Structure-Property Relationship of Thermoset Nanocomposites

Proefschrift

ter verkrijging van de graad van doctor
aan de Technische Universiteit Delft,
op gezag van de Rector Magnificus prof. ir. K.C.A.M. Luyben,
voorzitter van het College voor Promoties
in het openbaar te verdedigen op maandag 3 Juni 2013 om 12:30 uur

door

Muhammad Iftikhar Faraz
Master of Science in Manufacturing Engineering
University of Engineering and Technology Lahore, Pakistan

Geboren te Faisalabad, Pakistan

Dit proefschrift is goedgekeurd door de promotor:
Prof.dr.S.J.Picken

Copromotor: Dr.Ir. N.A.M. Besseling

Samenstelling promotiecommissie:

Rector Magnificus	voorzitter
Prof.dr.S.J.Picken	Technische Universiteit Delft, promotor
Dr.Ir. N.A.M. Besseling	Technische Universiteit Delft, copromotor
Prof.dr. J. Dik	Technische Universiteit Delft
Prof.dr.ir. J.W.M. Noordermeer	University of Twente
Prof.dr. T. Peijs	Queen Mary University of London, UK
Dr. G.J.M. Koper	Technische Universiteit Delft
Dr.ir. K.M.B. Jansen	Technische Universiteit Delft
Prof.dr. A. Schmidt-Ott	Technische Universiteit Delft, reserveild

This research has been completed in partial fulfillment of the requirements of Delft University of Technology, The Netherlands, for the award of the PhD degree. This research was supported by HEC Pakistan and Delft University of Technology.

Published and distributed by: M.Iftikhar Faraz
E-mail: seeiftikhar@gmail.com

ISBN # 978-94-6203-378-8
Copyright © 2013 by M.Iftikhar Faraz
All rights reserved. No part of the material protected by this copyright notice may be reproduced or utilized in any form or by any means, electronic or mechanical, including photocopying, recording or by any information storage and retrieval system, without written permission of the author.

The cover is designed by Malik Aleem Ahmad
Printed by Wöhrmann Print Service, The Netherlands

Table of contents

Chapter 1 1

Introduction 1

1.1 History of polymer composites 1
1.2 Polymer nanocomposites 1
1.3 The uniqueness of nanocomposites 3
1.4 Issues of nanocomposites 3
1.5 Motivation 5
1.6 Structure of the thesis 6
1.7 References 7

Chapter 2 9

Background literature 9

2.1 Polymer-clay nanocomposite 9
2.1.1 Layered silicates structure 9
2.1.2 Modification of clay layers and organoclay structure 11
2.2 Polymer/clay nanocomposites' structure 12
2.2.1 Conventional /microcomposite structure 12
2.2.2 Intercalated structure 13
2.2.3 Exfoliated structure 13
2.3 Preparation of polymer nanocomposites 14
2.3.1 In situ polymerization 14
2.3.2 Solution intercalation 15
2.3.3 Melt processing 15
2.4 Matrices for nanocomposites 16
2.4.1 Thermosets 16
2.4.2 Thermoplastics 16

2.5 High-temperature resistant thermosets 17
2.5.1 Polyimides 18
2.5.2 Bismaleimides 19
2.5.3 Cyanate esters 20
2.6 Literature survey of thermoset nanocomposites 20
2.6.1 Exfoliation mechanism 21
2.6.2 Role of different factors on exfoliation 21
2.6.3 Mechanical properties 23
2.6.4 Interfacial interactions and reinforcement 23
2.6.5 Thermal and dynamic properties 24
2.6.6 High temperature-resistant thermoset nanocomposites 24
2.7 Issues of thermoset nanocomposites 25
2.8 References 26

Chapter 3 33

Synthesis of Carbon Nanofiber Filled Composites: Thermal, Morphological and Mechanical Characterization 33

3.1 Introduction 33
3.2 Experimental 35
3.2.1 Materials 35
3.2.2 Processing of carbon nanofiber Bismaleimide nanocomposites 36
3.3 Characterization 36
3.3.1 Thermal analysis 36
3.3.2 Mechanical testing 37
3.3.3 Fracture characterization 37
3.3.4 Fire testing 37
3.4 Results and discussion 37
3.4.1 Gelimat mixing 37
3.4.2 Thermal stability and flammability properties 38
3.4.3 Mechanical properties 42
3.5 Morphological study of BMI/CNFs composites 43
3.6 Conclusion 46
3.7 References 47

Chapter 4 51

Probing the Development and Viscoelastic Properties of Organo-Clay Dispersions 51

4.1 Introduction 51
4.2 Experimental 54
4.2.1 Materials 54
4.2.2 Preparation 54
4.2.3 Characterization 55
4.3 Results 55
4.4 Discussion 63
4.5 Conclusion 66
4.6 References 67

Chapter 5 71

Synthesis , Characterization and Modeling of Mechanical Properties of Bismaleimide/Clay Nanocomposites 71

5.1 Introduction 71
5.2 Experimental 73
5.2.1 Materials 73
5.2.2 Nanocomposite preparation 74
5.2.3 Characterization 74
5.3 Results and discussion 75
5.3.1 Intercalation/exfoliation characterization 75
5.3.2 Orientation of the platelets 76
5.4 Mechanical properties 78
5.4.1 Dynamic moduli 78
5.5 Mechanical modeling of nanocomposites 81
5.6 Conclusion 84
5.7 References 85

Chapter 6 91

Creep and Recovery Behavior of Bismaleimide/Clay Nanocomposites: Characterization and Modeling 91

6.1 Introduction 91
6.2 Experimental 93
6.2.1 Materials 93
6.2.2 Nanocomposite preparation 94
6.2.3 Creep and creep- recovery measurements 94
6.3 Modelling of creep 95
6.4 Results and discussion 97
6.4.1 Creep and recovery behavior of matrix 97
6.5 Creep behavior of nanocomposites 100
6.6 Modeling creep behavior of nanocomposites 101
6.7 Multiple cycle creep and recovery behavior 105
6.8 Conclusion 106
6.9 References 107

Chapter 7 111

Conclusions and recommendations 111

7.1 Conclusions 111
7.2 Recommendations 113

Summary 115

Samenvatting 117

Acknowledgements 119

Curriculum Vitae 124

Chapter 1

Introduction

1.1 History of polymer composites

Polymers are extensively used in every economic sector and the trend is rapidly growing. Polymers lack some properties needed to satisfy specific requirements of product applications. The use of additives has been considered a cheaper, faster and an easier way to modify the properties of polymers. These polymer systems containing rigid fillers are known as composites because they consist of at least two different phases. Polymer composites are capable of meeting or exceeding the designed expectations. For instance, inorganic fillers are added in polymers to improve a variety of physical properties, such as stiffness, strength, thermal stability, etc., and in some cases fillers are employed to reduce the product cost. A variety of fillers are presently being used in polymers, such as glass fibers, mineral fillers, metallic fillers, etc. These types of fillers range in size from several microns to a few millimetres.

Blends of polymers and fillers have been used since the time polymers were introduced as commodity materials on industrial scale. However, intensive research on advanced composites started in the late 70’s in the pursuit of stronger, lighter and corrosion resistance materials for defence applications and was generously funded by the US ministry of defence [1]. Later on, with the development of easier processes, methods and less expensive materials, the composites got wide applications in civil life as well. A wide range of composite applications can be found in aerospace, automotive, ships, sports, construction, and consumer products.

1.2 Polymer nanocomposites

Polymer nanocomposite may be defined as a composite system containing a polymer matrix and homogeneously dispersed filler particles having at least one dimension below 100 nm. Polymer nanocomposites have received enormous attention both in academia and industry over the past decades. The excellent properties of nanocomposites are attributed to the large surface to volume ratio of the nanofillers [2]. In the late 80’s Toyota research laboratories synthesized nanoclay (layered-silicate) based nylon-6 nanocomposites that exhibited significant improvement in mechanical properties and heat deflection

temperature [3-5]. Later on these materials were commercialized to be used in the timing belt covers of Toyota cars. After this discovery the number of papers dealing with nanocomposites increased rapidly. Applications of nanocomposites are found in an array of fields ranging from agriculture and food production to space science and medicine [6].

Some of the additional benefits of layered silicate nanocomposites compared to polymers filled with micrometer-scale particles include:

- *High strength-and stiffness-to-weight ratios.* Nanofillers typically have exceptionally high mechanical properties together with a low density which may result in strength and stiffness to weight ratios of nanocomposites that are unachievable with traditional composites. For example 5 % nanofiller can provide the same increase in modulus as 40 % traditional mineral filler (talc) or 15 % glass fibers [7].

- *Improved barrier and diffusion properties*. High aspect ratio platelets increase the path length for diffusion of molecules [8-10].

- *Superior flame retardancy*; the barrier function of the silicate layers reduces the transport of oxygen and waste gases. The char layer formed by the silicate-layers protects the burning polymer from the surrounding atmosphere [11-13].

- *Better surface and optical properties*; the nanocomposites can be transparent because the particle size is below the wavelength of visible light [14, 15].

Although the raw material of the nanoclays might be very cheap the additional processing cost to improve their compatibility with polymer matrices can increase the cost of filler much more than the traditional fillers. However, very low quantity of filler used can lead to competitive price of nancomposites [14].

It is worth mentioning that in addition to improvement in mechanical properties, nanocomposites offer multifunctional properties. For example carbon nanotubes have excellent electrical conductivity, leading to electrically conducting composites. For platelet shaped nanoparticles, thermal and barrier properties are important. These multifunctional aspects of nanocomposites are a major driving force for continued research and development.

1.3 The uniqueness of nanocomposites

When the size of particles changes from macro size to nano size the surface area per unit volume drastically increases and their physical properties also change. The large surface-to-volume ratio of the nanoscale inclusions plays a vital role in improving the properties of nanocomposites [2, 16]. It is thought that many of the characteristics of nanocomposites are determined by the interfacial interactions. High aspect ratio particles provide extremely large interfacial area between the particles and the host material and are expected to lead to a strong reinforcement at low filler content [17].

In general shape and size of the particles have a direct effect on properties of nanocomposites. Other factors like the level of filler dispersion in the matrix, geometric arrangement of particles, efficient load transfer from particles to matrix and physical or chemical interactions of the particles with the host matrix affect the properties of nanocomposites.

1.4 Issues of nanocomposites

Despite the potential benefits of nanocomposites reported in several publications, their application is limited, and the industry is still waiting for a major breakthrough in this technology. In many cases only moderate improvement in properties is obtained and in some cases the incorporation of silicate into polymers leads to deterioration of performance [18-21]. Some critical issues have to be addressed to realize the full potential of the nanocomposites. Such issues include:

- *Dispersion of nanoparticles in polymer*. Uniform dispersion of the nanoparticles is the first step in the processing of nanocmposites. Beside the problems of agglomeration of nanoparticles, exfoliation of clay platelets (delamination of platelets stacks into single layers) is essential. It is necessary for optimal and more importantly uniform material properties. However, it often has proven to be difficult to form uniform and stable dispersion of nanoparticles in polymers.

- *Orientation of nanoinclusions.* The methods to control the orientatation of the anisotropic nanofillers (carbon nanotubes) in polymer matrix are not well developed. The lack of control of their orientation leads to decrease in reinforcing efficiency of nanotube and other functional properties in composites.

- *Understanding structure formation and control of interactions.* The properties of nanocomposites are largely determined by the microstructure formed at nanoscale level. In case of layered silicate composites the structure is usually oversimplified. Better understanding of the complicated structure formed and its quantitative characterization is much needed. Both the polymer matrices and the nanofillers used in composites have diverse physical and chemical structures and a wide variety of interactions may form between them. Interfacial interactions play a vital role in determining the structure. The use of surfactants to improve the dispersion of silicates modifies the interactions between the particle-particle and particle-matrix. The information available is limited and contradictory. Very little unambiguous information exists on the various competitive interactions of the coated silicate surface, the size and characteristics of the uncoated area and the strength of interfacial adhesion.

- *Interphase properties*. In composite materials an interphase is formed between the bulk matrix and the filler. The interphase properties are different from the constituent components. The interphase has an impact on the properties of the composites. The properties of the interphase, thickness of the interphase and its relation to macroscopic properties of the nanocomposites is not completely clear. There is no reliable method available to measure the volume and thickness of the interphase.

- *Quick characterization tools.* Methods that can quickly quantitatively assess the degree of intercalation/exfoliation in nanocomposites are required. It can provide more comprehensive information on the structure and enables studies of structure-property relationships.

- *Modeling limitations.* There is considerable uncertainty in theoretical modeling and experimental characterization of nanocomposites. Models that can account for practical limitations like the impact of non-uniform particle dispersion, the effect of surface modification on load transfer and interface effects are still under development.

- *Efficient manufacturing and cost effectiveness*. High volume production and low cost always gains the industrial support for the introduction of a technology. Currently the manufacturing cost of nanomaterials and nanocomposites is not

competitive with established polymers existing in the market. Production of nano materials at low cost and high volume is required. Furthermore manufacturing with high efficiency and widening the applications of the nanocomposites will make them cost effective.

1.5 Motivation

Thermosetting matrices have been widely used in fiber reinforced composites and occupy the largest market share of this type of material. Their inherent characteristics like ease of processing, excellent thermal and dimensional stability, and good resistance to solvents are the greatest advantages in comparison thermoplastic matrix materials. This makes thermoset matrix materials the preferred choice for use in composites. The development of polymer matrix fiber reinforced composites brought a revolution in light weight structural materials. A vast transformation in the engineering, design and performance of structural materials was witnessed in the second half of the twentieth century. Aerospace industry benefitted enormously from this technology. An excellent example of growing use of composites can be seen in the materials used in two new super-jets – the Airbus A380 and the Boeing 787 Dreamliner. The wings and fuselage of these airplanes consist of an unprecedented amount of up to 50% by weight of composite materials, enabling substantial weight savings, improved aerodynamic efficiency, and savings in the fuel cost [22].

Now with the emergence of nanometer–sized particles the paradigm of composite research has started to shift towards nanocomposites and efforts are under way to realize their true potential. However, unlike continuous fiber composites the literature on nanocomposites is dominated by thermoplastic matrices. Thermoset nanocomposites are relatively unexplored. Moreover, the examples of thermoset nanocomposites reported in the literature are predominantly based on generic low glass transition temperature epoxy systems, polyesters and polyurethanes. High-temperature resistant thermoset nanocomposites have been rarely investigated. However, in order to meet the stringent demands of new era of aero technology the aerospace industry is vey keen to use high performance and high-temperature resistant polymer matrix based composite materials. They are targeting the aircraft to be constructed using as much as three quarters composites. The widely used epoxy based advanced composites have a limited service temperature range and can not be applied in the areas where temperature is expected to be relatively high like in or around the engine, the parts subjected to engine exhaust gases,

military and supersonic air craft and space crafts. Thus, the use of high-temperature resistant matrices is highly desired to meet the strategic targets of the future aviation industry.

The use of nanoparticles in polymer matrices has already shown promising results in several publications. The combination of nanoparticles and a high-temperature resistant polymer can contribute to the advanced composites by further improving their performance and reducing the cost. It warrants the development of knowledge and understanding about high-temperature resistant thermoset nanocomposites. Thus we were motivated to study the high-temperature resistant thermoset nanocomposites. The main objectives of the research are:

- *Synthesis of high-temperature resistant thermoset nanocomposites*
- *Analysis of the thermo-mechanical properties*
- *Understand the structure-property relationships*
- *Modeling of the mechanical properties*

We selected a high-temperature resistant thermoset resin of *bismaleimide*, having intermediate properties between epoxy and high performance polyimides and with a high performance to cost ratio. To have compatible and inexpensive nanoparticles, we selected *organically modified nanoclays*. The cost of bismaleimide resin is also relatively low compared to the competitive high performance matrices like polyimides, PEEK, etc.

1.6 Structure of the thesis

The work done on thermoset nanocomposites in this thesis is structured in several chapters to bring forth the structure–property-relationship of these nanocomposites. After describing the context of the work and overall study objectives in **chapter 1**, the necessary relevant background literature is presented in **chapter 2.** It contains the information about the nanoclays, preparation methods of nanocomposites, polymer/clay nanocomposite structure and discusses the literature on thermoset nanocomposites over the years and the current state of research.

Initially, at the start of this research, we used carbon nanofiber as a filler. In **chapter 3**, the synthesis of bismaeimide/carbon nanofiber composites, results of thermo-mechanical characterization and fractography are presented.

The addition of carbon nanofibers exhibited poor reinforcing effects and the dispersion quality was rather bad. The cost of carbon nanofibers is also high, so ultimately we decided to use organoclay as the filler. In **chapter 4** the strategy used to prepare the oganoclay dispersions, study of their rheology and the development of the rheology over time is described. The viscoelastic behavior is also modeled with a *critical gel- like model*.

In **chapter 5**, the synthesis of bismaleimide/clay nanocomposites, structure characterization and their thermo-mechanical properties are reported. Moreover, the mechanical properties of the nanocomposites are modeled by a micromechanical model, the *Halpin-Tsai model*.

In chapter **6**, the creep and recovery behavior of the investigated thermoset-nanocomposites is described in detail. Furthermore, critical appraisal of some widely used viscoelastic models is made. The creep behavior is modeled by a *modified form of Burgers' model*. Some interesting facts about the role of filler on the composite dynamics are also presented.

The conclusions drawn from the overall work and recommendations are summarized in **chapter 7**.

1.7 References

[1] Pilato LA, Michno MJ. Advanced composite materials: Springer; 1994.

[2] Mai YW, Yu Z-Z. Polymer nanocomposites: Woodhead publishing LTD; 2006.

[3] Fukushima Y, Okada A, Kawasumi M, Kurauchi T, Kamigaito O. Swelling behavior of montmorillonite by poly-amide-6. Clay Minerals. 1988;23(1):27-34.

[4] Usuki A, Kojima Y, Kawasumi M, Okada A, Fukushima Y, Kurauchi T, et al. Synthesis of Nylon 6-clay hybrid. J Mat Res. 1993;8(5):1179-1184.

[5] Kojima Y, Usuki A, Kawasumi M, Okada A, Fukushima Y. Mechanical properties of nylon 6-clay hybrid. Mat Res. 1993;8(5):1185-1189.

[6] Twardowski TE. Introduction to nanocomposite materials: Properties, Processing, Characterization: DESTech Publications, Inc; 2007.

[7] Akkapeddi MK. Glass fiber reinforced polyamide-6 nanocomposites. Polymer Composites. 2000;21(4):576-585.

[8] Yano K, Usuki A, Okada A. Synthesis and properties of polyimide-clay hybrid films. Journal of Polymer Science Part a-Polymer Chemistry. 1997;35(11):2289-2294.

[9] LeBaron PC, Wang Z, Pinnavaia TJ. Polymer-layered silicate nanocomposites: an overview. Appl Clay Sci. 1999;15(1-2):11-29.

[10] Ray SS, Okamoto M. Polymer/layered silicate nanocomposites: a review from preparation to processing. Prog Poly Sci. 2003;28(11):1539-1641.

[11] Kiliaris P, Papaspyrides CD. Polymer/layered silicate (clay) nanocomposites: An overview of flame retardancy. Prog Poly Sci. 2010;35(7):902-958.

[12] Beyer G. Flame retardancy of nanocomposites - from research to reality - Review. Polymers & Polymer Composites. 2005;13(5):529-537.

[13] Kashiwagi T, Harris RH, Zhang X, Briber RM, Cipriano BH, Raghavan SR, et al. Flame retardant mechanism of polyamide 6-clay nanocomposites. Polymer. 2004;45(3):881-891.

[14] Giannelis EP. Polymer layered silicate nanocomposites. Advanced Materials. 1996;8(1):29-&.

[15] Fornes TD, Paul DR. Modeling properties of nylon 6/clay nanocomposites using composite theories. Polymer. 2003;44(17):4993-5013.

[16] Pissis P. Molecular dynamics of thermoset nanocomposites. In: R. Kotsilkova, editor. Thermoset nanocomposites for engineering applications: Smithers Rapta Technology; 2007. p. 143-206.

[17] Luo JJ, Daniel IM. Characterization and modeling of mechanical behavior of polymer/clay nanocomposites. Comp Sci Tech. 2003;63(11):1607-1616.

[18] Alexandre M, Dubois P. Polymer-layered silicate nanocomposites: preparation, properties and uses of a new class of materials. Materials Science and Engineering 2000;28(1-2):1-63.

[19] Pozsgay A, Csapo I, Szazdi L, Pukanszky B. Preparation, structure, and properties of PVC/montmorillonite nanocomposites. Materials Research Innovations. 2004;8(3):138-139.

[20] Yuan MQ, Pan XJ, Wan CY. Investigation of melt-intercalated PET-clay nanocomposites. Polymers & Polymer Composites. 2004;12(7):619-625.

[21] Yasmin A, Abot JL, Daniel IM. Processing of clay/epoxy nanocomposites by shear mixing. Scripta Materialia. 2003;49(1):81-86.

[22] Wagner HD. Nanocomposites - Paving the way to stronger materials. Nature Nanotechnology. 2007;2(12):742-744.

Chapter 2

Background literature

2.1 Polymer-clay nanocomposite

Various types of nanofillers with various sizes and shapes (particles, platelets, wires, fibers, rods etc.) have been used to prepare polymer nanocomposites. However, layered silicates (clays) have been the most widely used filler in polymer nanocomposites. Easy accessibility in nature, low cost, environment friendly and high aspect ratio are amongst the greatest advantages of the clay particles over the other fillers to promote its use in nanocomposites [1]. Carbon nanofiber, Carbon naotubes, synthetic whiskers and inorganic particles (alumina, silica etc...) are among the other fillers used. But their availability is limited and processing cost is high. For the low aspect ratio inorganic particles the properties are also not optimized [2].

2.1.1 Layered silicates structure

Clay minerals are the layered silicates consisted of regular stacks of aluminosilicate layers. The layered silicates have high aspect ratio and large surface area. The layers are built from octahedral and tetrahedral sheets [3]. In the tetrahedral sheets silicon atom is surrounded by four oxygen atoms, whereas in the octahedral sheets, metal like aluminum or magnesium is surrounded by eight oxygen atoms [1]. The tetrahedral and octahedral sheets are fused together by sharing oxygen atoms. Unshared oxygen atoms are present in hydroxyl form. The simplest arrangement of the sheets fusion is in the form of 1:1 in which one octahedral sheet is fused with one tetrahedral sheet known as kaolin group. The second arrangement is a 2:1 crystal lattice consisted of one octahedral sheet sandwiched between two tetrahedral sheets and is known as phyllosilicates [4].

The layered silicates most commonly used for polymer nanocomposites are montmorillonite (MMT) which belong to structure family of 2:1 phyllosilicates, more specifically smectites. The structure of phyllosilicates is shown in Fig. 2.1 [4]. The layer thickness is around 1 nm and lateral dimensions may vary from 30 nm to several microns depending on the source and preparation method of clay. The layers are separated by a regular

van der Waals gap between them called the interlayer or the gallery [4]. The sum of the thickness of single layer and interlayer space represents the repeating unit of multilayer structure and is called d-spacing (d_{001}) or basal spacing.

Isomorphic substitutions of aluminium by magnesium in the octahedral sheet generate negative charges which are counter balanced by alkaline-earth or hydrated alkali-metal cations situated inside the galleries [4]. Based on the extent of substitutions in the silicate crystals, a term called layer charge density is defined. This charge is not locally constant and varies from layer to layer; therefore, it must be considered an average value over the whole crystal. MMT has a mean layer charge density of 0.25-0.5 equiv.mol^{-1} [1].

The layers are held together by relatively weak electrostatic and van der Waals forces in MMT and interlayer distance varies depending on layer charge density, radius of cation and its degree of hydration [1]. The interlayer spacing and weak interlayer forces facilitate hydration of cations between layers in aqueous solutions known as clay swelling. The swelling causes an increase in interlayer spacing and other molecules can also intercalate between the layers consequently expansion of the layered lattice. Thus as a result of swelling and intercalation the individual layers can be easily separated by shearing, giving platelets with high aspect ratio [1]. The relatively easy exfoliation and high aspect ratio of MMT makes them very attractive as reinforcing filler for polymers. The aspect ratio has a large influence on the improvement of polymer properties and important in polymer/clay interfacial interactions. The MMT aspect ratio can be in the range of 10-1000 and surface area about 750 m^2/g. But practically due to breaking of the clay platelets during mixing process at high shear results in an aspect ratio about 30-300 [3].

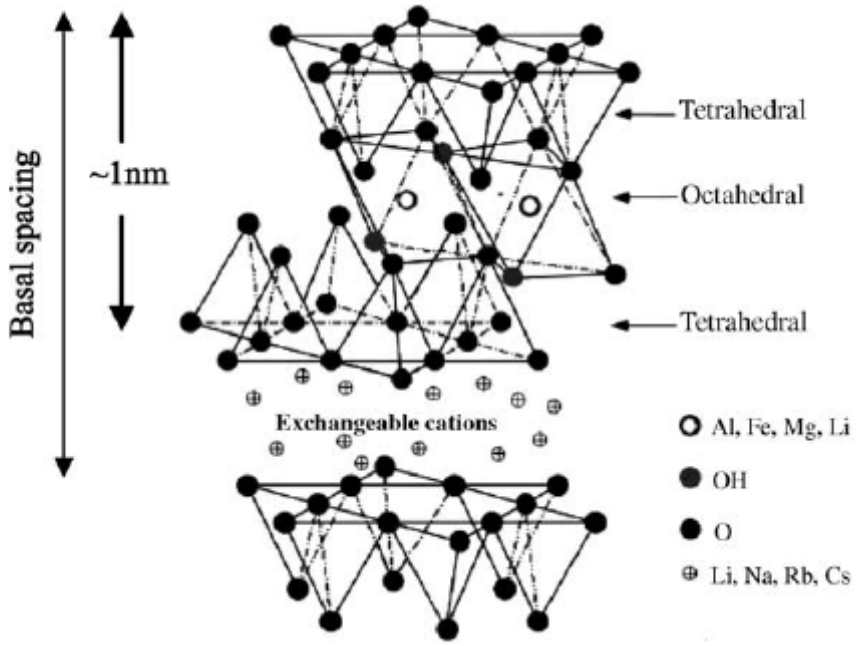

Figure 2.1 Structure of 2:1 layered silicates [4].Reproduced from reference 4

2.1.2 Modification of clay layers and organoclay structure

The neat sodium montmorillonites are not used with many polymers because of their high surface energy and intrinsic hydrophilicity which renders them incompatible with the hydrophobic polymers. In order to make them hydrophobic the inorganic cations present in galleries are exchanged with organic cationic surfactants like alkylammonium or alkylphosphonium having long aliphatic chains. The organic modification does not only impart hydrophobic character but also causes an increase in the interlayer spacing and decrease in surface energy of the clay platelets [4]. Larger the gallery spacing and weaker the interaction forces easier would be the exfoliation and distribution of the layers in the polymer. The cationic surfactants can also provide functional groups which interact with the polymer or initiate polymerization and therefore increase interfacial interactions [4]. That is also another advantage of organo clays and they are preferred over unmodified clay for polymer/clay nanocomposites.

With regard to the structure of interlayer in organoclays, it is believed that cationic head group of the alkylammonium molecule preferentially resides at the layer surface and the organic tail radiate away from the surface. The equilibrium layer spacing at a given temperature is defined by two parameters: the charge density of the layered silicates driving the packing of the chains and the chain length of the organic tails [1]. Depending on the

charge density of clay the organic chains may lie parallel to the silicate layer, forming mono or bilayers, a pseudo trilayer or even tilted paraffin structure as shown in Fig. 2.2.

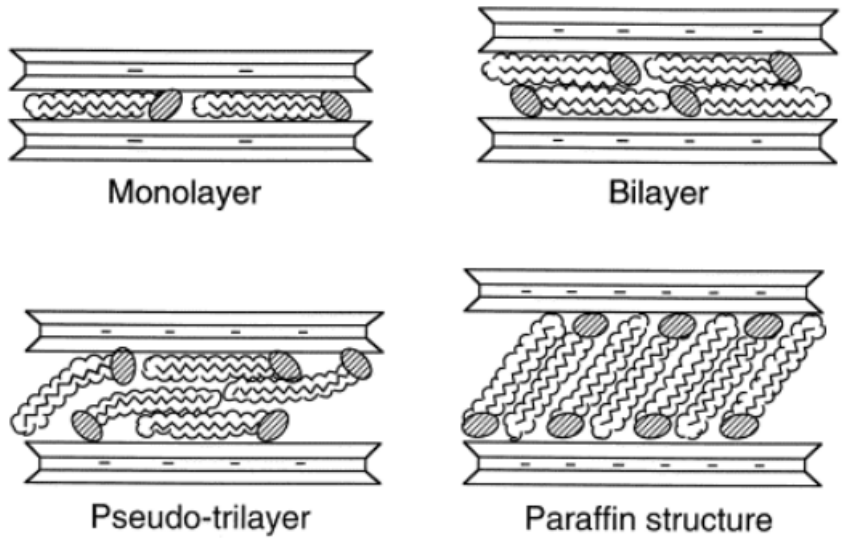

Figure 2.2 Various configurations of organic chains in clay galleries[1]

2.2 Ploymer/clay Nanocomposites' structure

Homogeneous dispersion of the nanoparticles is a primary condition of preparation of nanocomposites. When the clay particles are mixed with the polymer the microstructures formed are classified according to the level of exfoliation of clay particles. The kinetics of exfoliation depends on many factors including clay nature, organic modifier, interfacial interactions and preparation method. Therefore, depending on the nature and properties of polymer and clay as well as preparation methodology of nanocomposites different composite microstructures can be obtained.

2.2.1 Conventional microcomposite structure

In this type of structure the clay particles are dispersed as aggregates and stacks of platelets together like the original particles within the polymer matrix. The polymer is unable to intercalate between the clay layers and they are not broken down. It is also known as phase separated structure. It is the most unwanted structure and properties of the polymer are merely improved in this case.

2.2.2 Intercalated structure

In this type of structure the polymer chains are inserted into the clay galleries and the interlayer spacing is increased but the periodic array of clay layers is maintained. The polymer chains inside the galleries cause to decrease the electrostatic forces between the layers but are not totally dissolved.

2.2.3 Exfoliated structure

This structure is obtained when the clay layers are completely separated from each other and individual layers are randomly dispersed in the matrix. Exfoliated structure is of typical interest, it maximizes the polymer-clay interactions and entire surface of layers is available for the polymer (larger interfacial area). This should lead to significant change in physical and mechanical properties. The complete dispersion of clay layers provides optimum number of reinforcing elements to carry the load and deflect the cracks. The coupling between tremendous surface area of the layers and matrix facilitate stress transfer to the reinforcement phase allowing for improvement in mechanical properties [5].

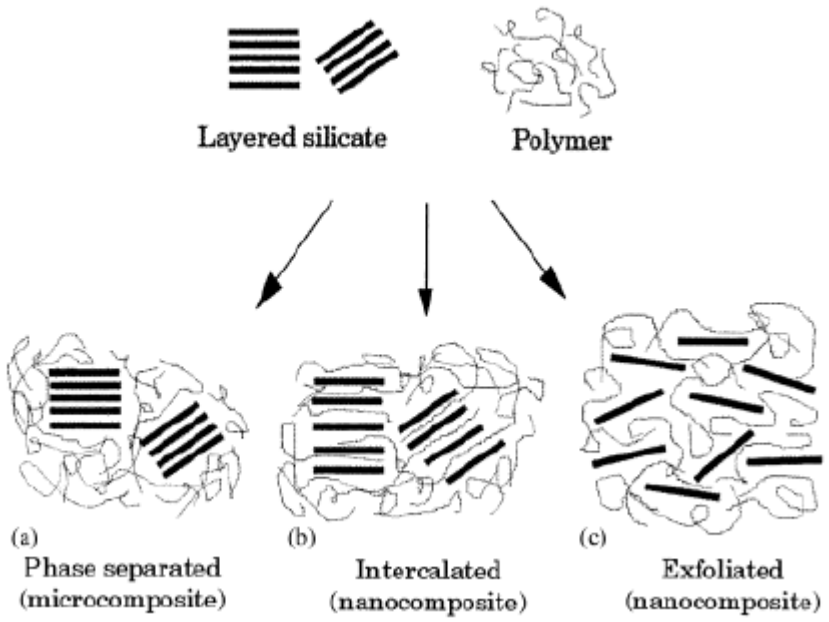

Figure 2.3 Probable microstructures of polymer/clay composites. From[6].

However, it is difficult to achieve complete exfoliation and with few exceptions most of the polymer nanocomposites reported in literature were found to have intercalated or mix

of intercalated and exfoliated structure [7]. Usually, intercalated stacks or tactoids with a range of gallery distances form in the composite. A composite having good mechanical properties and high degree of dispersion may contain stacks of silicates with 3 to 10 layers [8, 9]. The composite structure is more complicated than expected besides tactoids and individual layers also large particles and silicate network may be present in the composite [10]. The wide ranges of structural units are present in nanocomposites varying considerably in surface area and undergo various deformation processes during the deformation. One or more type of structural formations may determine the micro and macro-mechanical deformation processes and thus the properties of the composites. The interactions play a role to determine the extent of exfoliation and structure formation but the adhesion of the dominating unit to the matrix is crucial for the determination of composite properties [11].

2.3 Preparation of polymer nanocomposites

Many methods have been proposed to prepare polymer /clay nanocomposites. They can be classified into three main categories: solution processing, in situ polymerization and melt processing.

2.3.1 In situ polymerization

This method involves swelling of clay in monomer or monomer solution and subsequently polymerization of the monomer. The monomer inside the galleries is polymerized by heat or radiation by the diffusion of an initiator or catalyst fixed through cationic exchange to the layers before swelling them by the monomer. The polarity of clay layers and monomer determines the diffusion rate and equilibrium concentration of the monomer within the clay galleries. Consequently the exfoliation and dispersion of clay layers can be tailored by the clay and monomer chemistry [7]. For the nanocomposites prepared by this approach the growing chains are closely attached (grafted) on to the nanoparticles and act as coupling agents as well as matrix material at the same time. Polymerization is carried out within the clay galleries as well as outside the galleries. The growth of the chains by polymerization results into the exfoliation and formation of a disordered structure. This method can be used for the production of both thermoplastic and thermoset nanocomposites. However mostly thermoset nanocomposites of epoxy, polyurethane and polyester were

prepared by this method [12-15]. Polyolefin composites can not be easily produced by in situ polymerization.

2.3.2 Solution intercalation

In solution mixing technique same principle is applied as in situ polymerization but without the difficulties of initiation and catalysis reactions. In this method a solvent system is used in which the polymer is soluble and at the same time nano-clays are able to swell. In general the clay is first swollen in the solvent to make a homogeneous dispersion then a soluble polymer is added in the solution. After that the solvent is evaporated and polymer chains are intercalated into the layers and finally polymerize under suitable conditions. This method involves a large number of solvent molecules to be desorbed from the silicate layers to accommodate the polymer chains inside the galleries. From an energetic point of view the loss in conformational entropy of the confined polymer chains in the galleries is compensated by gain in entropy of the desorbed solvent molecules during evaporation. This method is widely applied for water soluble polymers. Unmodified clays are relatively easily exfoliated in water and thus the mixing of solution made from polymer with the slurry of silicates is relatively easy. For non water soluble polymers and organically modified clays organic solvents are used. It is also widely used for the preparation of thermoset nanocomposites. This method is not attractive for industry due to the use of large amount of solvent, expensive and environment unfriendly.

2.3.3 Melt processing

This method involves mixing of the nano-clays within the polymer matrix in the molten state. The nano-clays are mechanically mixed with thermoplastic by conventional methods such as extrusion and injection molding at an elevated temperature [3]. Almost all the thermoplastics can be processed by this technique [16-19]. It has become most popular method in industry because of its simplicity, economical and fast production rate. This approach is especially useful for polyolefins. This method is rarely used for preparation of thermoset nanocomposites.

2.4 Matrices for nanocomposites

Polymers are broadly classified into thermoplastics and thermosets. Nanocomposites based on both types of theses matrices have been reported in literature. Thermoplastics and thermosets matrices have different physical and mechanical properties because of different structural characteristics.

2.4.1 Thermosets

Thermosets are network forming polymers, usually build up from two components reacting together to form an amorphous crosslinked network. They are rigid below the glass transition temperature (T_g) and rubbery above T_g. They cannot be dissolved or melted once polymerized. Curing is normally thermally activated that is why they are called thermosets. Chemical reactions are involved during curing. Curing begins with the reaction of small monomers or oligomer molecules and they grow into chains and branches. As the reaction proceeds more and more molecules join together and eventually several chains linked together into a network of infinite molecular weight. The properties of the thermosets are mainly determined by the network structure. The network consists of several chains and crosslinking points or junctions. For highly crosslinked systems the concentration of junction points is high hence the lengths of chains between them are shorter. Shorter chains have less flexibility and spatial conformations thus higher would be the modulus. For high crosslinked density systems the mobility of chains is also restricted and T_g is usually high. Moreover, glass-rubber transition becomes broader and less distinct with increase in crosslink density [20]. Epoxies, polyesters, polyurethane, polyimides and phenolics are among the thermoset resins widely used in engineering applications.

2.4.2 Thermoplastics

Unlike thermoset polymers thermoplastics have usually high molecular weight linear chains which are not chemically linked to each other. Depending on the flexibility of the chain, side groups and the stereo-regularity of the polymer can form an amorphous or semi-crystalline structure. For amorphous polymer the properties below T_g are driven by the entanglements formed by the long chains. These entanglements act as temporary crosslinks and strengthen the matrix. Semi-crystalline polymers have also crystalline regions containing

densely packed chains which increase the modulus of amorphous regions even above T_g. Thermoplastics can be melted and molded a number of times. Polyolefins, polyamides, polyethers etc. are among the thermoplastics.

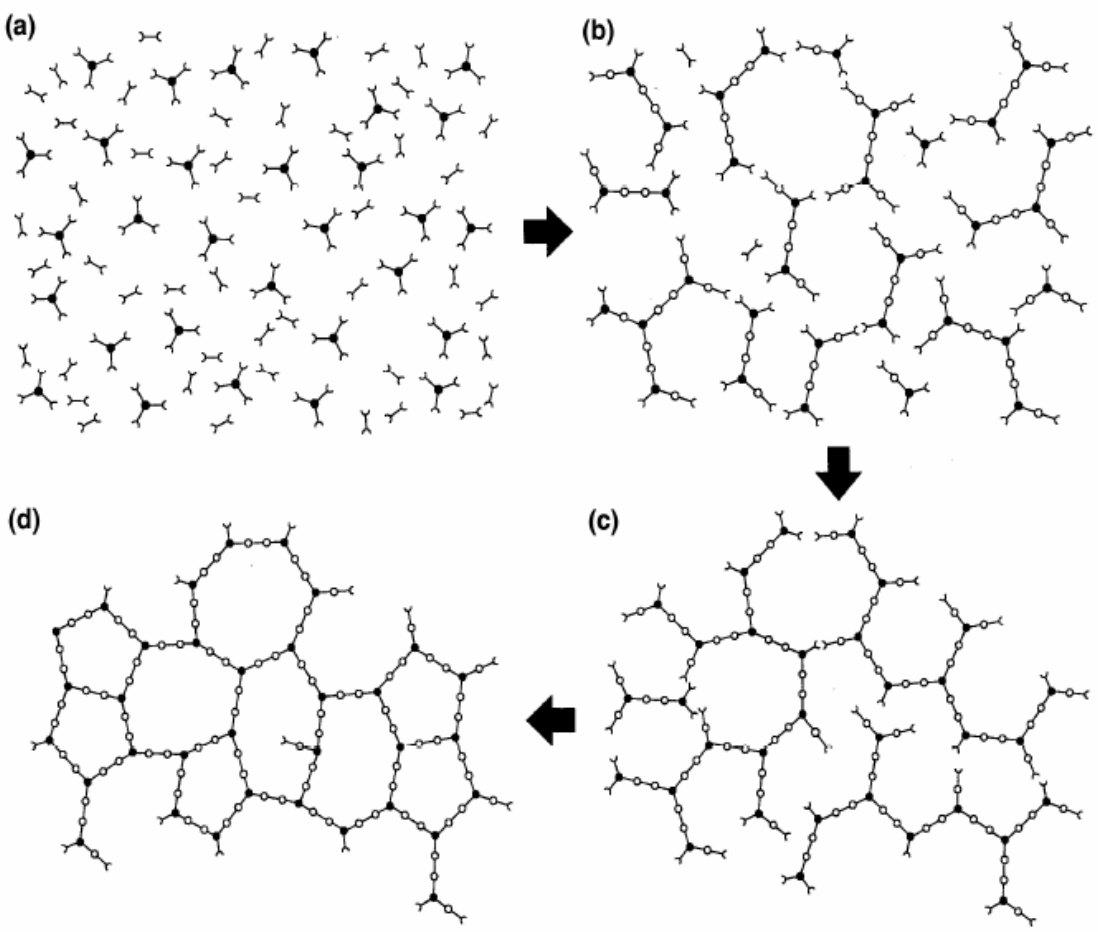

Figure 2.4 Schematic representation of curing process and network development for a thermoset system. (a) unreacted small monomers (b) initialization of monomers reaction and joining of small molecules (c) Network formation, gel state (d) Fully cured completed network. From [21]

2.5 High-temperature resistant thermosets

The market of fiber reinforced composites is dominated by the thermosetting matrices and particularly with the epoxy. Epoxy based fiber reinforced composites are being used in aerospace applications where the service temperature is around 100-120 °C [22]. However,

with the advancement of technologies and to broaden the applications of composites in aircraft structures the composite systems which can perform in the temperature range 200-400 °C are needed [22]. In order to meet these demands several high-temperature resistant (high-performance) thermosetting matrices have been developed over the years. These are designed to provide special properties in highly demanding environments. They can be tuned through compositional variations and innovative processing schedules. High-performance matrices usually possess high dimensional stability at elevated temperatures, excellent thermal and thermo-oxidative resistance, low water absorption, good chemical resistance and high mechanical properties. Cyanate esters, bismaleimides and polyimides are among the widely used high temperature-resistant thermosets. A brief review of the properties theses matrices is presented in following paragraphs.

2.5.1 Polyimides

Thermosetting polyimides are the most thermally stable polymers with service temperatures ranging from 250-350 °C [23]. The low molecular weight imide oligomers with unsaturated functional groups are capable of undergoing an addition reaction and form a densely cross-linked network. A wide range of polyimides have been synthesized over the years to improve the thermal stability and processability. PMR (Polymerization from monomeric reactants) type polyimides are among the most well-known and commercially successful polyimides. The PMR-15 polyimide has been widely used as high-temperature resistant resin for composite applications in the temperature range 260-288 °C [23]. The PMR-15 offers relatively easy processing and retention of properties at high temperature at a reasonable cost. For these reasons, it is widely used in both military and commercial aircraft engine components. Further efforts have been made to improve the thermo oxidative stability to meet the criteria of missile and gas turbine engines requiring thermal and thermo-oxidative stability at higher temperatures (350-400 °C) [24]. In this regard new generation PMR-polyimides have been synthesized, however, their molecular weight is relatively high and a concern from processing point of view.

The curing temperatures of PMR-polyimides are quite high and curing is done for a longer time to obtain high glass transition temperatures. For example in case of PMR-15 the high glass transition temperature close to 340 °C is obtained when it is cured at 316 °C for more than 16 hours [24]. This long thermal curing cycle is not appreciated. The brittleness and difficult processing are the concerns of polyimides.

Thermosetting polyimides have got the popularity as advanced materials in civilian and defence applications. The major use of PMR-polyimides is in aircraft engines, missiles and re-entry vehicles. In addition they are also finding applications in space craft, electronics and fuel cell membranes.

2.5.2 Bismaleimides

Among addition polyimides, bismaleimides (BMI) resins are the most important systems currently used for advanced composite applications due to their high performance to cost ratio [25, 26]. They can bridge the performance gap between the epoxy and high-temperature resistant polyimides. The monomers of Bismaleimides are capable of curing through thermally- induced addition reaction which gives highly cross-linked void free network of the polymer with high glass transition temperature about 300 °C, good thermal stability as well as better fire resistance and lower moisture absorption than the conventional epoxies [23]. Cured BMI can withstand service temperature up to 180 °C and can be improved further by manipulating chemical structures up to 270 °C [24]. Thus thermal stability is higher than that of epoxy but lower than that of high temperature resistant PMR-polyimides. However, BMI offer better processability than that of PMR- polyimides with low volatile emissions and low cost. BMI can be processed like epoxy resins by autoclave molding. At the same time they exhibit mechanical properties and damage tolerance similar to epoxy or even better [24]. Because of excellent processability, good mechanical properties and very good thermal stability bismaleimides have gained the popularity for the development of high performance composites.

However, high brittleness due to high crosslink density is a major concern of bismaleimides. This draw back renders it low damage tolerant and limiting its use in aerospace applications. The high cross link density and rigid maleimide groups also render it insoluble with normal solvents. A sizeable volume of literature is available dealing with the efforts done to improve the toughness and processability of bismaleimides. The strategies used for improving toughness and processability were chain extension, addition of long and flexible segments in backbone, copolymerization with olefinic via Diels- Alder reaction and blending with other systems [25-28]. In some cases toughness has improved at the cost of thermal stability [22]. The modification of bismaleimide resins with aromatic amines has been the most attractive and important approach for practical use [22].

BMI are blended with other resins like epoxy and unsaturated polyesters to improve their thermal stability. Aerospace composites are dominated by epoxy resins but now BMI

composites are gaining acceptance in the aerospace industry. They are used to design wings of extended supersonic air craft, and in other structural parts which experience engine exhaust in routine operation. BMI composites also find applications in jet engines, automobile engines, exhaust system components and self-lubricating bearings for high temperature use [24].

2.5.3 Cyanate Esters

Cyanate esters have emerged as a new class of thermosetting resins for use as pre-preg matrices in both the aerospace and electronics industries. They have been studied with various backbone structures with varying chemical, mechanical and electrical properties, and glass transition temperatures (T_g) ranging from 160 °C to 355 °C [29]. Cyanate esters resins donot have as good thermal stability as the bismaleimides but have superior dielectric loss properties and low moisture absorption than epoxy and bismaleimides. They also possess a reasonable toughness owing to relatively low crosslink density. Their processing characters are similar to epoxy and conventional manufacturing methods are applicable. Moreover, they have inherent low smoke generation and good flame retardancy properties. The only biggest disadvantage of cyanate esters is their high cost. Recent research efforts of blending with epoxy and bismaleimides has established a very promising approach to obtain a combination of balanced properties with low cost [29]. Microelectronics will be a huge potential area for cyanate esters owing to their superb dielectric properties and low power consumption. They are replacing epoxies in wiring boards and circuitry in electronics. The use of cyanate ester resins in aerospace structures is very limited [22].

2.6 Literature survey of thermoset nanocomposites

Epoxy/clay nanocomposites are the most widely studied among the thermosetting matrices because of wide utilization of epoxy in aeronautics, transport and electronic applications. Several research efforts have been made by varying the type of resin, organic modifiers, curing agents and processing conditions in order to gain fundamental understanding of materials and to optimize the fabrication and processing techniques. The exfoliation process, morphology and performance of epoxy clay nanocomposites with various organoclays have been widely reported by a number of researchers [30-38].

2.6.1 Exfoliation mechanism

Pak and Jana [33] hypothesized that the elastic forces generated in clay galleries during epoxy network formation are responsible for exfoliation. They explained that the elastic forces work for exfoliation and viscous forces and attractive forces (van der Waals, electrostatic force) work against the exfoliation. The elastic forces overcome the viscous and attractive forces and exfoliation takes place. The separation of the layers from a tactoid starts at the outermost layers because of the higher ionic bonding energy of the inner layers. Moreover as the viscosity works against the exfoliation so the exfoliation procedure should be completed before the gel point is reached. Networks are formed at this point and viscosity increases strongly. Lan et al. [31] reported that balancing of intra and extra gallery polymerization rates is critical to obtain exfoliated thermoset/clay nanocomposites. According to Wang et al. [39] the relative curing speed between the interlayer and extralayer is most important factor for clay exfoliation. For higher interlayer curing speed than extralayer will yield exfoliated nanocomposite.

2.6.2 Role of different factors on exfoliation

In order to process exfoliated thermoset nanocomposites some factors like the chemistry and structure of the organic modifer, curing agent, curing conditions, viscosity, functionality of the resin, etc. have to be considered. Kormann et al. [35] investigated the effect of curing agents on the exfoliation of organo clay in epoxy. The curing agent with low reactivity and high diffusion rate with in the galleries facilitated the exfoliation at high temperature curing conditions. The morphology observed was quite complex having intercalated, exfoliated and microcomposite regions. Pinnavia and co-workers [40] reported on the self polymerization of the epoxy resin in organoclays due to the presence of the alky-ammonium ions. This catalytic effect of alky ammonium ions also helps in exfoliation[41, 42]. Pinnavaia at al. [30] and another group of researchers [43] found that the organo-clays having long alkyl chains showed high degree of exfoliation. Kornamnn et al. [26] investigated the effect of cation exchange capacity of organo clays on exfoliation and found that relatively low charge density organoclays have better exfoliation. Tolle et al. [42] investigated the sensitivity of exfoliation to processing conditions. It turned out that the high temperature curing favours exfoliation. Exfoliated nanocomposites have been prepared by pre-aging of an intercalated epoxy/layered silicate mixture before curing with improved toughness [44].

Another group of researcher also observed a positive effect on exfoliation for preconditioning an epoxy resin mixture before curing. The improvement in exfoliation for a

preconditioned mixture was attributed to the homopolymerization of the epoxy due to the catalytic effect of ammonium ions [45].

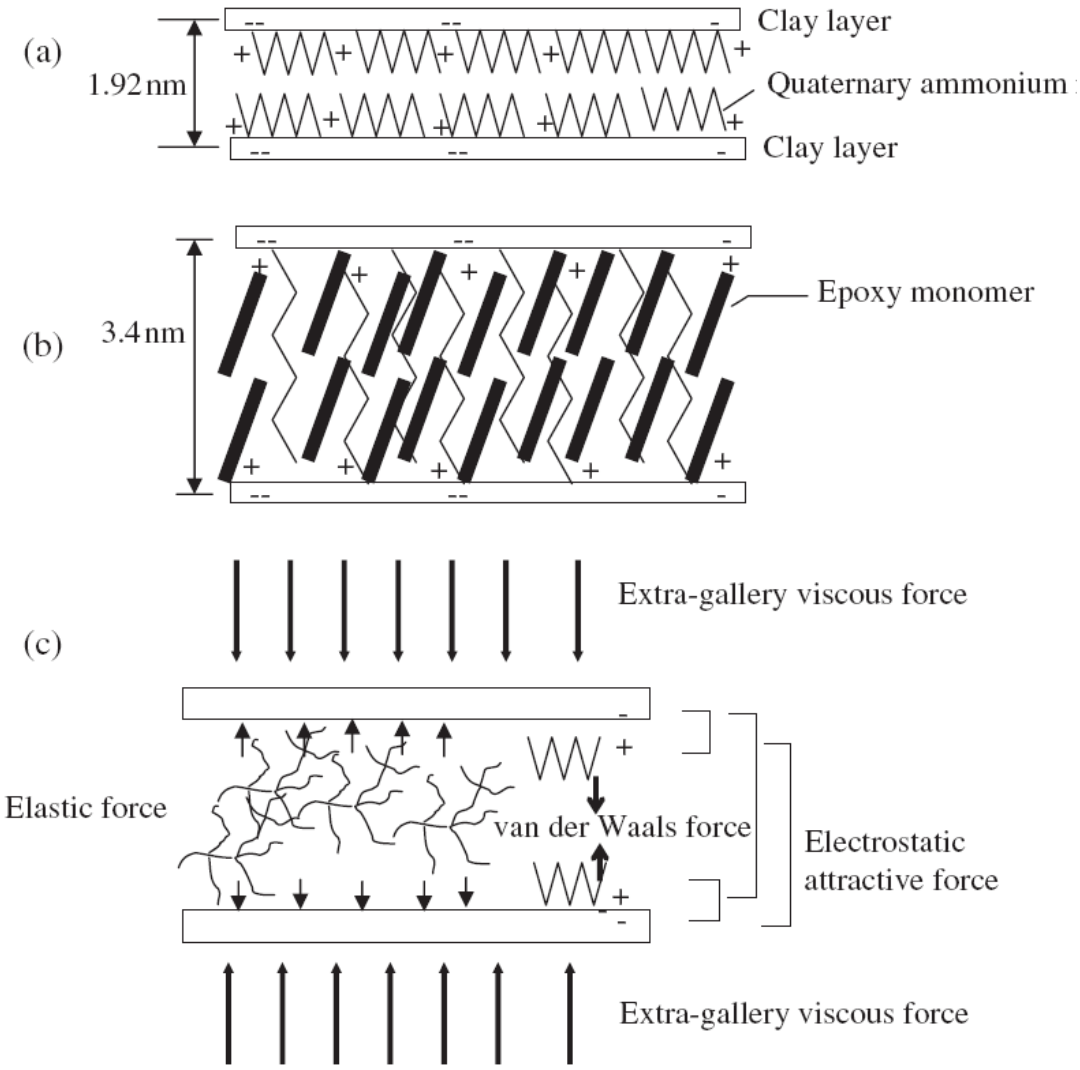

Figure 2.6 Schematic representation of exfoliation mechanism and forces acting on a pair of clay layers for an epoxy organo-clay system. From[33]

The preparation of a well dispersed epoxy/clay nanocomposites has also been an active area of research. In this regard different processing techniques have been tried. Moderate stirring with a magnetic stirrer is not sufficient for exfoliation [43]. High energy shearing devices are well proven, including ultraturrax or ultrasonic horn [46]. High level of dispersion and exfoliation of silicate layers in epoxy was achieved by using three-roll mill as means of applying external shearing force [47].

2.6.3 Mechanical properties

The addition of nanoclay has influenced the physical and mechanical properties of the epoxy. From the pioneering work of Pinnavia and co workers [30] a 10-fold increase in tensile strength and modulus was observed for a well exfoliated clay in a rubbery epoxy at 15 wt% loading. They also concluded that the reinforcement effect depends on the ductility of the epoxy. For a rigid high T_g epoxy system the improvement in mechanical properties was very marginal but for a system having T_g lower than ambient a significant increase in properties was observed. Similarly many other authors reported linear increase in tensile strength and modulus with the concentration of clay for elastomeric epoxy systems [32, 48, 49]. An increase in tensile, compressive and flexural modulus with the addition of clay for glassy epoxy systems also reported in [14, 50-52]. However, there are studies that report decrease in tensile strength and strain at break by incorporation of clay in epoxy [53-56]. It turns out from these studies that high degree of exfoliation was responsible for improvement in properties. However, despite the improvement in mechanical properties complete degree of exfoliation was never achieved [30, 49, 52, 57].

Some authors have also reported the nanocomposites prepared from other thermosetting matrices like unsaturated polyester and polyurethanes [15, 58-60]. Kornmann and co-workers [58] prepared unsaturated polyester –clay nanocomposites and found an increase in the modulus and fracture toughness with the concentration of clay particles. The clay particles were partially exfoliated. Another group of researchers [15] established structure-property relationships in polyester/clay nanocomposites. Despite the formation of nanocomposite structure of mixed type containing regions of intercalated and exfoliated the tensile modulus and the loss and storage moduli showed a progressively decreasing trend with increasing clay concentration. This decrease in mechanical properties was attributed to decrease in degree of crosslinking in the presence of organoclays. Joulazadeh et al. [60] investigated the effect of two different organoclays on the stiffness of the polyurethane. The exfoliation was limited by the degree of crosslinking density. The modulus increased up to 1.5 wt% clay loading and then decreased due to poor dispersion at high loading.

2.6.4 Interfacial interactions and reinforcement

Several explanations have been given about the reinforcement properties of the polymer clay nanocomposites based on the interfacial properties and restricted mobility of the polymer chains. Shi et al. [61] proposed that the direct bonding of polymer to clay layers

would be the dominant factor. Another group of researchers [55] systematically designed the interfacial strength for an epoxy clay system and studied its effect on mechanical, thermal and fracture properties. The strong interface system created by the reactive surfactant that can bridge between the layers and matrix produced best mechanical properties compared to the low strength and normal interface system. Kojima et al.[62] proposed an explanation that the formation of constrained region in the vicinity of the layers where polymer chains have constrained mobility contributes to the modulus.

However, still the understanding about the mechanics of nanocomposites is not well established and it is not so straight forward to fix a single mechanism for the reinforcing effect. It is a widely held view that the reinforcing effect of the nanofillers will appear if the nanoparticles are finely dispersed in the matrix and well coupled to the polymer molecules. If the bulk mechanical properties are not improved it is stated that the dispersion is not good enough or the interfacial bonding is not strong. However, these statements are not always self-evident, even well dispersed nanofillers naturally aggregate to form clusters. The large scale aggregated character of the nanofillers is a big obstacle in the nanocomposite technology and perceived as the most important factor that compromises the nanocomposites mechanical performance [63, 64].

2.6.5 Thermal and dynamic properties

Epoxy/clay nanocomposites have also exhibited improvement in fire resistance properties [65-67]. The effect of clay on glass transition temperature is not clear and mixed results with increase, decrease and neutral effects have been reported [14, 37, 52, 68].

2.6.6 High temperature-resistant thermoset nanocomposites

A few studies have been reported based on high temperature-resistant thermosetting matrices nanocomposites [69-71]. PMR-type polyimides are highly thermally stable and have been used in aerospace composite applications where reliability and durability are critical concerns. Abdalla et al. [69] synthesized polyimide PMR-15/clay nanocomposites with both organically modified and unmodified clay. An intercalated structure was formed. A significant improvement in thermal and mechanical properties was observed with 2.5 wt % loading of modified clay without reduction in elongation at break. However, thermal stability of the organic modifier is one of the main concerns for the preparation of high temperature-

resistant polyimide/clay nanocomposites. The ammonium based surfactants used for the modification of clay have shown the degradation well below the cross linking temperature of polyimide (e.g. PMR-15 curing temperature is 316 °C). Due to the processing difficulties and high processing cost of high temperature polyimides continuous efforts are under way to modify the chemistry of polyimides and find alternatives [72].

Meng et al. [71] synthesized Bismaleimide organo clay nanocomposites and investigated the effect of processing method, conditions and modifier on the exfoliation process of the clay layers. The combination of insitu polymerization method, compatible modifier and initially prolonged low temperature curing produced best exfoliation results up to 2 wt% of clay. The impact strength was significantly improved for exfoliated organoclay nanocomposites. A group of researchers [73] showed an improvement in the wear resistance for bismaleimide/carbon nanotubes composites up to 2 wt%. Yan et al. [74] synthesized a modified low viscosity bismaleimide and functionalized silica nanoparticles composites. The impact and flexural strength improved significantly. Storage modulus at room temperature also increased but glass transition temperature decreased.

2.7 Issues of thermoset nanocomposites

Although superior properties have been reported for thermoset nanocomposites but many difficulties appear for manufacturing nanocomposite materials. The potentials of the nanostructured materials have not been fully translated into macroscopic properties and the successful commercialization is still far away. Many issues concerning the control of nanocomposite structure and understanding of structure-property relationship in order to obtain the desired property enhancement are unsolved, which limit the industrial applications. All these problems ask for intensive research in the field of nanocomposite synthesis, characterization and applications.

The following main points may be derived based on a detailed review of the literature on thermoset nanocomposites:

- The desired nanocomposite structure (complete exfoliation) is difficult to control. A relatively lower level of exfoliation has been obtained for thermoset nanocomposites compared to thermoplastic nanocomposites. Dispersion of nanofillers is a serious concern as the nanofillers have to be dispersed well before the curing starts.
- Thermoset nanocomposites are quite programmable materials and a number of variables are involved in determining the structure and properties. Technological

difficulties exist related to the programmable choice of a surface organic modifier, curing agent and processing conditions.

- Fast and easy methods are needed for the preparation of thermoset nanocomposites to make it commercially attractive and for larger volume production.
- Quick and reliable characterization techniques are needed to characterize the nanofiller/resin dispersion at an early stage of nanocomposite preparation. The macroscopic rheological methods need to be proved in nanodispersions for characterization of the degree of dispersivity, and the polymer particle and particle – particle interactions.

- Improved knowledge of structure- property relationship is required to develop the fundamental understanding of the enhancement of nanocomposites properties.

- The use of nano-filler based matrix seems to be a promising novel concept in fibre reinforced composite technology and it is not well investigated. So it is needed to pay attention to investigate the hybrid nanofilled fiber composites in detail.

Many research potentials can be identified from the above listed issues of thermoset nanocomposites. However, keeping in view the demand for high temperature-resistant thermosetting matrices in advanced composites and scarcity of research dealing with the nanocpmposites based on theses matrices, we were motivated to study the high-temperature resistant thermoset nanocomposites.

2.8 References

[1] Mittal V. Polymer layered silicate nanocomposites: A Review. Materials. 2009;2(3):992-1057.

[2] Vlasveld DPN. Fiber reinforced polymer nanocomposites PhD. Delft University of Technology, PhD Thesis, 2005.

[3] Hussain F, Hojati M, Okamoto M, E.Gorga R. Review article: Polymer-matrix Nanocomposites, Processing, Manufacturing,and Application:An Overview. J Comp Mat. 2006;40(17):1511-1575.

[4] Ray SS, Okamoto M. Polymer/layered silicate nanocomposites: A review from preparation to processing. Prog Poly Sci. 2003;28 (11):1539–1641.

[5] Wu SH, Wang FY, Ma CCM, Chang WC, Kuo CT, Kuan HC, et al. Mechanical, thermal and morphological properties of glass fiber and carbon fiber reinforced polyamide-6 and polyamide-6/clay nanocomposites. Mat Lett. 2001;49(6):327-333.

[6] Alexandre M, Dubois P. Polymer-layered silicate nanocomposites: preparation, properties and uses of a new class of materials. Materials Science and Engineering 2000;28(1-2):1-63.

[7] Pavlidou S, Papaspyrides CD. A review on polymer layered silicate nanocomposites. Prog Poly Sci. 2008;33(12):1119-1198.

[8] Fornes TD, Paul DR. Modeling properties of nylon 6/clay nanocomposites using composite theories. Polymer. 2003;44(17):4993-5013.

[9] E. Manias, A. Touny, L. Wu, K. Strawhecker, B. Lu, Chung TC. Polypropylene/montmorillonite nanocomposites. Review of the synthetic routes and materials properties. Chem Mater. 2001;13(10):3516-3523.

[10] Százdi L, Ábrányi Á, Jr BP, Vancso JG, Pukánszky B. Morphology characterization of PP/clay nanocomposites across the length scales of the structural architecture. Macromolecular Materials and Engineering. 2006;291(7):858-868.

[11] Dominkovics Z. Polymer/layered silicate nanocomposites: structure formation, interactions and deformation mechanisms. Budapest University of Technology and Economics, PhD Thesis, 2011.

[12] Heidarian M, Shishesaz MR, Kassiriha SM, Nematollahi M. Study on the effect of ultrasonication time on transport properties of polyurethane/organoclay nanocomposite coatings. Journal of Coatings Technology and Research. 2011;8(2):265-274.

[13] Liu WP, Hoa SV, Pugh M. Fracture toughness and water uptake of high-performance epoxy/nanoclay nanocomposites. Comp Sci Tech. 2005;65(15-16):2364-2373.

[14] Ngo TD, Ton-That MT, Hoa SV, Cole KC. Preparation and properties of epoxy nanocomposites. Part 2: The effect of dispersion and intercalation/exfoliation of organoclay on mechanical properties. Poly Eng Sci. 2012;52(3):607-614.

[15] Bharadwaj RK, Mehrabi AR, Hamilton C, Trujillo C, Murga M, Fan R, et al. Structure-property relationships in cross-linked polyester-clay nanocomposites. Polymer. 2002;43(13):3699-3705.

[16] Hari J, Dominkovics Z, Fekete E, Pukanszky B. Kinetics of structure formation in PP/layered silicate nanocomposites. Express Polymer Letters. 2009;3(11):692-702.

[17] Liu XH, Wu QJ. PP/clay nanocomposites prepared by grafting-melt intercalation. Polymer. 2001;42(25):10013-10019.

[18] Arora A, Choudhary V, Sharma DK. Effect of clay content and clay/surfactant on the mechanical, thermal and barrier properties of polystyrene/organoclay nanocomposites. J Poly Res. 2011;18(4):843-857.

[19] Chavarria F, Shah RK, Hunter DL, Paul DR. Effect of melt processing conditions on the morphology and properties of nylon 6 nanocomposites. Poly Eng Sci. 2007;47(11):1847-1864.

[20] Stepto RFT. Polymer networks : Principles of their formation structure and properties. London: Blackie Academic&Professional; 1998.

[21] Prime RB. Thermosets. In: Turi EA, editor. Thermal characterization of polymeric materials, vol. 2 San Diego: Academic Press; 1997. p. 2420.

[22] Nair CPR, Mathew D, Ninan KN. Cyanate ester resins, recent developments. In: Abe A, Albertsson AC, Cantow HJ, Dusek K, Edwards S, Hocker H, et al., editors. New Polymerization Techniques and Synthetic Methodologies, vol. 1552001. p. 1-99.

[23] Mangalgiri PD. Polymer-matrix composites for high-temperature applications. Defence Science Journal. 2005;55(2):175-193.

[24] Ratna D. Handbook of thermoset resins: Smithers Rapra Technology 2009.

[25] Gu AJ, Liang GZ, Lan LW. A high-performance bismaleimide resin with good processing characteristics. J App Poly Sci. 1996;62(5):799-803.

[26] Ursache O, Gaina C, Gaina V, Musteata VE. High performance bismaleimide resins modified by novel allyl compounds based on polytriazoles. J Poly Res. 2012;19(10):9968-9968.

[27] Huang P, Gu A, Liang G, Yuan L. High-Performance Hyperbranched Poly(phenylene oxide) Modified Bismaleimide Resin with High Thermal Stability, Low Dielectric Constant and Loss. J App Poly Sci. 2011;120(1):451-457.

[28] Cristea M, Gaina C, Ionita DG, Gaina V. Dynamic mechanical analysis on modified bismaleimide resins. J Ther Anal Calo. 2008;93(1):69-76.

[29] Hamerton I. High-performance thermoset-thermoset polymer blends:a review of the chemistry of cyanate ester-bismaleimide blends. High Perfor Polym. 1996;8:83-95.

[30] Lan T, Pinnavaia TJ. Clay reinforced epoxy nanocomposites. Chem Mater. 1994;6:2216-2219.

[31] Lan T, Kaviratna PD, Pinnavaia TJ. Mechanism of clay tactoid exfoliation in epoxy clay nanocomposites. Chem Mater. 1995;7(11):2144-2150.

[32] Wang Z, Pinnavaia TJ. Hybrid organic-inorganic nanocomposites: Exfoliation of magadiite nanolayers in an elastomeric epoxy polymer. Chem Mater. 1998;10(7):1820-1826.

[33] Park JH, Jana SC. Mechanism of exfoliation of nanoclay particles in epoxy-clay nanocomposites. Macromo. 2003;36(8):2758-2768.

[34] Kornmann X, Lindberg H, Berglund LA. Synthesis of epoxy-clay nanocomposites: influence of the nature of the clay on structure. Polymer. 2001;42(4):1303-1310.

[35] Kornmann X, Lindberg H, Berglund LA. Synthesis of epoxy-clay nanocomposites. Influence of the nature of the curing agent on structure. Polymer. 2001;42(10):4493-4499.

[36] Boukerrou A, Duchet J, Fellahi S, Djidjelli H, Kaci M, Sautereau H. Synthesis and characterization of rubbery epoxy/organoclay hectorite nanocomposites. Express Polymer Letters. 2007;1(12):824-830.

[37] Mouloud A, Cherif R, Fellahi S, Grohens Y, Pillin I. Study of morphological and mechanical performance of amine-cured glassy epoxy-clay nanocomposites. J App Poly Sci. 2012;124(6):4729-4739.

[38] Mittal V. Epoxy-layered silicate nanocomposites: effect of cross-linking amines and fillers on curing, morphology and oxygen permeation. Journal of Reinforced Plastics and Composites. 2012;31(11):739-747.

[39] Wang Q, Song CF, Lin WW. Study of the exfoliation process of epoxy-clay nanocomposites by different curing agents. J App Poly Sci. 2003;90(2):511-517.

[40] M.S.Wang, Pinnavaia TJ. Clay polymer nanocomposites formed from acidic derivatives of montmorillonite and an epoxy resin. Chem Mater. 1994;6(4):468-474.

[41] Chin IJ, Thurn-Albrecht T, Kim HC, Russell TP, Wang J. On exfoliation of montmorillonite in epoxy. Polymer. 2001;42(13):5947-5952.

[42] Tolle TB, Anderson DP. Morphology development in layered silicate thermoset nanocomposites

Comp Sci Tech. 2002;62:1033-1041.

[43] Lu JK, Ke YC, Qi ZN, Yi XS. Study on intercalation and exfoliation behavior of organoclays in epoxy resin. Journal of Polymer Science Part B-Polymer Physics. 2001;39(1):115-120.

[44] Tolle TB, Anderson DP. The role of preconditioning on morphology development in layered silicate thermoset nanocomposites. J App Poly Sci. 2004;91(1):89-100.

[45] Pustkova P, Hutchinson JM, Roman F, Montserrat S. Homopolymerization effects in polymer layered silicate nanocomposites based upon epoxy resin: Implications for exfoliation. J App Poly Sci. 2009;114(2):1040-1047.

[46] Chen C, Benson-Tolle T, Baur JW, Putthanarat S. Processing - Morphology regulation of epoxy/layered-silicate nanocomposites. J App Poly Sci. 2008;108(5):3324-3333.

[47] Yasmin A, Luo JJ, Daniel IM. Processing of expanded graphite reinforced polymer nanocomposites. Comp Sci Tech. 2006;66(9):1182-1189.

[48] Wang Z, Pinnavaia TJ. Nanolayer reinforcement of elastomeric polyurethane. Chem Mater. 1998;10(12):3769-+.

[49] Lipinska M, Hutchinson JM. Elastomeric epoxy nanocomposites: Nanostructure and properties. Comp Sci Tech. 2012;72(5):640-646.

[50] Nigam V, Soni H, Saroop M, Verma GL, Bhattacharya AS, Setua DK. Thermal, morphological, and X-ray study of polymer-clay nanocomposites. J App Poly Sci. 2012;124(4):3236-3244.

[51] Kinloch AJ, A.C.Taylor. The mechanical properties and fracture behavior of epoxy-inorganic micro-and nano-composites. J Mat Sci. 2006;41(11):3271-3297.

[52] Liu WP, Hoa SV, Pugh M. Organoclay-modified high performance epoxy nanocomposites. Comp Sci Tech. 2005;65(2):307-316.

[53] Yasmin A, Abot JL, Daniel IM. Processing of clay/epoxy nanocomposites by shear mixing. Scripta Materialia. 2003;49(1):81-86.

[54] Isik I, Yilmazer U, Bayram G. Impact modified epoxy/montmorillonite nanocomposites: synthesis and characterization. Polymer. 2003;44(20):6371-6377.

[55] Zaman I, Le Q-H, Kuan H-C, Kawashima N, Luong L, Gerson A, et al. Interface-tuned epoxy/clay nanocomposites. Polymer. 2011;52(2):497-504.

[56] Khanbabaei G, Aalaie J, Rahmatpour A, Khoshniyat A, Gharabadian MA. Preparation and properties of epoxy-clay nanocomposites. Journal of Macromolecular Science Part B-Physics. 2007;46(5):975-986.

[57] Wang MS, Pinnavaia TJ. Clay polymer nanocomposites formed from acidid derivatives of montmorillonite and an epoxy resin. Chem Mater. 1994;6(4):468-474.

[58] Kornmann X, Berglund LA, Sterte J. Nanocomposites based on montmorillonite and unsaturated polyester. Poly Eng Sci. 1998;38(8):1351-1358.

[59] Dalir H, Farahani RD, Nhim V, Samson B, Levesque M, Therriault D. Preparation of highly exfoliated polyester-clay nanocomposites: process-property correlations. Langmuir. 2012;28(1):791-803.

[60] Joulazadeh M, Navarchian AH. Study on elastic modulus of crosslinked polyurethane/organoclay nanocomposites. Poly Adv Tech. 2011;22(12):2022-2031.

[61] Shi HZ, Lan T, Pinnavaia TJ. Interfacial effects on the reinforcement properties of polymer-organoclay nanocomposites. Chem Mater. 1996;8(8):1584-&.

[62] Kojima Y, Usuki A, Kawasumi M, Okada A, Fukushima Y, Kurauchi T, et al. Mechanical properties of NYLON 6-clay hybrid. J Mat Res. 1993;8(5):1185-1189.

[63] Schaefer DW, Justice RS. How nano are nanocomposites? Macromo. 2007;40(24):8501-8517.

[64] Starkova O, Buschhorn ST, Mannov E, Schulte K, Aniskevich A. Creep and recovery of epoxy/MWCNT nanocomposites. Composites Part a-Applied Science and Manufacturing. 2012;43(8):1212-1218.

[65] Wu GM, Schartel B, Bahr H, Kleemeier M, Yu D, Hartwig A. Experimental and quantitative assessment of flame retardancy by the shielding effect in layered silicate epoxy nanocomposites. Combustion and Flame. 2012;159(12):3616-3623.

[66] Schartel B, Weiss A, Sturm H, Kleemeier M, Hartwig A, Vogt C, et al. Layered silicate epoxy nanocomposites: formation of the inorganic-carbonaceous fire protection layer. Poly Adv Tech. 2011;22(12):1581-1592.

[67] Katsoulis C, Kandare E, Kandola BK. The effect of nanoparticles on structural morphology, thermal and flammability properties of two epoxy resins with different functionalities. Poly Deg Stab. 2011;96(4):529-540.

[68] Marouf BT, Bagheri R, Pearson RA. Observation of two alpha-relaxation peaks in a nanoclay-filled epoxy compound. J Mat Sci. 2008;43(21):6992-6997.

[69] Abdalla MO, Dean D, Campbell S. Viscoelastic and mechanical properties of thermoset PMR-type polyimide-clay nanocomposites. Polymer. 2002;43(22):5887-5893.

[70] Gintert MJ, Jana SC, Miller SG. A novel strategy for nanoclay exfoliation in thermoset polyimide nanocomposite systems. Polymer. 2007;48(14):4166-4173.

[71] Meng HR, Hu X. Synthesis and exfoliation of bismaleimide-organoclay nanocomposites. Polymer. 2004;45(26):9011-9018.

[72] Dean D, Abdalla MA, Vaidya U, Ganguli R, Battle CJ, Abdalla M, et al. Processable PMR-type polyimides: process-property relationships, curing kinetics, and thermooxidative stability. High Perfor Polym. 2005;17(4):497-514.

[73] Liu L, Fang Z, Gu A, Guo Z. Aminofunctionalization effect on microtribological behavior of carbon nanotube/bismaleimide nanocomposites. J App Poly Sci. 2009;113(6):3484-3491.

[74] Yan H, Li P, Zhang J, Ning R. Mechanical properties of novel bismaleimide nanocomposites with Si3N4 nanoparticles. Journal of Reinforced Plastics and Composites. 2010;29(10):1515-1522.

Chapter 3

Synthesis of Carbon Nanofiber Filled Composites: Thermal, Morphological and Mechanical Characterization

Abstract[1]

In this chapter we report the synthesis, thermo-mechanical properties and fractography studies of carbon nanofiber (CNF) filled bismaleimide nanocomposites. High shear thermo-kinetic mixing technique was applied to prepare thermoset nanocomposites, innovative in nature as normally used for thermoplastics. The thermal and mechanical properties of composites containing 1 wt% and 2 wt% CNFs were investigated by tensile testing, dynamic mechanical analysis, thermogravemetric analysis, and flame testing methods. Thermogravimetric analysis (TGA) demonstrated a modest improvement in thermal stability of the matrix was obtained by the addition of CNFs. A moderate increase in storage modulus and glass transition temperature (T_g) of the matrix was obtained upon the incorporation of CNF. Fractographic analyses of the composites were carried out by scanning electron microscopy (SEM) to determine the failure mechanism. In general a fairly well dispersion was observed, along with agglomeration at some points and fibre matrix interfacial debonding. The reduction in tensile strength for nanocomposites was attributed to the poor adhesion of the fibres with the matrix.

3.1 Introduction

In recent years, polymer nanocomposites have received immense attention owing to many competitive advantages like high strength, high stiffness, thermal stability, electrical and thermal conductivity. The incorporation of nanoparticles, such as carbon nanotubes and nanoclays, have shown to produce remarkable improvements in mechanical and physical

[1] Parts of this chapter have been published in : M.I.Faraz, S.Bhowmik, C.De Ruijter, F.Lautid, R.Benedictus and Ph.Dubois, J.App.Poly.Sci., 2010, 117, 2159-2167

properties of polymers [1-7]. Therefore, at present, the addition of nanoparticles is seen as a potential method for tailoring polymer properties to desired applications.

The discovery of carbon nanotubes has generated significant attention in the field of material science due to their exceptional mechanical, electrical, and thermal properties. Tensile moduli and strength values, ranging from 270 GPa to 1TPa and 11-200 GPa respectively, have been reported for carbon nanotubes[8, 9]. This outstanding strength makes it a hundred times stronger than steel at one sixth of the weight[10]. Carbon nanotubes (CNT) are categorized into single-wall (SWNT), multi-wall (MWNT) nanotubes and carbon nanofiber (CNF) depending upon their diameter. Carbon nanofiber has diameter ranging about 60-200 nm whereas SWNT and MWNT have 0.7-1.5 nm and 10-50 nm respectively [11].

Fibre reinforced composites are widely used in aerospace, civil and military applications due to their high specific strength. It is greatly desired that structural composites must perform well in the harsh multifactor environment. Potential applications of polymer composites in the fields of aerospace, electronic hardware, and automobiles are placing demands for materials with higher thermal stability, higher electrical and thermal conductivity, and improved electromagnetic transparency. Due to the exceptional nanoscale behaviour of CNFs in each of these areas, it is plausible that the behaviour of polymeric composites could be improved through the addition of CFNs. Carbon nanofibers were selected as filler for the present investigations by virtue of their outstanding performance with respect to the above mentioned challenges. Carbon nanofibers were selected in favour to CNTs because they can be produced industrially at low cost and high production volume [12]. The use of CNFs within thermoplastics has been shown to improve performance by several researchers [11, 13-16]. Ghose et al. have fabricated CNF composites with high temperature polyimide (PETI 330) for high performance applications. Thermal and electrical conductivity were improved but voids were found in the samples, so mechanical properties were not improved [17].

This study was aimed at preparation of high temperature-resistant thermoset nanocomposite so the selection of the matrix was of utmost importance. It is reported that polyimides are excellent high temperature resins for high performance composites. However, their processability, and void formation due to volatiles is still a problem to be addressed. A subclass of polymides known as, Bismaleimides have a high stability at high temperatures and good hot/wet performance, and have attracted attention in the advanced composite industry due to their high performance to cost ratio. It has been demonstrated that Bismaleimides show

retention of properties at elevated temperature, dimensional stability, low shrinkage, and good mechanical strength, as well as, high resistance against various solvents, acids and water [18]. Bismaleimides can be processed under epoxy-like conditions, but excel in physical and mechanical properties compared to epoxy. However, due to a high cross-link density, they are very brittle and have low damage tolerance. Much of the research efforts have emphasized primarily on structural modification to improve toughness, processability and cost [19-25].

A high temperature Bismaleimide pre-polymer, commercially available as “Homide 250”, developed by Hos-Technik, was selected for this study. The presence of rigid maleimide groups and high cross-link density after curing results in high thermal stability with low volatile emissions. Melting point is merely in the range of 90-120 °C which makes processing easier. State of the art literature reveals that only few examples are available on Bismaleimide containing CNT or CNF nanoparticles [26-28]. Therefore, considerable scope remains open for research. In addition, all previous efforts were focussed with two component systems, and solution mixing techniques which are time consuming, high cost, and low output. In the present study, melt blending technique, which is most common for thermoplastics, is attempted by using a high speed thermokinetic mixer, specially designed for handling systems which are difficult to disperse. To our knowledge, this is the first study to examine the use of such a high shearing mixer to disperse carbon nanofibers in BMI.

The objective of this study was to prepare BMI/CNFs composites by a thermokinetic mixing method and examine its thermal and mechanical behaviour. A detailed morphology analysis of fractured surfaces is presented by using scanning electron microscopy (SEM) to investigate failure mechanism, fibre dispersion and CNF/matrix adhesion.

3.2 Experimental

3.2.1 Materials

A pre-polymer of high temperature Bismaleimide under the trade name Homide 250 was purchased from HOS-technik, Austria. Heat treated, vapor grown carbon nanofibers (PR-19-XT-LHT) having average diameter of 150 nm and length of 50 - 200 microns were provided by Pyrograf Products, Inc, USA.

3.2.2 Processing of carbon nanofiber Bismaleimide nanocomposites

Nanocomposites with 1 and 2wt% of carbon nanofiber were prepared by melt compounding process. A high thermokinetic mixer “Gelimat blender”, (Werner and Pfleiderer Gelimat 1-S) thermokinetic mixer was used to prepare the batches. The Gelimat system is specially designed to disperse particles within the polymer by heating, mixing, and compounding, in a period of a few minutes in order to minimize any thermal degradation of the material. High speed rotating blades of the Gelimat accelerate the particles and impart high kinetic energy which is converted to thermal energy upon hitting the walls of chamber. Factors like rotor speed, charge size and material properties dictate compounding time [29].The Gelimat was run at a shaft speed of 2000 rpm (13.8m/s at the tip of the blade) at a temperature of 130 °C. This temperature was selected based on rheological results, since at this temperature the resin is fully melted and has lowest viscosity. At higher temperatures the gel time of BMI decreases rapidly and it starts curing at 160 °C. A quantity of 300g of material was fed into the thermokinetic mixer for each batch, resulting in an output of 265 g after compounding.

Rectangular specimens (dimensions 110x40x3mm) were prepared by compression molding using a 100 Ton Joos press with controlled heating and pressure. The consolidation temperature, pressure, and time were 200 °C, 60 bar and 30 min respectively. After molding they were post-cured at 220 ^{0}C for 10 hrs. Specimens for tensile testing were cut from this moulded bar with dimensions according to ISO-527.

3.3 Characterization

3.3.1 Thermal analysis

Thermal stability of the polymer and nanocomposites was studied by Thermogravimetric analysis (TGA) using a Perkin Elmer Pyris Diamond TG/DTA at a heating rate of 10 °C/min under both nitrogen and air atmosphere from 25 °C to 800 °C. Dynamic mechanical analyses were performed by Perkin Elmer Diamond DMTA, in three point bending mode under a nitrogen atmosphere at a heating rate of 3 °C/min and a frequency of 1HZ from 25 to 300 °C using small rectangular specimen with dimensions of 50x5x3 mm.

3.3.2 Mechanical testing

Tensile tests of the samples were carried out by using a Zwick 20 kN static tensile test machine (model 1455) at a testing speed of 5mm/min according to ISO 527-1. Five specimens were tested for each sample and average tensile strengths are reported.

3.3.3 Fracture characterization

The morphologies of the fractured tensile specimens and CNFs dispersion in the composite samples were evaluated using Scanning Electron Microscopy (SEM) model (Jeol JSM-7500F) operated at an accelerated voltage of 40 kV.

3.3.4 Fire testing

Limiting Oxygen Index (LOI), a standard test method to measure the minimum concentration of oxygen for sustaining candle like downward flame combustion, was measured on specimens 80x10x3mm according to ISO 4589.

3.4 Results and discussion

3.4.1 Gelimat mixing

The excellent dispersing properties of the Gelimat thermokinetic mixer can be used to increase the surface area between the polymer and nanoparticles. High shear stresses generated by the equipment have the potential to breakdown aggregates and disperse the reinforcing particles in the polymer matrix [30]. The influence of carbon nanofiber on the compounding time and energy consumption is shown in Fig. 3.1. The data obtained by the Gelimat run, i.e. energy required (current), induction time (which is the time difference between the moment the blends are inserted into the mixing chamber and the blends have reached the melting point), consolidation time, and other values are summarized in Table 3.1. The current relates to energy required by Gelimat to melt and mix the polymer with additives. The energy required for the 2% CNF composite is the highest, as indicated in table 1. This can be attributed to an increase in viscosity with increasing nanofiber content. The induction time and mixing time of 2% CNF composite is reduced from 670 to 130s and 70 to 42s, respectively as compared to the neat polymer due to the high thermal conductivity of CNFs.

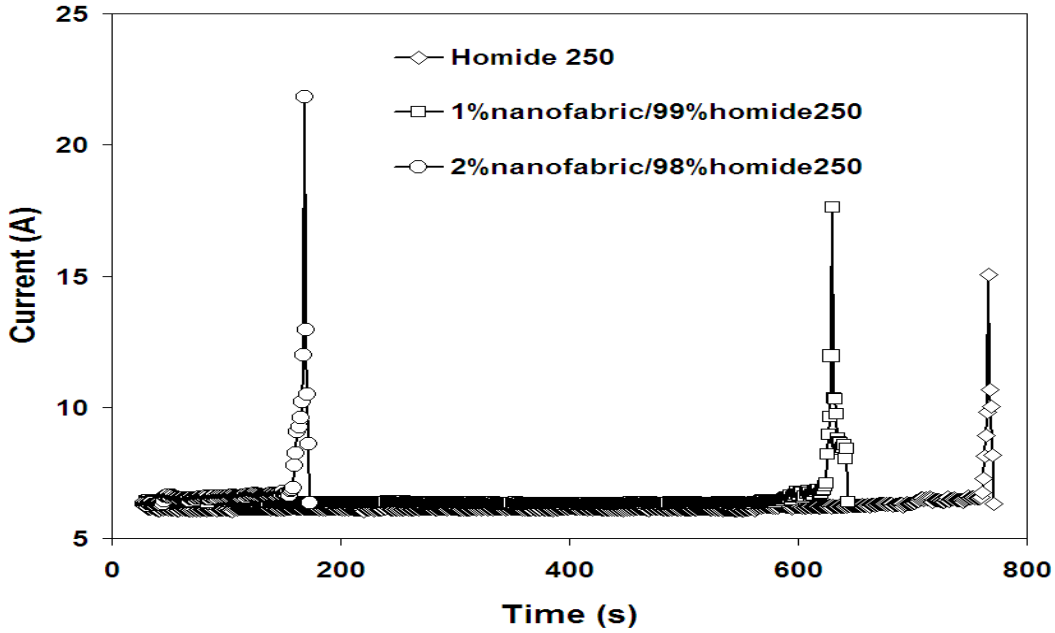

Figure 3.1 Effect on compounding time and energy consumption with the addition of carbon nanofibre in matrix

Table 3.1 Gelimate mixed composites time and current values

Sample CNF	Induction time	Peak time	End time	Max.current
%	Sec	Sec	Sec	A
0	670	736	740	15
1	558	600	604	17.6
2	130	141	172	21.8

3.4.2 Thermal stability and flammability properties

To investigate the decomposition behaviour of the composites thermogravimetric analysis (TGA) was performed both in nitrogen and air. The TGA results are summarised in Table 3.2 and curves are shown in Fig. 3.2 (a) and 3.2 (b) for nitrogen and air respectively. A different behaviour is observed depending on the applied atmosphere (air or nitrogen). Under air, the incorporation of CNFs have an effect on the thermal resistance, i.e. the first decomposition step leads to the formation of more char residue. However, this char is less thermally stable in comparison with that formed during thermal degradation of pristine BMI polymer (Fig. 3.2 b), its degradation is accelerated when CNF are used. This is because once the degradation has

started, the CNFs played the role of a catalyst to accelerate the decomposition due to presence of iron particulates [31]. It can be seen that the TGA curves are quite stable until the onset of decomposition but after that a very rapid decomposition occurs typically in air (Fig. 3.2 b). The char is thermally stable during non oxidative thermal decomposition (Fig. 3.2a). No char is left in air and around 40% char is left in a nitrogen environment. It can be concluded that incorporation of CNFs does not significantly enhance the thermal stability of the corresponding nanocomposite system for the range of fibre concentrations investigated in this study. However, thermal stability is still reasonably high to be acceptable. Kashiwagi et. al. [32] and Zhou et al. [33] have also observed that thermal stability remains insensitive to the incorporation of CNFs. It can be affected by physiochemical bonding states and microstructural features of the composites, including attendant branching and stiffening effects [34], which needs to be investigated further.

Table 3.2 Thermo-mechanical properties of nanocomposites

Sample	$T_{d\ N2}$ ^0C	T_{dair} ^0C	Char %	T_g ^0C	Tensile MPa	Modulus GPa	LOI %
0%	380	379	42	235	72	3.8	27.2
1% CNF	387	381	43	245	61	-	28.8
2% CNF	385	381	44	245	58	4.2	29.2

Char taken at 800°C in nitrogen atmosphere. T_d =decomposition temperature, T_g= glass transition temperature, LOI= limiting oxygen index

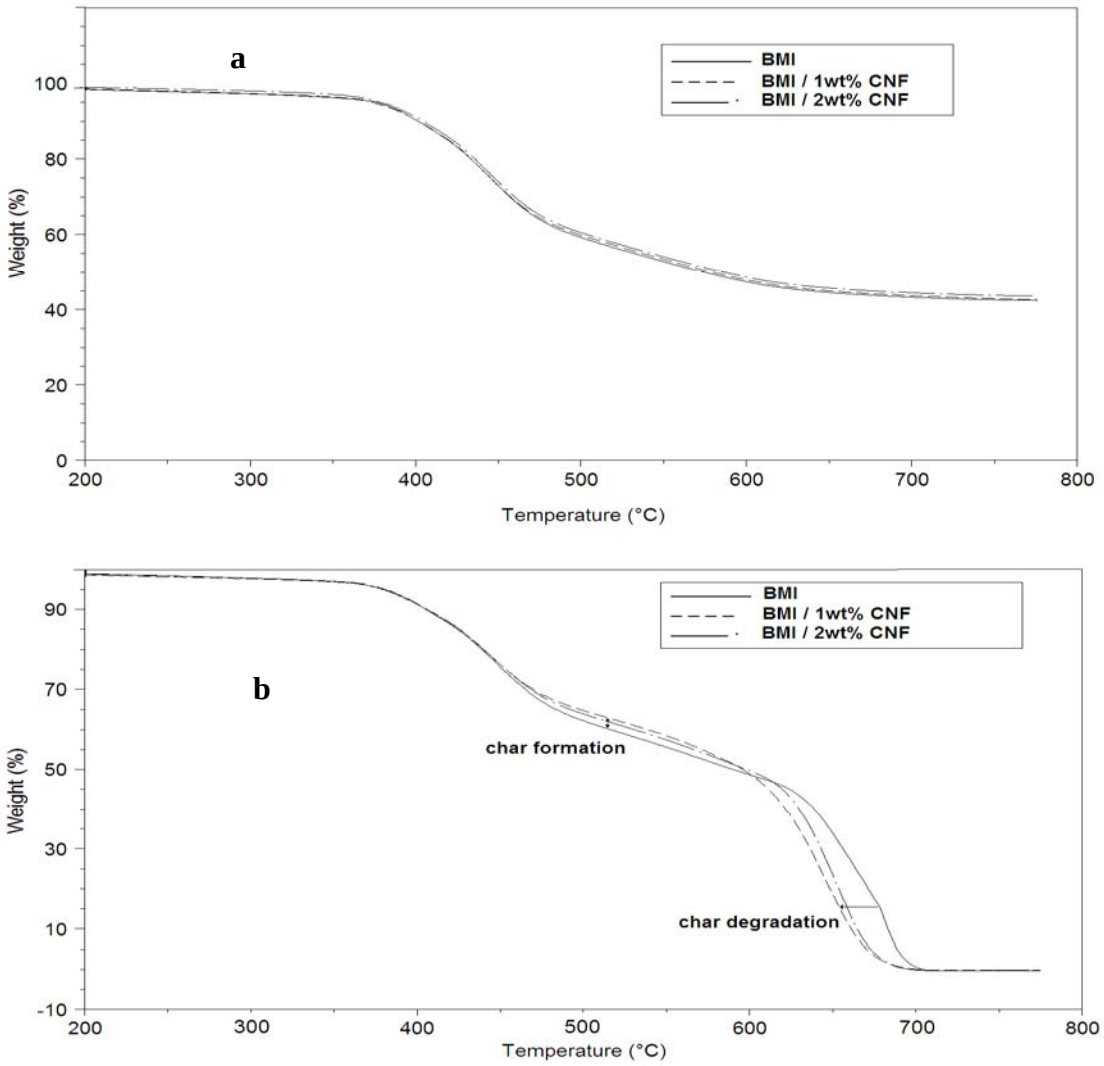

Figure 3.2 TGA curves showing decomposition behavior run under (a) air (b) nitrogen

Limiting Oxygen Index (LOI), is a very common method to assess flammability of polymers. A high value of this index relates to the low flammability and less easily ignited materials. The addition of CNF has increased the LOI value from 27.2 to 29.2 as shown in Table 3.2. This indicates that CNFs also act as flame retardant. The decreased flammability can be attributed to the formation of cohesive char residue [31, 35]. The char left after the TGA run in nitrogen showed a very integrated morphology, free of any cracks, openings and bubbles as is observed by SEM, shown in Fig. 3.3. Moreover, no dripping was observed during burning, reducing fire spread hazard. This char acts as a barrier to prevent the diffusion of heat and gases from the flame through the polymer and stops the fuel, i.e. degraded products, to reach the flame [32, 35]. However, when CNFs only are added to a resin the effect on flame retardancy will not be sufficient to pass the regulatory standards, but in combination with a suitable flame retardant a synergistic effect might be expected [36].

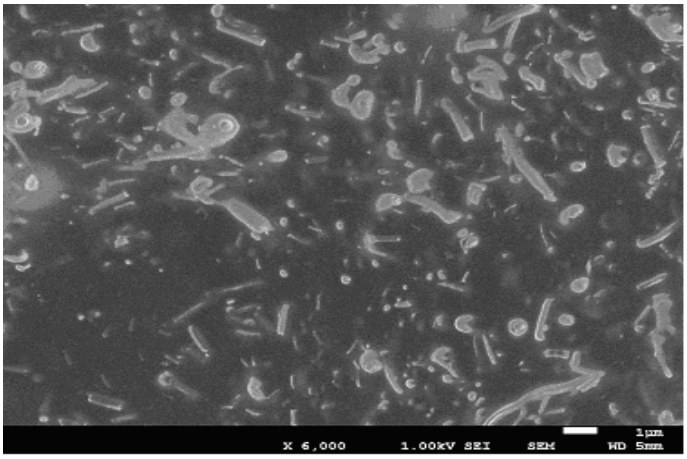

Figure 3.3 SEM image of 2% CNF composite char left after TGA run under nitrogen

Dynamic mechanical analysis has been performed in order to determine the dynamic mechanical properties and viscoelastic behavior. An increase in glass transition temperature (T_g) of about 10°C was observed for the nanocomposites as given in Table 3.2. Glass transition temperatures were determined from the maximum of the loss modulus curves as shown in Fig. 3.4 (b). This increase in T_g could be attributed to constrained chain mobility imposed by rigid CNFs [33, 37]. This conclusion is further supported by increase in storage modulus of the nanocomposites compared to the neat polymer as shown in Fig. 3. 4 (a). The improvement of the storage modulus is more significant above T_g. The storage modulus increased from 1238 MPa to 1900 MPa at 250°C for 2% of CNFs, i.e. an improvement of 53%. The rigid CNF network structure formed may contribute to this stiffness above T_g [38].

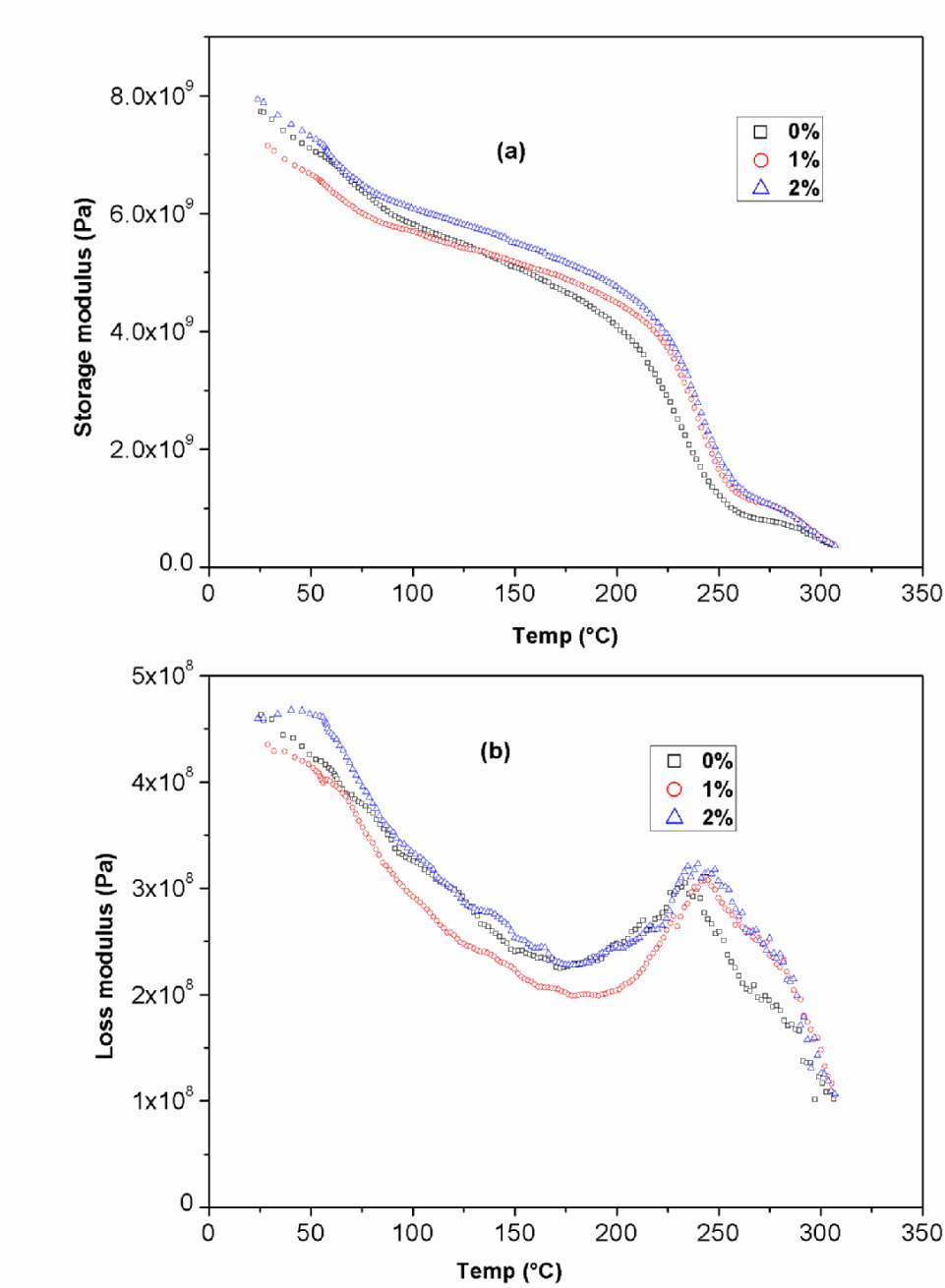

Figure 3.4 DMA curves of nanocomposites (a) storage modulus (b) loss modulus

3.4.3 Mechanical properties

The mechanical properties of the composites depend on many factors, including filler aspect ratio, degree of dispersion, filler-matrix adhesion and some other processing defects. The average tensile strength values for BMI/CNFs composites are reported in Table 3.2. Five specimens were tested for each formulation. All specimens failed in a brittle manner, and no

obvious yield point was found in the tensile curves. A decrease in tensile strength is observed for each composition in comparison to the neat polymer and tensile strength is decreasing with increasing fibre content. There were some fibre bundles observed with 2wt% of CNF as shown in Fig. 3.6(e) by SEM fracture analysis. These fibre bundles may act as stress concentration sites upon loading and result in premature failure. The findings of present investigation is in line with many other researchers, who have also observed that higher concentration of CNFs did not perform well, in terms of mechanical properties which could be due to the formation of voids and other defects [38, 39] and as a consequence results in reduction of the tensile strength. It is also obvious that there is more resistance to deformation in the presence of CNF as can be seen from Fig. 3.6 (a and d). This reduced deformation of nanocomposites is due to the formation of strong cross linking network of CNF with matrix which results in restriction of polymer chain mobility of amorphous phase and hence the reduced flexibility [28, 38, 39].This increase in stiffness is also confirmed by the increase in elastic modulus of the nanocomposites as shown in Table 3.2. Hence carbon nanofibers have reinforcing effect both below and above glass transition temperature. Fibre pull-out effect is dominant for each formulation as shown in Fig. 3.6(c, f and g). The absence of matrix material on the nanofibers together with the presence of voids indicates complete pull-out and can be concluded that there is a weak adhesion between the nanofibers and the matrix. The lower interfacial adhesion results in inefficient load transfer between the fibre and matrix and failure will occur at lower loading [40]. This behaviour has also been observed by other researchers and they have shown that chemical functionalization could be an effective solution to improve the dispersion and adhesion for enhancing stress transfer [28, 38]. Thermal stresses induced during curing of thermosets, due to mismatch of the thermal expansion coefficients of the components mat also affect the mechanical strength.

3.5 Morphological study of BMI/CNF composites

Scanning electron microscopy was used to observe the surface morphology and nanofibre dispersion of tensile fractured surfaces. All the images were taken from crack propagation areas, at different magnifications. Fig.3.5 (a-d) shows SEM images of neat BMI fractured surfaces. The surface close to the initial crack is relatively smooth. Obvious cleavage steps and cleavage plains are observed as shown in Fig. 3.5 (a). Further away from the initial crack the surface appears rougher and matrix tearing takes place (Fig.3.5 b) which could be observed at a higher magnification. A number of small cleavage planes are observed

in rougher surfaces as shown in Fig. 3.5 (c). A smooth and flat surface is observed at higher magnification between the cleavage steps (Fig. 3.5 d) which is showing a typical brittle failure.

In Fig. 3.6 (a-g) fractured surfaces of nanocomposites with 1wt% (a-c) and 2wt% (d-g) of CNFs are shown. The nanocomposites surfaces (Fig. 3.6(a-d) are rougher as compared to the neat matrix. It shows that carbon nanofibers are distorting the crack propagation and more energy is dissipated in fracture. Overall, there is a uniform distribution of CNFs within the polymer matrix at 1wt% as shown in Fig. 3.6 (a-b). However, the nanofibers are broken or pulled out of the matrix and there is no matrix material observed around the fibers as shown in Fig. 3.6 (b-c). This indicates a poor adhesion between the fibers and the matrix. It is also exhibited that at some points, the nanofibers are completely pulled out, and voids are formed as shown by arrows in Fig. 3.6 (c). These voids consume more energy for fracture, and therefore, a more rough surface is observed, although it fails at lower load [28].

At a concentration of 2 wt% of CNFs, at some points bundles are formed, as shown in Fig. 3.6 (e-f) pointed by circles. These bundles act as stress concentration points and result in pre-fracture failure [28, 38]. There is increase in fiber pull-out and debonding at higher loading as shown in Fig. 3.6(f). A more zoomed view of a debonded fiber is shown in Fig.3.6 (g) pointed by an arrow. Therefore, it can be concluded that deboning is the dominant failure mechanism.

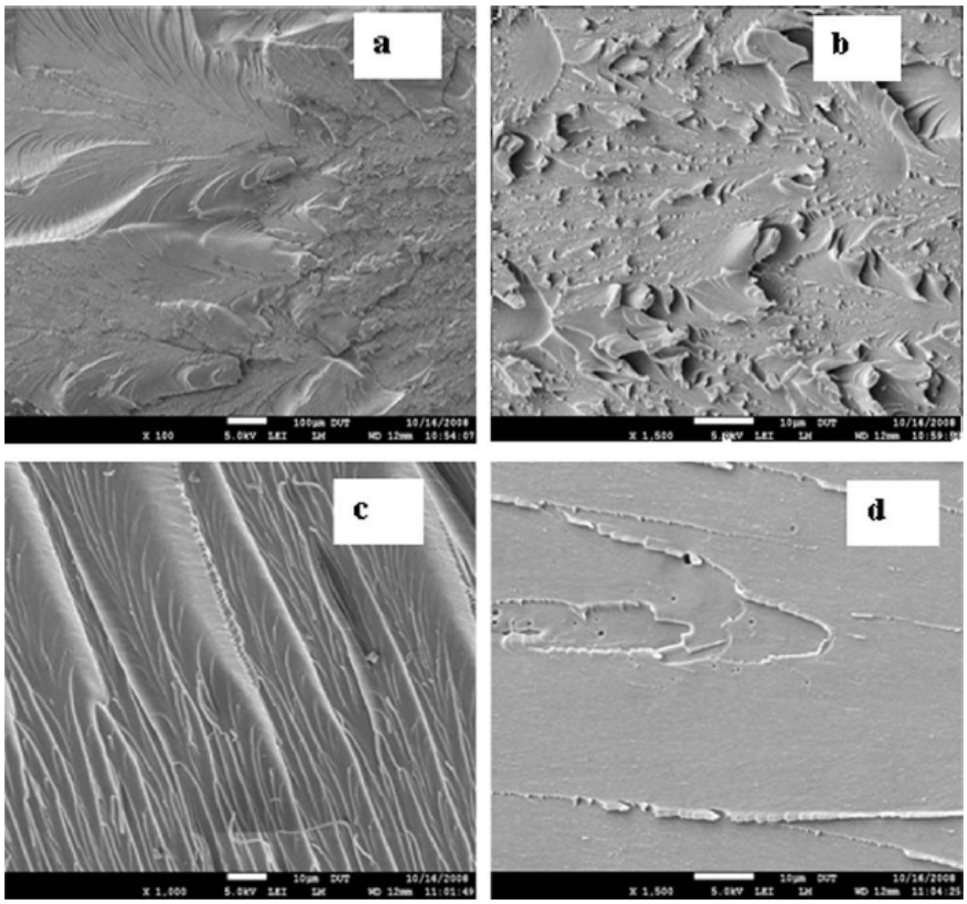

Figure 3.5 SEM images of fractured surface of neat BMI at different locations and magnifications. (a) Fracture initiation (b) Matrix tearing (c) Cleavage planes (d) Brittle failure

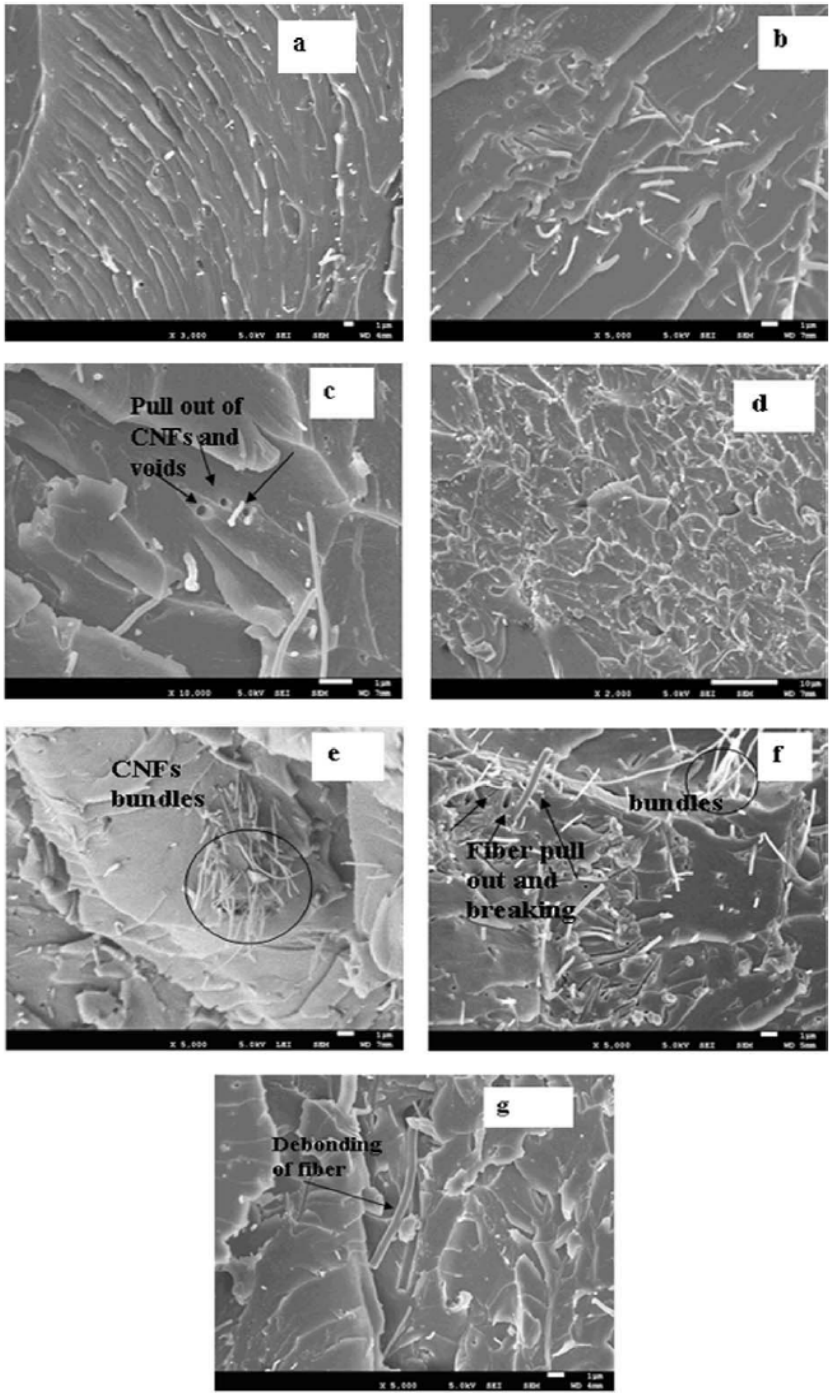

Figure 3.6 SEM images of fractured surfaces of BMI/CNFs nanocomposites containing 1 wt%(a-c) and 2 wt% (d-g) of CNFs, at different locations and magnifications

3.6 Conclusion

A new high temperature-resistant thermoset bismaleimide pre-polymer and carbon nanofiber composites were prepared by melt compounding method using a high shear thermo-

kinetic mixer (Gelimat blender). The approach adopted to mix the CNF with the resin by gelimat blending is very first time applied for the preparation of thermoset nanocomposite and is commonly used for thermoplastics. This technique has the benefits of saving much time and high output rate. A moderate improvement in glass transition temperature and modulus of the matrix obtained by the incorporation of the CNF. The incorporation of CNF also improved the fire resistance of the matrix by the formation of more char residue layer protecting the matrix. The poor adhesion of the fibers with the matrix leads to the reduction in tensile strength of the matrix with the incorporation of the CNF. Fibre bundles are also found in fractured surfaces indicating a poor dispersion quality.

3.7 References

[1] Ray SS, Okamoto M. Polymer/layered silicate nanocomposites: A review from preparation to processing. Prog Poly Sci. 2003;28 (11):1539–1641.

[2] Wanger HD. Nanocomposites Paving the way to stronger materials. Nature Nanotechnology. 2007;2:742-744.

[3] Tai N-H, Yeh M-K, Liu J-H. Enhancement of the mechanical properties of carbon nanotube/phenolic composites using a carbon nanotube network as the reinforcement. Carbon. 2004;42(12-13):2774-2777.

[4] Hammel E, Tang X, Trampert M, Schmitt T, Mauthner K, Eder A, et al. Carbon nanofibers for composite applications. Carbon. 2004;42(5-6):1153-1158.

[5] Njuguna J, Pielichowski K, Desai S. Nanofiller-reinforced polymer nanocomposites. Poly Adv Tech. 2008;19:947-959.

[6] Hackman I, Hollaway L. Durability and mechanical properties of polymer layered silicate nanocomposites. In: Teng Ca, editor. Proceedings of the International Symposium on Bond Behaviour of FRP in Structures, UK: International Institute for FRP in Construction; 2005.

[7] Aravind Dasari, Szu-Hui Lim, Zhong-Zhen Yu, Mai Y-W. Toughening, thermal stability, flame retardancy, and scratch–wear resistance of polymer–clay nanocomposites. Aus J Chem. 2007;60: 496–518.

[8] Li F, Cheng HM, Bai S, Su G. Tensile strength of single-walled carbon nanotubes directly measured from their macroscopic ropes. App Phy Lett. 2000;77(20):3161-3163.

[9] Lu JP. Elastic properties of single and multilayered nanotubes The J Phy Chem Soli. 1997;58(11):1649-1652.

[10] Lau K-T, Hui D. The revolutionary creation of new advanced materials—carbon nanotube composites. Compo Par B. 2002;33:263-277.

[11] Zeng J, Saltysiak B, Johnson WS, Schiraldi DA, Kumar S. Processing and properties of poly(methyl methacrylate)/carbon nano fiber composites. Composites: Part B 2004;35(2): 173–178.

[12] Thostenson ET, Li C, Chou T-W. Review : Nanocomposites in context. Comp Sci Tech. 2005;65(3-4):491-516.

[13] Coopera CA, Ravicha D, Lipsb D, Mayerb J, Wagnera HD. Distribution and alignment of carbon nanotubes and nanofibrils in a polymer matrix. Comp Sci Tech. 2002;62 (7-8):1105–1112

[14] Carneiro S, Covas JA, Bernardo CA, G. Caldeira, F. W. J. Van Hattum, J.-M. Ting, et al. Production and assesment of polycarbonate composites reinforced withvapour-grown carbon fibers. Comp Sci Tech. 1998;58:401-447.

[15] J.Kuriger R, Alam MK, P.Anderson D, L.Jacobsen R.
Processing and chracterization of aligned vapour grown carbon fiber reinforced polypropylene. Compsites Part A. 2002;33:53-62.

[16] Sui G, Zhong WH, Ren X, X.Q.Wang, Yang XP. Structure, mechanical properties and friction behavior of UHMWPE/HDPE/carbon nanofibers. Mat Chem Phy. 2009;115: 404–412.

[17] Ghose S, Watson KA, Working DC, Siochi EJ, Connell JW, Criss JM. Fabrication and chracterization of high temperature resin/carbon nanofiber composites. High Perfor Polym. 2006;18:527-544.

[18] Hamerton I. High-performance thermoset-thermoset polymer blends:a review of the chemistry of cyanate ester-bismaleimide blends. High Perfor Polym. 1996;8:83-95.

[19] Stenzenberger HD. Recent developments of thermosetting polymers for advanced composites. Comp Struc. 1993;24:219-231.

[20] Cai Y, Liu P, Hu X, Wang D, Xu D. Microstructure-tensile properties relationships of polyurethane/poly(urethane-modified bismaleimide–bismaleimide) interpenetrating polymer networks. Polymer. 2000;41:5653-5660.

[21] Hsiao S-H, Chang C-F. Syntheses and thermal properties of ether-containing bismaleimides and their cured resins. J Poly Res. 1996;3:31-37.

[22] Liu Y-L, Chen Y-J. Novel thermosetting resins based on 4-(N_maleimidophenyl) glycidylether:II.Bismaleimides and polybismaleimides. Polymer 45 (2004) 1797–1804. 2004;45:1797-1804.

[23] K. Dinakaran, Alagar M, Kumar RS. Preparation and characterization of bismaleimide/1,3-dicyanatobenzene modified epoxy intercrosslinked matrices. Eur Polym J. 2003; 39 2225–2233.

[24] Nair CPR. Advances in addition-cure phenolic resins. Prog Poly Sci. 2004;29: 401–498.

[25] Gu A, Liang G, Lan L. A high performance bismaleimide resin with good processing characteristics. J App Poly Sci. 1996;62:799-803.

[26] Liu L, Gu A, Fang Z, Tong L, Xu Z. The effects of the variations of carbon nanotubes on the micro-tribological behavior of carbon nanotubes/bismaleimide nanocomposite. Composites: Part A 2007; 38 1957–1964.

[27] Aijuan Gu, Liang G, Liang D, Ni M. Bismaleimide/carbon nanotube hybrids for potential aerospace application: I. Static and dynamic mechanical properties. Poly Adv Tech. 2007; 18(10): 835–840.

[28] Prolongo SG, Campo M, Gude MR, Chaos-Moran R, Urena A. Thermo-physical characterisation of epoxy resin reinforced by amino-functionalized carbon nanofibers. Comp Sci Tech. 2009;69(3-4):349-357.

[29] T. G. Gopakumar, Page DJYS. Compounding of nanocomposites by thermokinetic mixing. J App Poly Sci. 2005;96(5):1557-1563.

[30] Gopakumar TG, Page DJYS. Polypropylene/Graphite nanocomposites by thermo-kinetic mixing. Poly Eng Sci. 2004;44(6):1162-1169.

[31] Takashi Kashiwagi, Erik Grulke, Jenny Hilding, Richard Haris, Award W, Douglas J. Thermal degradation and flammability properties of Poly(propylene)/carbon nanotube composites. Macrom Rap Comm. 2002;23:761-765.

[32] Takashi Kashiwagi, Minfang Mu, Karen Winey, Bani Cipriano, S.R. Raghavan, Seongchan Pack, et al. Relation between the viscoelastic and flammability properties of polymer nanocomposites. Polymer. 2008;49(4358–4368):4358.

[33] Zhou Y, Pervin F, Jeelani S. Effect vapor grown carbon nanofiber on thermal and mechanical properties of epoxy. J Mat Sci. 2007;42(17):7544-7553.

[34] Seo M-K, Park S-J. Thermomechanical properties of graphite nanofiber/poly(methyl methacrylate) composites. Mat Sci Eng A. 2009;508(1-2):28-32.

[35] Kashiwagi T, Fangming Du, Winey KI, Groth KM, Shields JR, Bellayer SP, et al. Flammability properties of polymer nanocomposites with single-walled carbon nanotubes: effects of nanotube dispersion and concentration. Polymer. 2005;46:471-481.

[36] Ye L, Wu Q, Qu B. Synergistic effects and mechanism of multiwalled carbon nanotubes with magnesium hydroxide in halogen-free flame retardant EVA/MH/MWNT nanocomposites Poly Deg Stab. 2009;94(5):751-756.

[37] F.T.Fisher, A.Eitan, R.Andrews, L.S.Schadler, L.C.Brinson. Spectral response and effective viscoelastic properties of MWNT-reinforced polycorbonate. Adv Comp Lett. 2004;13(2):105-111.

[38] S. Kumara, T. Rath , R.N. Mahaling, C.S. Reddya, C.K. Dasa, K.N. Pandey, et al. Study on mechanical, morphological and electrical properties of carbon nanofiber/polyetherimide composites. Mat Sci Eng B. 2007;141(1-2):61-70.

[39] Lozano K, Barrera EV. Nanofiber-Reinforced Thermoplastic Composites. I.Thermoanalytical and Mechanical Analyses. J App Poly Sci. 2001;79(1):125-133.

[40] Schadler LS, Giannaris SC, Ajayana PM. Load transfer in carbon nanotube epoxy composites. App Phy Lett. 1998;73(26):3842-3844.

Chapter 4

Probing the Development and Viscoelastic Properties of Organo-Clay Dispersions

Abstract

In this chapter we report the rheological characteristics and development of organoclay dispersions in nonpolar organic solvent. The development over time of the dispersions with various clay concentrations was examined by rheometry, applying small-amplitude oscillatory deformation. The dispersions exhibit an evolution with distinct stages. After a lag phase, the dynamic moduli grow as a function of time according to power laws. Dispersions with clay concentrations below a threshold value, which seems to coincide with a particle overlap concentration, are initially predominantly viscous but develop over time into predominantly elastic systems. Above this critical threshold concentration of clay, dispersions are predominantly elastic from the first measurement, and exhibit critical-gel like visco-elastic characteristics. For these dispersions, the frequency dependence of the complex modulus fits satisfactorily to critical-gel expressions. The unique characteristic of preserving critical-gel like behavior throughout the evolution process is interpreted in terms of the dispersions microstructure.

4.1 Introduction

Clay-based polymer nanocomposites have been the subject of immense investigations in recent years. The improvement in mechanical properties as well as thermal stability is achieved at low levels of clay content. The improved properties are largely dependent on the dispersal and degree of exfoliation of clay platelets in the polymer matrix [1, 2]. It remains a challenging job for the scientists and processing engineers to achieve good degree of dispersion and exfoliation. Besides nanocomposites, dispersed clay particles are also used in many other applications including paints, coatings, adhesives, pharmaceuticals, cosmetics and oil field drilling fluids. In developing polymer clay nanocomposites or other applications of clay dispersions it is essential to be able to characterize the state of dispersion of clay.

Understanding the interaction between clay platelets and solvent molecules as well as the structure of clay platelets in a suspension is critical for tailoring and characterizing polymer clay nanocomposites, because the final properties should be determined by the structure and morphology of the clay in suspension.

Montmorillonite (MMT) is a type of clay widely used for different purposes because of its high aspect ratio and good swelling properties [2]. It is hydrophilic in its natural form owing to polarity of the surfaces thus unsuitable to be mixed with hydrophobic organic media. Therefore it is organically modified to make it compatible with hydrophobic organic matrices. Moreover, the organic modification also decreases interaction among the platelets and facilitates exfoliation. The organic modification is done by exchanging the cations on the clay surfaces with cationic organic surfactant. The monolayer of the surfactant has two regions. The head region is polar whereas the tail region consists of alkyl chains which are apolar. With the exchange of cationic surfactant the clay platelets become largely hydrophobic and are swellable by apolar organic solvents because of good interactions between the surfactant and the solvent. The platelets experience both attraction and repulsion forces. Due to dispersion attraction forces the platelets tend to stack but the repulsion forces keep them apart. Thus, the equilibrium platelet separation is determined by the combination of these two opposing forces. The degree of interaction between the surfactant and solvent also defines the separation of platelets [3].

Over the years different structural and dynamic aspects of clay dispersions have been investigated. Most of the studies have been carried out with aqueous solvents and unmodified clays [4-7]. Colloidal behavior of organically modified clay dispersions in apolar organic solvents is less investigated. The dispersion of organoclay in various organic media is important for many technical applications so it is needed to pay more attention to these systems. The behavior of organoclay dispersions is determined by many factors like structure and chemistry of the surfactant, cation exchange capacity and interaction between modifier and polymer precursors [8]. Despite a number of theoretical studies on polymer-clay nanocomposites the exfoliation of clay platelets in polymer clay nanocomposites is still not well understood [8, 9]. Therefore it is important to study organoclay dispersions.

Connolly et al. [3] investigated effect of surfactant and solvent on the structure of clay suspension. They found that the basal spacing of the clay platelets increases with increasing chain length of surfactant. Furthermore, non polar solvents showed better degree of exfoliation compared to the polar ones. The stack size was estimated theoretically from the dispersions of various clay sizes with various concentrations. But the results were not

according to the model predictions due to the aggregation of platelets on large scale. Derek et al. [10] analyzed the effect of solvent solubility parameters on dispersability of organically modified clay in various solvents and found that the dispersion forces determine the suspension stability. Moreover, the clay platelets have better degree of exfoliation in less polar solvents. King et al. [11] characterized the structure and rheology of organo clay dispersions in organic solvents. A gel-like structure was formed by the clay suspension having predominant elastic behavior. The elastic behavior of dispersions was modeled by considering jamming of randomly oriented tactoids. The mechanical moduli and yield stress exhibited scaling behavior as a function of clay platelets volume fraction. Lionetto et al. [12] observed gel like properties for organically modified hectorite clays dispersed in organic solvent. The applied shear and increase in concentration of clay improved the gel elasticity. Zhong et al. [13] showed the formation of network like structures for organically modified montmorillonite dispersions in organic solvent with good degree of exfoliation. A quite pronounced yield stress existed for the suspensions. Yield stress, mechanical moduli and viscosity showed scaling behavior with clay concentration.

From the literature it turns out that the apolar solvents have better interactions with the organoclays and are helpful for the exfoliation. In addition to that, these suspensions have gel like behavior. However, gellation is a very complex phenomenon having different mechanisms and no general consensus is established yet [14]. By scanning through literature it also turns out that the effect of time on organoclay dispersions has not been investigated. Physical gels experience structural changes with time and bond formation, breaking and reformation processes continues during the time evolution [15]. Thus it is interesting to investigate the effect of time on the clay dispersions; how these evolve over time. Secondly many high performance engineering polymers are not soluble with common organic solvents. So the solvents should have optimum combination of properties which would allow to dissolve the polymers as well as being suitable for the dispersion of the nanoparticles. Recent studies have shown that aromatic amine based solvents have displayed good dispersion characteristics for nanofillers in polymers. Among those NMP has exhibited excellent dispersion characteristics for the nanofillers and also is a good solvent for many polymers [16]. Polymer nanocomposites prepared by solution casting using NMP as the solvent have shown promising properties [17-19]. In view of this it is useful to study the behavior of organo clay dispersions in NMP. To the best of our knowledge no study has been reported about the development of organoclay dispersions in NMP yet.

The aim of this study is to examine the development of organo clay dispersions in NMP. This main objective is met by setting the following objectives: (1) Study the evolution of the dynamic mechanical properties of dispersions during aging (2) Systematically study the effect of clay concentration on viscoelastic behavior (3) Develop understanding of the underlying mechanisms. We have critically analyzed the gelling process and its kinetics by following the rheology under small oscillatory deformation. Different stages of development have been identified and mechanisms governing the behavior are proposed. A threshold concentration of clay content for the transition of viscoelastic behavior was found. Viscoelastic behavior of dispersions was characterized during their evolution at different times. Some interesting viscoelastic features of the dispersions are noticed and a typical gel model is applied to describe the behavior. Concentration dependent viscoelastic behavior is interpreted in terms of dispersion microstructure.

4.2 Experimental

4.2.1 Materials

Cloisite 30B was obtained from Southern Clay Products, USA. It is an organically modified montmorillonite. It is modified with bis-(2-hydroxyethyl) methyl tallowalkyl ammonium cations. Tallowalkyl ammonium is a quaternary ammonium cationic surfactant, which renders the clay platelets hydrophobic and compatible with the polymers. The cationic exchange capacity (CEC) is 90 meq/100 g clay. The solvent *N*-Methyl-2-pyrrolidone (NMP) was obtained from Sigma Aldrich.

4.2.2 Preparation

The desired amount of clay was mixed in NMP and the large aggregates of clay were broken by manual stirring. Ultrasonication was employed to disperse the clay in NMP solvent in a plastic vial of 25 ml. The Sonotrode UIS -250LS by Hielscher Ultrasonics, GmbH was used. The instrument was operated at 50% amplitude and 50% cycle time for 2 hrs to prepare a master batch dispersion with 5 wt% clay. Exfoliation of the clay was determined by a Bruker AXS D8 Discover X-ray diffractometer (XRD) using CuKα-radiation having wavelength of 1.54 Å. A good degree of exfoliation was observed as the characteristic peak at $2\theta = 4.82^0$ indicating the platelets d-spacing disappeared after ultrasonication, as shown in Fig. 4.1(**Appendix**). Desired concentrations were obtained by diluting the master batch with

NMP. In different experiments the master batch and diluted samples were further sonicated for different durations e.g. 5 min, 30 min, 1 hr and 2 hrs.

4.2.3 Characterization

All the rheological measurements were done at 23 °C, using a strain controlled TA instruments rheometer AR-G2 equipped with parallel plate geometry of 40 mm diameter. The boundary of the linear regime was determined by running a strain sweep from 0.1-100% strain, at a fixed frequency of 10 rad/s. It turns out that up to 0.5% strain amplitude the sample was in the linear regime. Before measurements, samples were sheared at 400/s for 10 min. to have the same starting conditions with different samples. No waiting time was allowed after the pre-shear for measuring the oscillatory deformation response. In several experiments the development of the sample was monitored by a continuous oscillatory deformation at a fixed frequency of 10 rad/s and small strain amplitude of 0.5%. For several samples at various stages of development the viscoelastic response was measured by running a frequency sweep from 100 to 0.1 rad/s at 0.5% strain.

4.3 Results

We investigated the development of the clay dispersions (Cloisite 30B in NMP) by oscillatory rheometry. The samples were diluted from the master batch and ultrasonically treated for different durations. Immediately after this last sonication a sample was transferred to the rheometer to monitor over time the response to a small-strain oscillatory shear deformation at a fixed frequency (0.5% strain amplitude, 10 rad/s). Fig. 4.2 shows the development over the first 10 minutes for one of the representative samples. We have shown here only one case but we have data for various other clay concentrations prepared in the same way, showing the similar behavior. It is obvious from Fig. 4.2 that the storage and loss moduli ($G' \& G''$) increase with time. The development of the dynamic moduli exhibit a number of distinct features: initially there seems to be a certain lag phase during which the curves are flat and the moduli hardly change. Then, a crossover occurs, at which the slopes increase over a very short time, after which we observe that the increase of the moduli with time follows a power law or scaling law, as evident from linearity of the log-log plot. Similar trends and features were observed for all the cases.

We cannot identify any clear relationship between the sample composition or treatment histories and the evolution of the dynamic moduli. The levels of the moduli during the lag phase, the duration of the lag phase and the scaling exponents for the power-law phase do not seem to exhibit a clear correlation with clay concentration or pre-treatment. We plotted the loss tangent ($\tan\delta = G''/G'$) with time for the development of dispersions and found that the value of $\tan\delta$ seems to be the same within experimental scatter for all samples. We found a value for $\tan\delta$ roughly within a range of 0.44 ± 0.2 for most of the cases. On the basis of these observations, we conclude that $\tan\delta$ is independent of time and sample preparation. The development of the storage and loss moduli of the dispersions during the power-law phase of the development can be summarized by the following relation:

$$G' = \frac{G''}{\tan\delta} = \frac{G''}{0.44 \pm 0.2} = At^{\nu} \quad \text{..... (4.1)}$$

where ν is the scaling exponent for the power-law growth of the dynamic moduli. This exponent varies between samples with different pre-treatments. However, we cannot identify any clear relationship between ν, and the composition and/or pre-treatment. The second equality in equation 1 represents the power law behavior of the dispersions development.

A number of clay dispersions underwent a pre-treatment somewhat different from what was described above. The samples were just shaken after the dilution from master batch and stored for some time. After transferring the sample to the rheometer, high pre-shear (400 s^{-1} for 10 minutes) was applied before starting to monitor the response to the small amplitude, fixed frequency oscillation. The results are shown in Fig. 4.3. For these samples the developments of mechanical moduli exhibit far longer lag phases. But apart from the longer lag phase, the features are the same as for the other samples; even after 16 hrs the moduli did not reach a plateau.

Comparing the curves of Fig. 4.2, there appears to be a correlation between the levels of the moduli during the lag phase, and the slopes of the power-law phase (ν). We have determined the scaling exponents $\nu' \,\&\, \nu''$ and the corresponding values of the dynamic moduli at the crossover (G_*' and G_*'') and collected them in log-log plots in Fig. 4.4. Surprisingly, we see that the points tend to gather around single straight lines. This is indicative of power-law relations between ν' and G_*', and between ν'' and G_*''. These latter power-law relations can be represented by the following expression:

$$\nu' = B\left(G_*'\right)^{\eta} = B\left[\frac{G_*''}{\tan\delta}\right]^{\eta} \quad \ldots\ldots\ldots\ldots\ldots\ldots\ldots \quad (4.2)$$

the second equality follows from relation (4.1).

In order to further investigate the viscoelastic properties of the dispersions at different stages of their development during the investigated time window of 18 hr, we employed oscillation sweeps, in which we varied the frequency from 0.1 to 100 rad/s, at 0.5% strain amplitude for a number of samples. We applied the oscillation sweeps immediately after termination of a pre-shearing treatment (400 s^{-1} for 10 min.). During the first hour there were continuous oscillation sweeps. After this hour we further monitored the development of a dispersion using a single frequency (10 rad/s), during which we also applied oscillation sweeps at different intervals. We show in Fig. 4.5 the results from the oscillation sweeps done immediately after pre-shearing and after 18 hrs. We show only results for two samples but we have data for various other clay concentrations. It is obvious from the figure that after 18 hrs of development the dynamic moduli (G' and G'') show a weakly frequency dependent response. For the entire frequency range, the storage modulus is higher than the loss modulus, which signifies a predominantly elastic behavior. Moreover, for the dispersions with a certain clay content ($\geq$ 0.5wt%) this predominantly elastic behavior is exhibited already immediately after the pre-shearing treatment. Only for very low clay concentration below this threshold value we see that initially, immediately after pre-shearing, the storage modulus is smaller than the loss modulus, signifying a viscoelastic fluid rather than solid as shown in Fig. 5 for clay concentration of 0.35 wt%. However, even for these cases the dispersions develop to an extent that the storage modulus surpasses the loss modulus after some time. It is also interesting to point out another feature, namely that the logarithms of the storage modulus and loss modulus are parallel with small slopes. It means that the ratio of G'' over G' which equals the loss tangent ($\tan\delta$) is independent of frequency. This behavior resembles that of a so-called critical gel. The viscoelastic behavior of a critical gel is described by the following relations [20]:

$$G'_c(\omega) = \frac{G''_c(\omega)}{\tan\left(n\pi/2\right)} = S\Gamma\left(1-n\right)\cos\left(n\pi/2\right)\omega^n \quad \ldots\ldots\ldots\ldots\ldots\ldots \quad (4.3)$$

$$\left|G^*(\omega)\right| = S\Gamma(1-n)\omega^n \quad \ldots\ldots\ldots\ldots\ldots\ldots\ldots\ldots\ldots \quad (4.4)$$

Where $|G^*|$ is the magnitude of the complex modulus, S is the gel stiffness and n is the relaxation exponent. We see that according to these expressions the loss tangent is independent of frequency and equals $\tan(n\pi/2)$. Fig. 4.6 shows plots of the magnitude of the complex modulus as a function of frequency. We fitted our experimental data to the critical-gel equation (4.4) in order to determine S and n at different stages of the development of the clay dispersions. This reveals that for all elastic dispersions the critical gel model fits well to the experimental data. For the samples with clay concentrations below the threshold, for which we have seen that the storage modulus was smaller than the loss modulus in the early stages, the critical-gel like behavior is not attained during the first hour. How the parameters S and n evolve over time is shown in Fig. 4.7. The values of the relaxation exponent n are much smaller than unity. The values gather around a single value of 0.1 for different samples. The stiffness S increases with time and concentration. For some cases we can see that S seems to level off at long times.

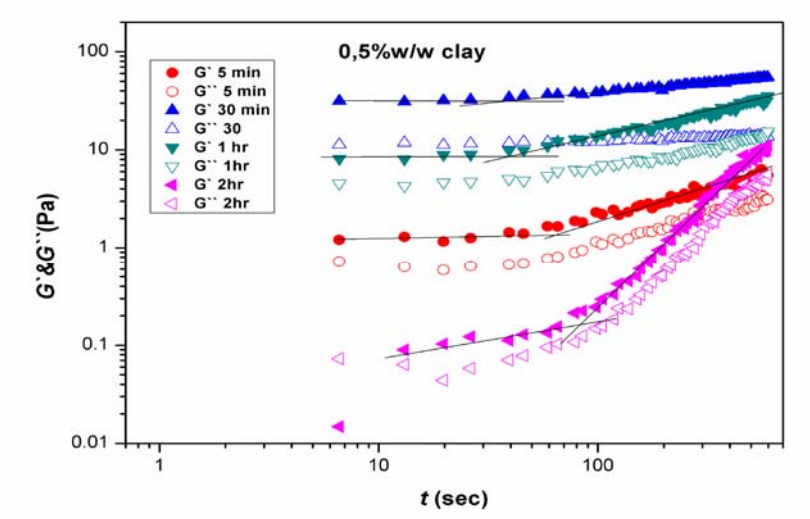

Figure 4.2 Development of the dynamic moduli at ω = 10 rad/s for 10 min for clay in NMP dispersion for different sonication times.

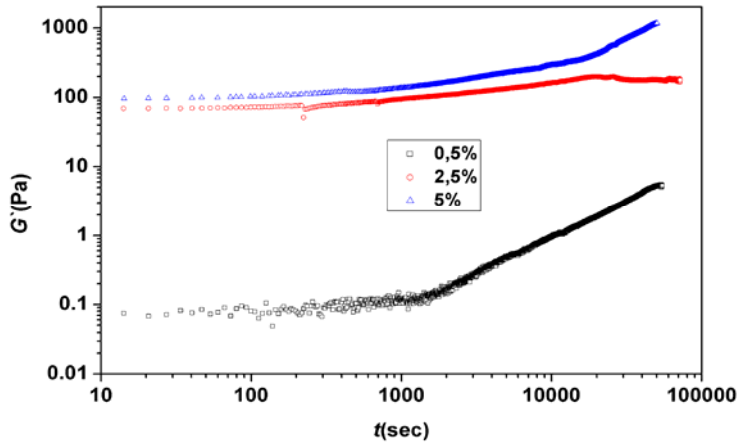

Figure 4.3 Development of the modulus of the samples that were not sonicated after dilution and pre-sheared at 400/s for 10 min. before starting to monitor the response to small-amplitude, fixed-frequency oscillation

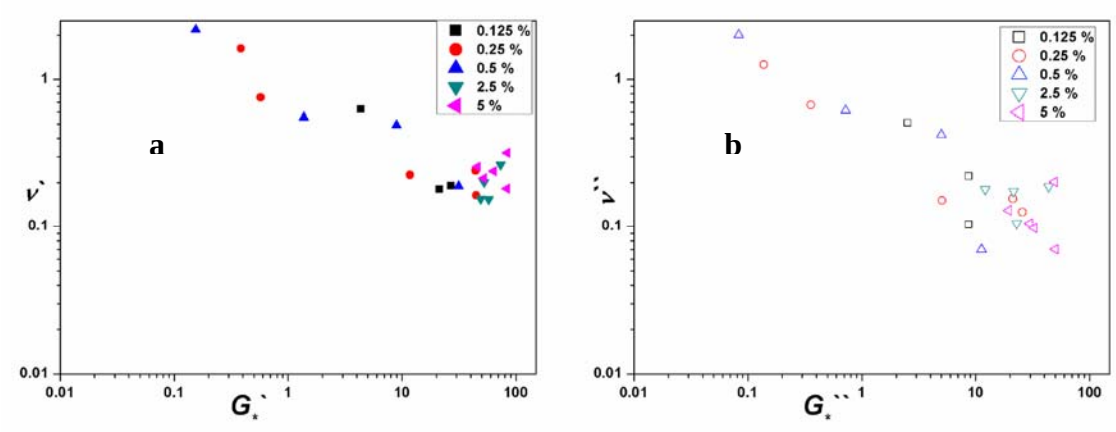

Figure 4.4 The relation between the values of the dynamic moduli at the end of the lag phase and the exponent of the power-law phase for different clay concentrations. (a) Storage modulus $G_*^{'}$ (b) Loss modulus $G_*^{''}$ (Obtained from Fig. 2 at crossover points)

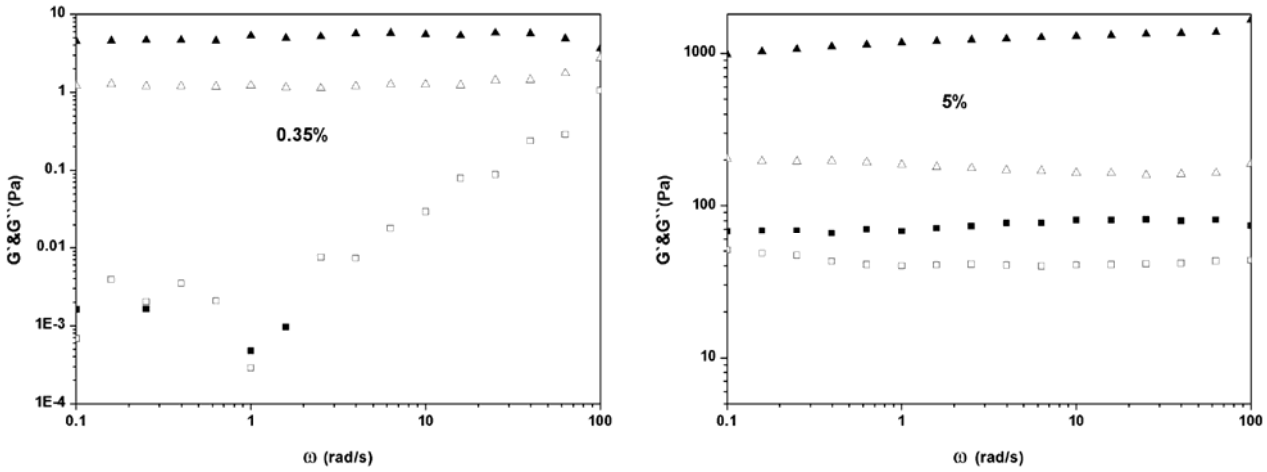

Figure 4.5 Frequency response for clay dispersions at 10 rad/s for different clay concentrations (weight percentage indicated in the graphs). All filled symbols represent storage modulus ($G^{/}$) and open symbols loss modulus ($G^{//}$) .$G^{/}$ at the beginning (■) $G^{//}$ at the beginning (□) $G^{/}$ after 18hrs (▲) $G^{//}$ after 18hrs (Δ)

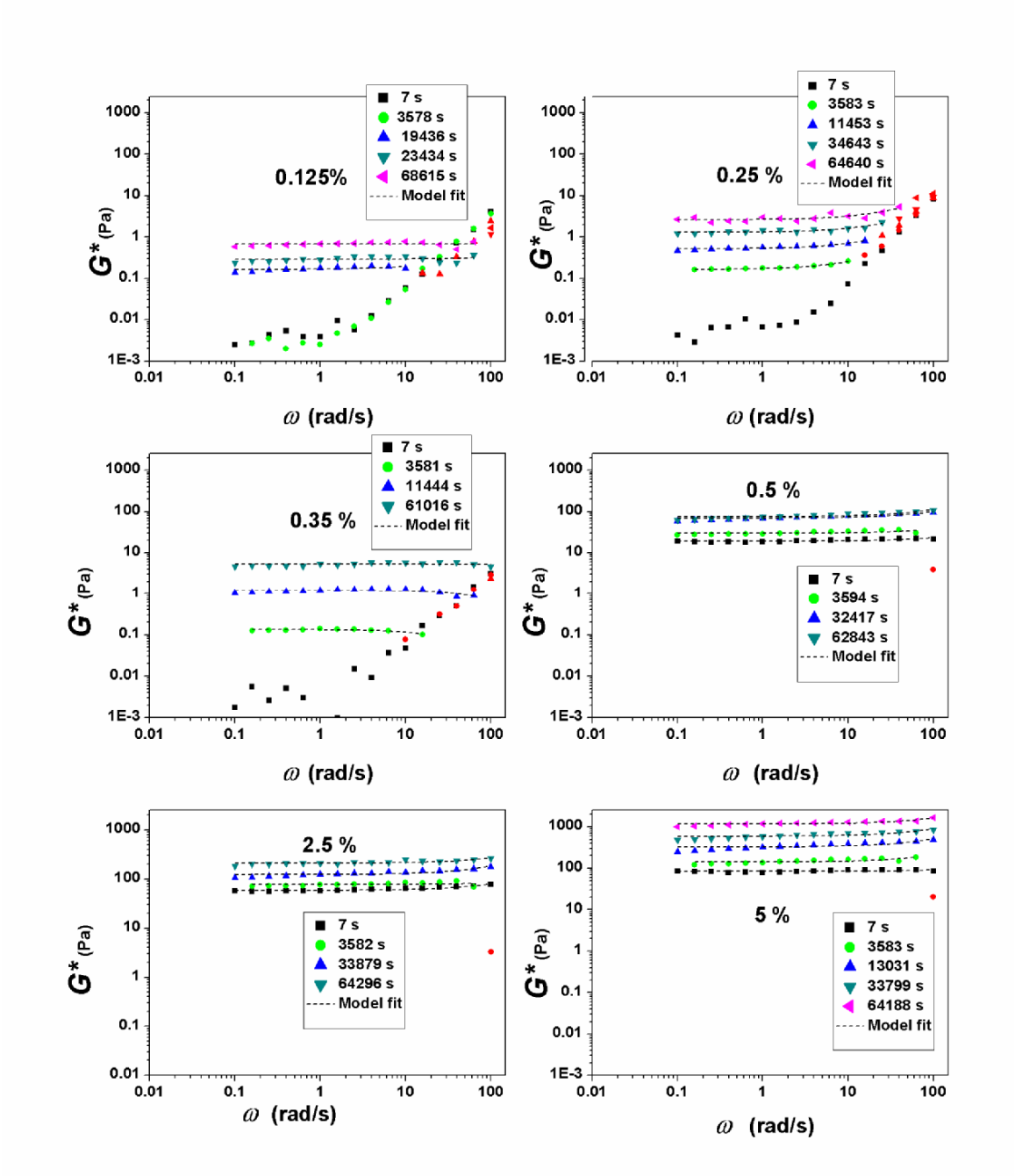

Figure 4.6 Fitted curves of the magnitude of the complex modulus as a function of frequency with critical gel model for different clay concentrations, at different times during the evolution of clay dispersions (Dashed lines through the data points are model fits)

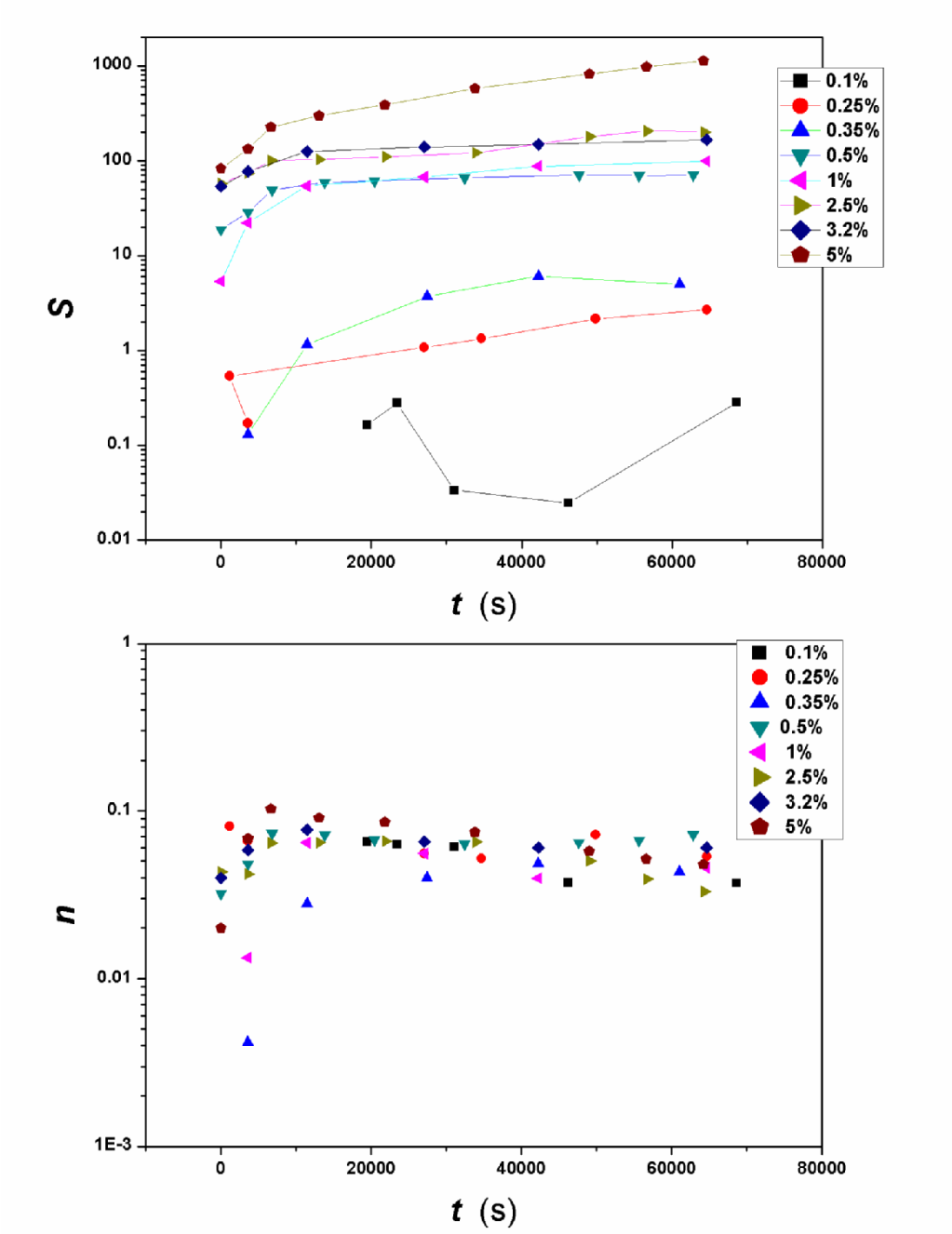

Figure 4.7 The evolution of gel stiffness(S) and relaxation exponent (n) for clay dispersions determined by critical gel model fits with the data of dynamic sweeps during 18hrs at different times for different clay concentrations

4.4 Discussion

Use of NMP as solvent and the ultrasonication method, which we have employed, yields well exfoliated organoclay dispersions, as demonstrated in Fig. 1. The clay platelets do not aggregate back into stacks at the timescale of two weeks. The size of the crystallite (stack) for dry Cloisite 30B is calculated by following the Scherrer equation given as:

$$\Gamma = \frac{K\lambda}{\beta cos\theta} \quad \text{..... (4.6)}$$

Where Γ is the mean dimension of the crystallite, λ is the wavelength of the X-rays, θ is Bragg diffraction angle, K is so called shape factor takes the value of about 0.9 and β is the width of diffraction peak at half of its maximum intensity. The XRD spectrum of Cloisite 30B as shown in Fig. 1 was considered for the purpose of stack size calculation. The size of the platelets stack obtained for Cloisite 30B by using the Scherrer equation is 53 Å. It means there are roughly 3 platelets per stack as the d-spacing of the Closite 30B is roughly18.2 Å determined from the XRD data in Fig. 1. Exfoliation becomes relatively easy for such a low number of platelets per stack. However, we note that Γ may also represent a stacking correlation length, indicating somewhat irregular spacing of the platelets due to intercalation and exfoliation. So the stack size estimated by the Scherrer equation can not be confidently claimed.

From our rheological investigations, it has become clear that the exfoliated clay dispersions evolve over time. Furthermore, this evolution has two distinct stages. The first stage is certain delay or lag time over which the mechanical moduli hardly change. After this lag phase there is a rather sharp crossover towards a power-law increase of the moduli. The lag phase can be explained as the phase during which interparticle connections gradually increase, but during which the dispersion is still structured as a collection of non-percolating clusters.

It is also observed the initial elastic behavior emerges at a critical thershold of clay content (≥ 0.5 wt%). For example there are roughly two level off regions of ratio of loss over storage modulus i.e. loss tangent ($\tan\delta$) as a function of clay content shown in Fig. 4.8(a). For one region below the threshold of clay content the $\tan\delta$ is larger than unity (viscous) and above the threshold for the other region it is less than unity (elastic). The systematic effect of clay concentration on transition from viscous to elastic behavior is an important finding. Most of the investigations have been carried out with gel-like clay dispersions and the relation of

particle concentration with rheological properties (viscosity, moduli, shear thinning etc.) was discussed. The viscous clay dispersions are rarely reported.

The viscous dispersions also turned into elastic after long time. The viscous systems are not structured initially having low number of interparticle connections. The particles are randomly distributed and far apart from each other. The particles move to make connection with other particles. Time is needed to form percolated network of particles. In contrast to that for the dispersions having clay content above the threshold value, the particles are close enough that even a rotational diffusion is sufficient to connect with another particle; consequently the network is formed immediately. With the formation of a network like structure the system is dynamically arrested and behaves like an elastic solid.

Although the lag time is present even for the systems which are predominantly elastic already, it is much shorter than the time taken by the viscous systems to turn into elastic state which is of the order of an hour instead of seconds. The long lag time in case of elastic samples which were pre-sheared (400/s for 10 min) can perhaps be attributed to the alignment of the particles as a result of high shearing force. The particles that were oriented lost the internal connectivity of the network. Therefore, it takes longer time to rebuild as shown in Fig. 4.3.

In case of aqueous dispersions of clay, the most common explanation given for the formation of elastic gels is interaction between oppositely charged faces and edges of the platelets leading to a "house of card" like structure [21]. However, we don't expect such electrostatic interactions in organo clays in apolar solvents. They would resemble more closely to hard platelets in a solution. In this scenario it is interesting to probe the underlying mechanism governing the viscoelastic behavior for such dispersions.

If the platelets have lower attractive interactions compared to thermal energy, then the rheology of the clay suspensions is expected to change significantly when the clay volume fraction ϕ is raised above an effective "overlap volume fraction", ϕ^*, below which the platelets can rotate freely without hindering each other and above which the bodies of revolution of clay platelets overlap. The body of revolution of a platelet on average occupies a volume about equal to the cube of its diameter. Then the overlap volume fraction is given by:

$$\phi^* = \frac{D^2 t}{D^3} = \frac{t}{D} \quad \ldots\ldots\ldots\ldots\ldots\ldots \quad (4.7)$$

where D is the average diameter of platelet and t is thickness.

From the relation it is clear that the overlap volume fraction is inversely related to the platelets aspect ratio. As the clay platelets have a high aspect ratio overlapping occurs at quite low ϕ. The overlap concentration threshold may also play a role in determining the degree of exfoliation. It may be difficult to achieve the complete degree of exfoliation for the overlap concentration of clay particles due to space restrictions. Thus the exfoliation is limited by gel formation. The concentration of clay particles commonly used for the nanocomposites is generally higher than the overlap concentration. As a result complete exfoliation in nanocomposites is hardly ever achieved. From the experimental results the onset of elastic behavior occurs at a volume fraction of 0.003 (0.5wt %). By considering this as the overlap concentration, ϕ^*, the estimated aspect ratio corresponding is roughly 300. This calculated value of the aspect ratio matches closely to the aspect ratio values reported for MMT type platelets in the literature [22]. Thus relating the onset of elasticity to overlap particles like is quite reasonable.

The dispersions with $\phi > \phi^*$ there is a modest increase in relative modulus with aging, however, for the case of $\phi < \phi^*$ there is significant increase in relative modulus with aging approximately three orders of magnitude as shown in Fig. 4.8(b). The change in behavior from viscous to elastic and the maximal increase in relative modulus occurs at the same threshold value of clay content. Therefore, the relative increase in modulus is related to the initial state of the system. For the viscous dispersions with $\phi < \phi^*$ the initial modulus is very low but with aging these dispersions turn elastic consequently the increase in relative modulus is significant. In contrast for elastic dispersions the system is already in the elastic state and the (relative) stiffness increases over time moderately.

An interesting aspect is the critical gel like behavior observed for the dispersions. In case of chemically cross linked polymeric systems this behavior is observed only at particular stage corresponding to the percolation threshold, and cannot be seen before or after it. In contrast to that, surprisingly, for the clay dispersions under consideration, the critical gel like behavior is maintained throughout the evolution process. We have checked this characteristic by fitting the critical gel equations at different times of dispersion evolution and noticed that once the critical state is achieved, it remains during the evolution as shown in Fig. 4.6. To our understanding this kind of behavior might be explained in this way. For the physical gel forming colloidal systems the structural organization continues throughout the process. The

tactoids and platelets are not so rigidly bonded in contrast to chemically cross-linked polymer networks. The particles are mobile and new bonds can be formed between the particles. Moreover the dangling ends of the particle networks can form new bonds and new chains of the particles are added to the network. However, the fractal like structure of the particle network is preserved despite the formation of new inter-particle or inter-tactoid bonds. Thus, the critical gel like scaling behavior persists for the system throughout the evolution process because of the conservation of the fractal structure. The critical gel-like character is maintained although the gel strength increases with time. The increase in gel strength is attributed to increase in network connections or network density with time.

4.5 Conclusion

Based on rheometry results it is clear that in this study the organoclay dispersions evolve over time and turn into elastic gels. The growth of mechanical moduli as a function of time follows a scaling law. The viscoelastic behavior depends on clay concentration and there is a critical threshold concentration separating the viscous and elastic dispersions. The concentration can be explained by considering critical overlap of the particle structure. Exfoliation is limited by gel formation. The frequency dependence of the dynamic moduli closely resembles that of a critical gel. The critical gel model predictions fit well to the experimental data. The sustainability of the critical gel like behavior throughout the evolution process may be explained by considering fractal-like structural aspects of clay configuration. Structural characterization by microscopic and scattering techniques and online monitoring of dispersions by rheometry coupled with microscopy would be handy to have better insight into the structure to obtain further understanding of the gel formation mechanism.

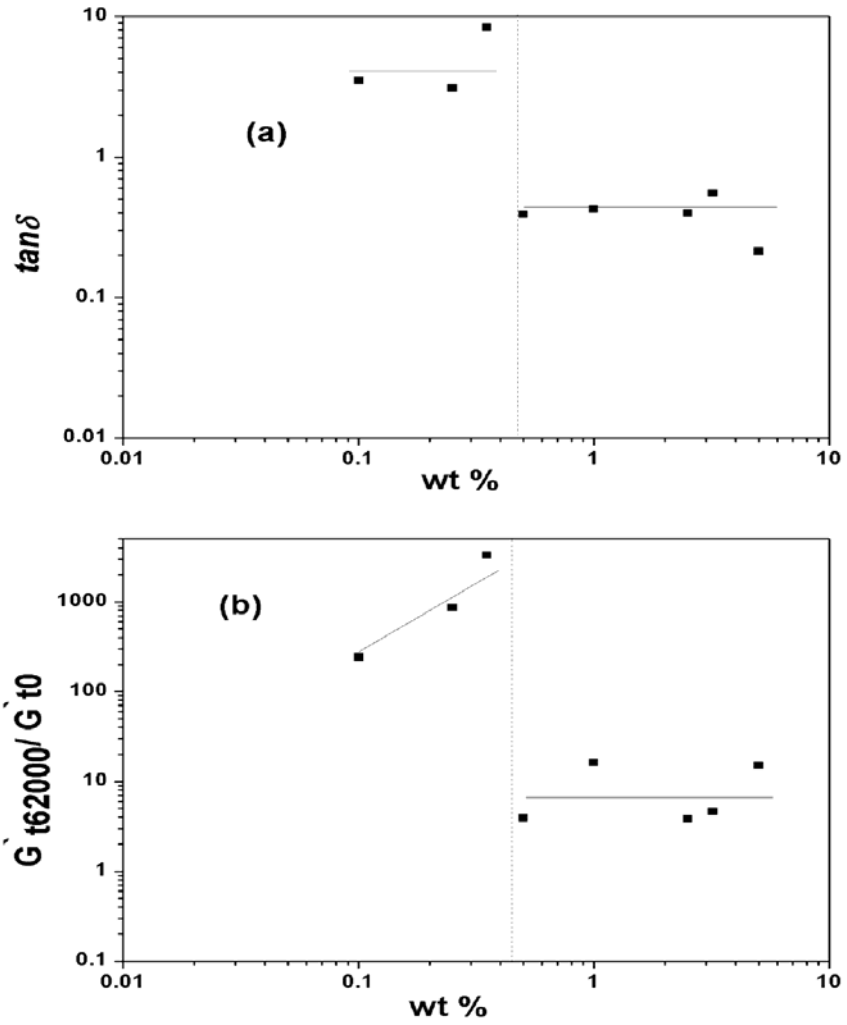

Figure 4.8 (a) Showing the initial loss tanδ for different clay samples at the start (time 0 sec) of rheometry measurement for dispersions (b) Relative increase in elastic modulus over the investigated time of evolution process (time 0 sec to 62000 sec) for various clay concentrations

4.6 References

[1] Ray SS, Okamoto M. Polymer/layered silicate nanocomposites: A review from preparation to processing. Prog Poly Sci. 2003;28 (11):1539–1641.

[2] Bitinis N, Hernandez M, Verdejo R, Kenny JM, Lopez-Manchado MA. Recent advances in clay/polymer nanocomposites. Advanced Materials. 2011;23(44):5229-5236.

[3] Conolly J, Duijneveldt JSv, Klein S, Pizzey C, Richardson RM. Effect of surfactant and solvent properties on the stacking behavior of non aqueous suspensions of organically modified clays. Langmuir. 2006;22(15):6531-6538.

[4] Jennifer M. Saunders, James W. Goodwin, Robert M. Richardson, Vincent B. A small-angle X-ray scattering study of the structure of aqueous laponite dispersions. J Physical Chemistry B. 1999;103(43):9211-9218.

[5] Willenbacher N. Unusual thixotropic properties of aqueous dispersions of laponite RD. J Colloid and Interface Science. 1996;182(2):501-510.

[6] Patil SP, Mathew R, T.G.Ajithkumar. Gelation of covalently edge-modified laponites in aqueous media. 1. Rheology and
nuclear magnetic resonance. JPhysical Chemistry. 2008;112(15):4536-4544.

[7] Pujala RK, Pawar N, H.B.Bohidar. Universal sol state behavior and gelation kinetics in mixed clay dispersions. Langmuir. 2011;27(9):5193-5203.

[8] Simons R, Qiao GG, Bateman SA, Zhang X, Lynch PA. Direct observation of the intergallery expansion of Polystyrene-Montmorillonite nanocomposites. Chem Mater. 2011;23(9):2303-2311.

[9] Fu Y-T, Heinz H. Cleavage energy of Alkylammonium-modified montmorillonite and relation to exfoliation in nanocomposites: Influence of cation density, head group structure, and chain length. Chem Mater. 2010;22(4):1595-1605.

[10] L.Ho D, Glinka CJ. Effect of solvent solubility parameters on organo clay dispersions. Chem Mater. 2003;15(6):1309-1312.

[11] King HE, Milner JST, Lin MY, Singh JP, Mason TG. Structure and rheology of organoclay suspensions. Physical Review 2007;75(2):21403-21422.

[12] Lionetto F, Maffezzoli A. Rheological characterization of concentrated nanoclay dispersions in an organic solvent. Applied Rheology. 2009;19(2):23423-23430.

[13] Zhong Y, Wang S-Q. Exfoliation and yield behavior in nanodispersions or organically modified monmorillonite clay. Journal of Rheology. 2003;42(2):483-495.

[14] Zaccarelli E. Colloidal gels :equilibrium and non equilibrium routes. Journal of Physics: Condensed Matter. 2007;19(2):323101-323149.

[15] Rubinstein M, Dobrynin AV. Associations leading to formation of reversible networks and gels. Current Opinion In Colloidal &Interface Science. 1999;4(1):83-87.

[16] Giordani S, Bergin SD, Nicolosi V, Lebedkin S, Kappes MM, Blau WJ, et al. Debundling of single-walled nanotubes by dilution: Observation of large populations of

individual nanotubes in amide solvent dispersions. Journal of Physical Chemistry B. 2006;110(32):15708-15718.

[17] Wang J, Iroh JO, Long A. Controlling the structure and rheology of polyimide/nanoclay composites by condensation polymerization. J App Poly Sci. 2012;125(1):E486-E494.

[18] Faghihi K, Soleimani M, Shabanian M, Abootalebi AS. The Structure-Property Relationship of Poly(amide-imide)/Organoclay Nanocomposites. High Temperature Materials and Processes. 2011;30(3):217-222.

[19] Delozier DM, Orwoll RA, Cahoon JF, Johnston NJ, Smith JG, Connell JW. Preparation and characterization of polyimide/organoclay nanocomposites. Polymer. 2002;43(3):813-822.

[20] Winter HH, Mors M. Rheology of polymers near liquid solid transitions. Advances in Polymer Science. 1997;134:167-230.

[21] Olphen HV. An introduction to clay colloid chemistry. New York: Wiley and sons; 1964.

[22] W.Beall G, E.Powell C. Fundamentals of Polymer-clay nanocomposites. Cambridge: Cambridge University Press; 2011.

Appendix

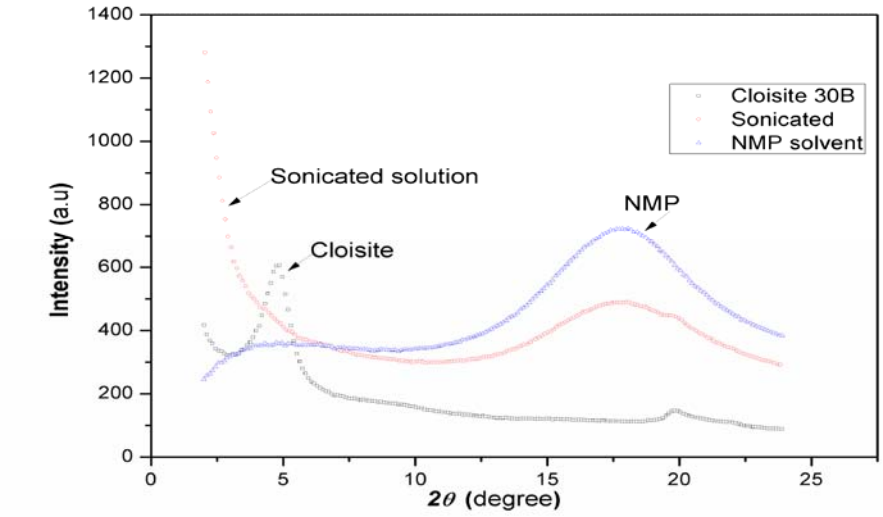

Figure 4.1 XRD spectrum of dry Cloisite 30B and of Cloisite 30B dispersed in NMP and sonicated for 2hrs showing the exfoliation of clay

Chapter 5

Synthesis, Characterization and Modeling of Mechanical Properties of Bismaleimide/Clay Nanocomposites

Abstract

In this chapter we report thermo-mechanical properties of organo-clay based nanocomposites with a high-temperature resistant thermoset resin. Nanocomposites up to 5 wt% of clay were prepared by a solution casting method and dispersed by ultrasonication. The structure and thermo-mechanical properties were characterised by X-ray diffraction (XRD) and dynamic-mechanical analysis (DMA) respectively. The characteristics of dispersion and influence of the preparation process on the structure of nanocomposites are critically discussed. XRD measurements indicate imperfect exfoliation and an anisotropic dispersion of clay particles in the nanocomposites. The elastic modulus and heat deflection temperature are systematically improved upon increasing the concentration of clay particles. The Halpin-Tsai model is used to model the mechanical properties and reproduces the experimental data reasonably well. Both the XRD results and the Halpin-Tsai model analysis indicate that the degree of exfoliation decreases with increasing concentration of clay particles. The capability of the model to explain the reinforcing mechanism in nanocomposites is critically discussed.

5.1 Introduction

Nanocomposites of polymer and layered-silicate particles are the subject of considerable interest in recent years because of their superior properties [1, 2]. Addition of the particles leads to a significant improvement of mechanical properties [3]. The reinforcement of polymers by the incorporation of nano-clay particles is achieved at very low loading levels of the clay compared to their counter part micro-composites [4]. This dual advantage of lower filler levels for the enhanced stiffness has been exploited to prepare light-weight components. This is a desirable feature in many applications, especially in transportation, where fuel efficiency is important. Moreover, nanocomposites exhibit a negligible loss in other matrix

properties, e.g. fracture toughness, ductility and surface finish [5]. The aviation industry is in search for high-temperature resistant matrices for high-performance composites, to meet the future demands of high speed and fuel efficiency. In this regard composites of Bismaleimides are getting attention due to their high temperature resistance, high dimensional stability, good resistance to chemicals and reasonable mechanical strength [6-9]. The processability of Bismaleimides is as easy as epoxy but performance is much better. Bismaleimides are thermosets which release very low amounts of volatiles during curing, therefore, there is less chance of void formation [10]. In contrast, the high-temperature resistant polyimides are cured by a condensation-type polymerization process involving the release of volatiles, which leads to void formation, which compromises performance [10]. Bismaleimides have a balanced combination of properties, processability and affordability. Brittleness is one of the major concerns for Bismaleimides, which leading to low damage tolerance. Different strategies have been adopted to improve its toughness with minimum loss of the thermal properties [8-11].

High-temperature resistant thermoset nanocomposites are rarely reported in the literature. However, the importance of these materials warrants thorough investigation. Hence, we were motivated to study Bismaleimide nanocomposites. We have selected a recently developed pre-polymer resin of Bismaleimide, which is claimed to be high-temperature resistant. It is a one-component system, in contrast to commonly used two-components Bismaleimide systems. It is challenging to find an optimal processing route for this resin to incorporate the filler. Moreover, a thorough characterization and fundamental understanding of the effects of nanofiller is needed to tailor it for the desired applications. In our previous study on the same polymer we used carbon nanofiber as filler and a melt blending technique to mix the filler with the matrix. It turned out that this did not lead to significant improvement of the mechanical properties [12]. In the present study we have adopted a different processing strategy and also used an organically modified nano-clay as the filler.

The reinforcing effect of the fillers depends on various filler parameters, such as shape, aspect ratio, modulus, volume fraction, interfacial adhesion, surface characteristics and orientation [13-16]. Thus, many factors could potentially influence the stiffness of the final nanocomposite, and a better understanding of the effects of each filler property is needed. Over the years the effect of various parameters on the mechanical properties of nanocomposites have been studied, and micromechanical models have been proposed to explain the behavior [13, 15, 17, 18]. These micromechanical models are based on

conventional composite theory, which assumes that each individual phase keeps the same properties as if the other phase were not there. These models and experimental studies indicate that the filler aspect ratio is an important parameter affecting the stiffness of a nanocomposite. Van Es [19] concluded that the stiffness of nanocomposites to a large extent is determined by the particle aspect ratio. The better the degree of exfoliation, the higher the effective aspect ratio, the larger the effect of the nano-filler on mechanical properties.

The Halpin-Tsai model has been found to explain the mechanical properties of the nanocomposites reasonably well. Paul et al. [13] modeled the mechanical behavior of nanocomposites using the Halpin-Tsai and Mori-Tanaka models, and found that an exfoliated platelet structure with a high aspect ratio provides superior reinforcing effect. The heat distortion temperature obtained by model predictions and experiment were in good agreement. The model predicts the heat distortion temperature (HDT) to increase with increasing aspect ratio. Picken et al. [18] modeled the mechanical behavior of nanocomposites using the Halpin-Tsai model for different filler geometries and found that the modulus increases with increasing aspect ratio. Weon et al. [15] studied the effect of clay aspect ratio and orientation on mechanical behavior of nanocomposites. The modulus and heat distortion temperature improved with high aspect ratio and alignment of the filler. Another group of researchers [20] used two types of clay particles with different aspect ratios and investigated their effect on thermo-mechanical properties. Nanocomposites prepared with high-aspect-ratio clay particles exhibited better mechanical reinforcement despite having an intercalated structure as compared to low aspect ratio particles of clay with an exfoliated structure. This behavior was well explained by the Halpin-Tsai model.

The present study aims at preparation of high temperature-resistant thermoset nanocomposites and characterization and modeling of their mechanical properties. A reasonable reinforcing efficiency and good thermal stability was achieved by the addition of nano-clay particles. The Halpin-Tsai model is applied to explain the mechanical properties of the nanocomposites.

5.2 Experimental

5.2.1 Materials

The resin used was a pre-polymer of Bismaleimide with trade name of “Homide 250” supplied by Hos-technik, Austria, in the form of a yellow powder. Organically modified clay, Cloisite 30B, was obtained from Southern Clay Products, USA. It is Montmorillonite (MMT)

modified with bis-(2-hydroxyethyl) methyl tallow alkyl ammonium cations. The solvent *N*-Methyl-2-pyrrolidone (NMP) was obtained from Sigma Aldrich.

5.2.2 Nanocomposite preparation

A pre-polymer resin solution of 30 wt% concentration in NMP solvent was prepared by magnetic stirring. An ultrasonication probe Sonotrode UIS-250LS by Hielscher Ultrasonics, GmbH was used to disperse the clay in NMP in a plastic vial of 25 ml. The instrument was operated at 50% amplitude and 50% cycle time for 2 hrs to prepare a master batch dispersion with 5 wt% clay. After that the master batch was diluted to 2.5 wt% and ultrasonicated for 1 hr. Then both the diluted clay dispersion and resin solutions were mixed in appropriate proportions to prepare a resin clay mixture with various concentrations of clay particles. The resin clay solution mixture was magnetically stirred for 8 hours. After that, the mixture was poured in a glass dish. The dish was placed in a vacuum oven at 80 °C for 3 hrs to evaporate the solvent and remove any entrapped air. In the mean time, the mixture was stirred intermittently with a spatula to avoid skin formation and agglomeration. The solvent was evaporated and the mixture dried to an extent that it could be easily poured into a mold. We used silicone-rubber molds with slots of dimensions length 25 mm, width 3 mm, and a depth 1 mm. After filing the mold, the samples were cured for 1 hr at each of the following temperatures: 80 °C, 120 °C, 140 °C, 160 °C, 180 °C and 200 °C .
The samples were removed from the molds after curing, and post cured at 220 °C for 4 hr. The samples were finished by removing the overflowed material and burrs using sand paper.

5.2.3 Characterization

In order to assess the state of dispersion of the clay platelets in the nanocomposites we used X-ray diffraction (XRD). The measurements were performed on a Bruker AXS D8 Discover X-ray diffractometer equipped with a Hi-Star 2D detector using Cu Kα-radiation (λ=0.154 nm) filtered by cross-coupled Göbel mirrors at 40 kV and 40 mA. The sample was placed at a distance of 10 cm from the detector and the range of the cone angle 2θ was 1.7^0 to 23.7^0. Both radial and azimuthal integrations were performed on the X-ray diffraction data.

Storage and loss moduli of the nanocomposites were measured using a Perkin Elmer DMA 7-e dynamic mechanical analyzer in a three point bending mode at a frequency of 1 Hz. The distance between the supports was 10 mm. The controlled oscillating strain applied was

0.15%. The temperature was scanned from 25-350 °C at a heating rate of 2 °C /min. The sample dimensions were 15x3x0.6 $mm^{3.}$

5.3 Results and discussion

5.3.1 Intercalation/Exfoliation characterization

X-ray diffraction is a common technique to probe the degree of exfoliation in polymer clay nanocomposites. Stacks of clay particles consist of platelets arranged like a deck of cards with regular interplatelet spacing. The X-rays are diffracted from the regular planes of the platelets and interfere, resulting into high intensity sharp peaks in the X-ray diffraction pattern. The interlayer distance is calculated from the 2θ value of these peaks using Bragg's law. If the clay platelets are completely separated and disordered upon mixing with the polymer matrix, the characteristic 001d-spacing peak of clay platelets disappears from the X-ray diffraction pattern. The XRD results of composites are shown in Fig. 5.1. For the dry powder Cloisite 30B the 001 d-spacing peak position is at an angle of $2\theta \approx 4.84^0$ corresponding to a basal spacing of 18.2 Å. Furthermore, a peak at $2\theta \approx 20^0$ relates to the internal structure of the clay platelets [21]. The unmodified resin showed a broad peak with a maximum at approximately $2\theta \approx 18^0$, which shows that the cured material has an amorphous structure, as expected for a thermosetting polymer [21]. In the case of nanocomposites, the 001d-spacing peak at $2\theta \approx 4.84^0$ has disappeared, indicating that the stacks of platelets have fallen apart and that the platelets inside the nanocomposites are fairly well exfoliated. The peak at $2\theta \approx 20^0$ is still present, as the internal structure of the clay platelets has not changed. It is worth to point out here that for 5% composite we can recognize the edge of a small peak at $2\theta \lesssim 2^0$ which indicates that the distance between the platelets has increased due to the interpenetration of the polymer chains inside the galleries of platelets. In nanocomposites such a structure in which the inter-platelets distance increases due to polymer penetration without totally loosing the deck-of-card-like arrangement of platelets is known as an intercalated structure.

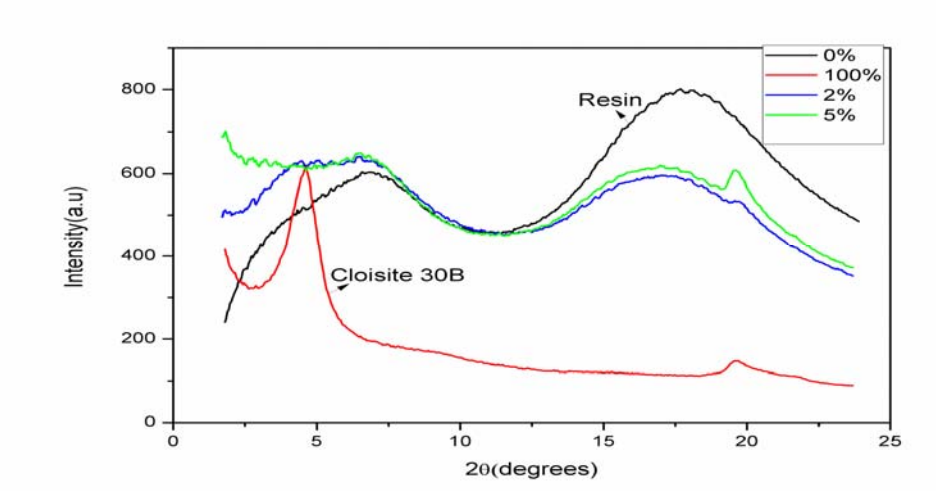

Figure 5.1 XRD patterns of cured matrix and their nanocomposites reinforced with Cloisite 30B

5.3.2 Orientation of the platelets

The solution casting technique used for the preparation of nanocomposite samples involves evaporation of the solvent during drying and curing. This drying process may have an influence on the structure and properties of the final material [22]. We used a mold with slots in which the solution mixture is casted and solvent evaporates during the drying process. The loss of solvent causes shrinkage in the vertical direction (which is the thickness direction) that is accompanied by solidification of the material. Shrinkage of the sample in the thickness direction, because of evaporation of solvent, is expected to lead to internal anisotropy, as chains and platelets get oriented parallel to the plane normal to the thickness direction. Orientation of polymer chains and birefringence caused by a drying process has been reported for some polymer films [23, 24]. For polymer clay mixtures the polymer chains as well as the platelets may get oriented and aligned during the drying process [22]. In order to investigate the alignment of the platelets we performed the XRD measurements with varying orientation of the sample. The details of sample geometry and scattering orientation are shown schematically in Fig. 5.2. X represents the width, Y thickness and Z the length of the sample. In different measurements, either the XZ plane or the YZ planes of the sample were oriented normal to the incident beam. The scattering pattern corresponding to incident X-rays normal to the XZ plane and normal to the YZ plane, termed here as y and x respectively, are shown in Fig. 5.3 and 5.4. We carried out the measurements for different concentrations of clay

particles and found that for 5 wt%, significant alignment of the platelets occurs, as indicated by the strongly azimuthal-angle-dependent reflections at small cone angles 2θ in figure 3b. This means that the platelets are indeed preferentially oriented parallel the thickness direction, as expected. This anisotropy is clearly shown in Fig. 4 as two discernible peaks can be observed when the scattered intensity is integrated over the cone angle and plotted vs the azimuthal angle. These peaks were absent for the 5% sample in y incident scattering and for other lower concentrations the peaks were absent in both of the scattering orientations.

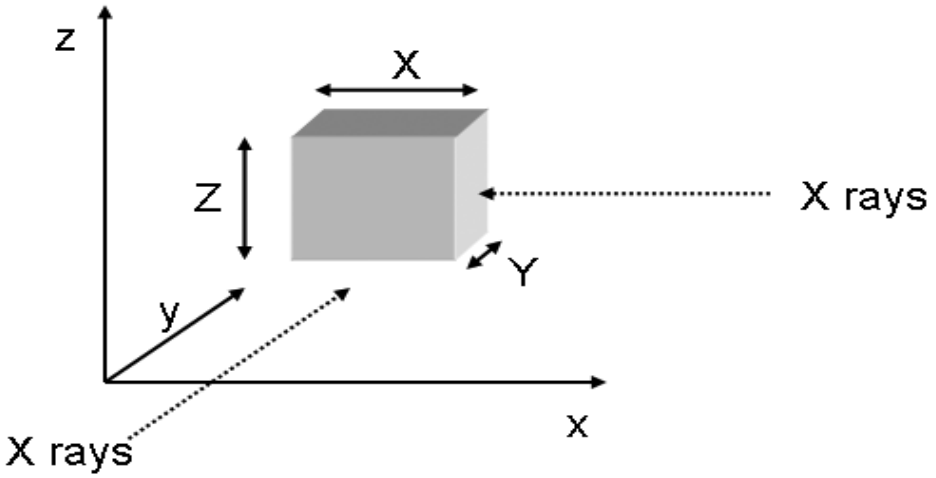

Figure 5.2 Schematic of the sample geometry and orientation for X-ray scattering to probe alignment of the platelets

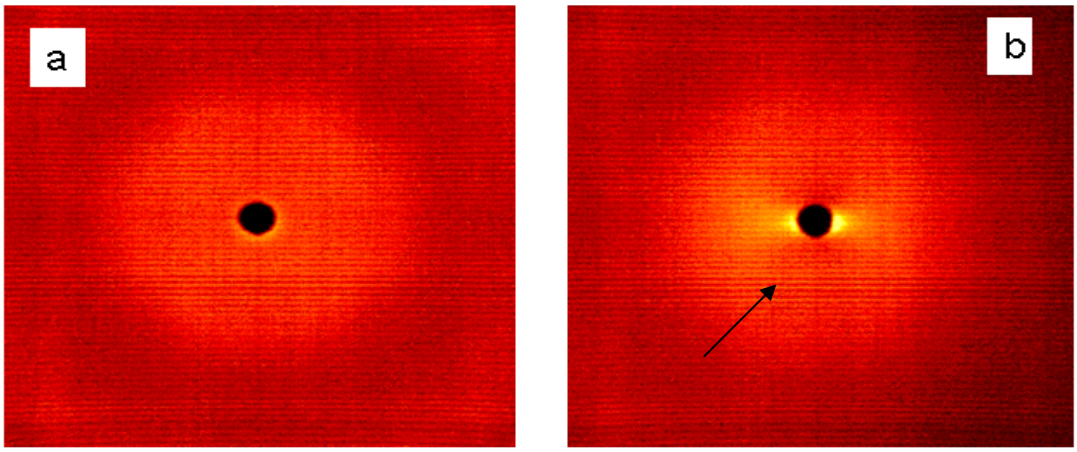

Figure 5.3 XRD spectrum of 5% nanocomposite; incident beam normal to the (a) XZ plane (b) YZ plane

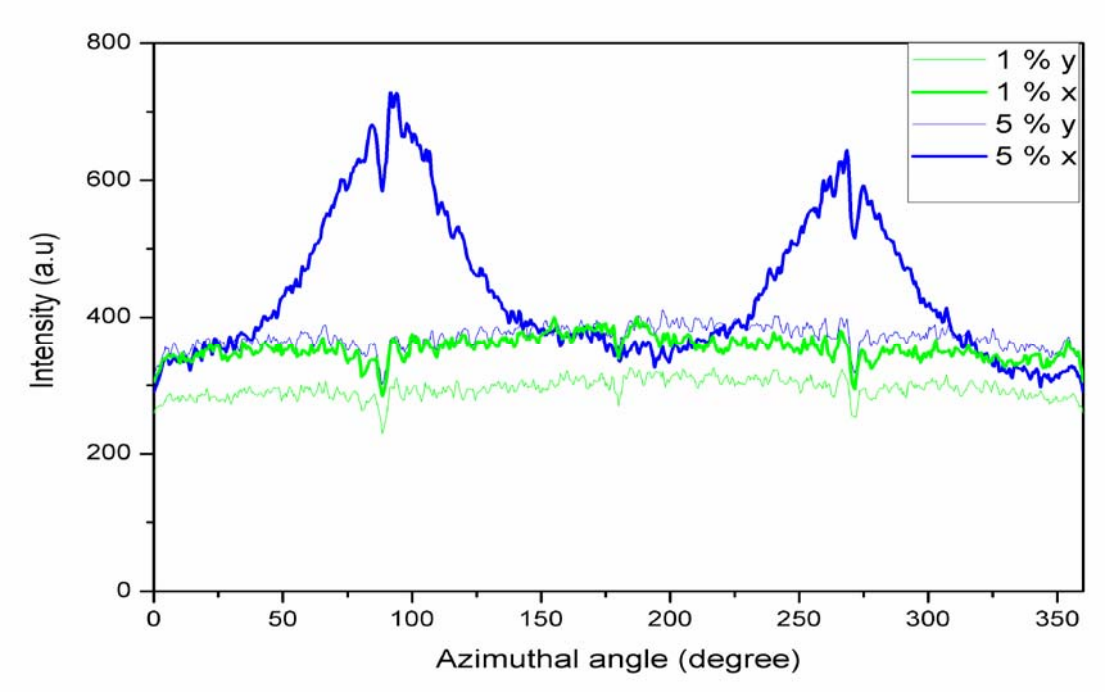

Figure 5.4 Dependence of the scattered intensity integrated over the cone angle, as a function of the azimuthal angle, for 1% and 5% composites obtained from the scattering of x incident and y incident X-rays.

5.4 Mechanical properties

5.4.1 Dynamic moduli

Dynamic mechanical analysis (DMA) is commonly used for the analysis of thermo-mechanical properties of materials. The storage modulus (E') and the loss modulus (E'') are two important parameters determined by DMA. The storage modulus is related to the energy stored elastically by the material upon deformation and the loss modulus is related to the energy dissipated by the material. So the storage modulus is related to the stiffness and the loss modulus to the viscous dissipation of the material. The dynamic moduli (E' & E'') as a function of temperature, measured at a fixed frequency of 1 Hz are shown in Fig. 5.5 for nanocomposites with various concentrations of clay particles. From the storage-modulus vs. temperature curves (E'-T) in Fig. 5.5 (a) it is clear that there is a systematic increase in the modulus with increasing concentration of clay particles. The modulus improves by 40% with

the addition of 5 wt% clay particles. Similarly, the loss modulus also increases with the increase in concentration of clay particles, as shown by E''-T curves in Fig. 5.5 (b).

For each clay concentration, the loss modulus exhibit two peaks. Theses represent two different dynamical processes. The first peak, at a low temperature of roughly T< 40 °C is usually denoted as the β peak. The β peak is related to the small-length-scale motions of the polymer molecules. There is a relatively sharp drop in the storage modulus at temperatures corresponding to the β peak as can be seen in Fig.5.5 (a).

The second peak, at a high temperature of about 250 °C is usually denoted the α peak. The α peak is related to the motions on larger length scales, and is associated with the glass transition temperature (T_g) [10]. These peaks are quite broad which makes the glass transition temperature less distinct. This broadness of the α peaks indicates that the matrix has a heterogeneous structure. The curing of Bismaleimides involves a number of reactions and some maleimide groups remain un-reacted during curing[10]. The α peak exhibits a moderate shift towards higher temperature upon addition of clay, which indicates an increase of T_g.

Upon increasing the temperature, the mobility of polymer chains increases. Consequently the material state changes from glass to rubber like, corresponding to a sharp reduction in the storage modulus [10]. As can be seen in Fig. 5.5 (a), the storage modulus decreases significantly at temperatures corresponding to the α peak. It diminishes to roughly 1.42 GPa (almost 50% reduction) for the matrix at glass transition (T_g) temperature. For the cross-linked polymer under investigation this reduction in modulus at T_g is much lower than for linear amorphous polymers. The storage modulus may drop by three orders of magnitude at T_g for linear amorphous polymers [10]. This smaller decrease of the modulus at T_g is attributed to the highly crosslinked network structure that obstructs the dynamics of the polymer chains.

The heat deflection temperature (HDT), which is an important parameter for engineering polymers can also be determined from E'-T curves. The HDT is a crucial parameter for engineering polymers to judge the limits of their service temperature. We have determined the HDT values from E'-T curves (Fig. 5.5 a) as the points at which the storage modulus equals 1 GPa as suggested in [25]. The HDT value of the present matrix material is significantly larger than that of most engineering polymers. This high thermal stability of the system stems from the highly crosslinked network structure and the rigid aromatic moieties in the backbone[10]. The values of both HDT and T_g of this material are quite high, which renders it a potential candidate for high-temperature resistant composites. From the

intersection points of the storage modulus curves in Fig. 5.5 (a) it is quite clear that the HDT is increasing with the concentration of clay particles. The HDT value of the unfilled matrix is approximately 260 °C. It increases to 320 °C with 5 wt% of clay particles.

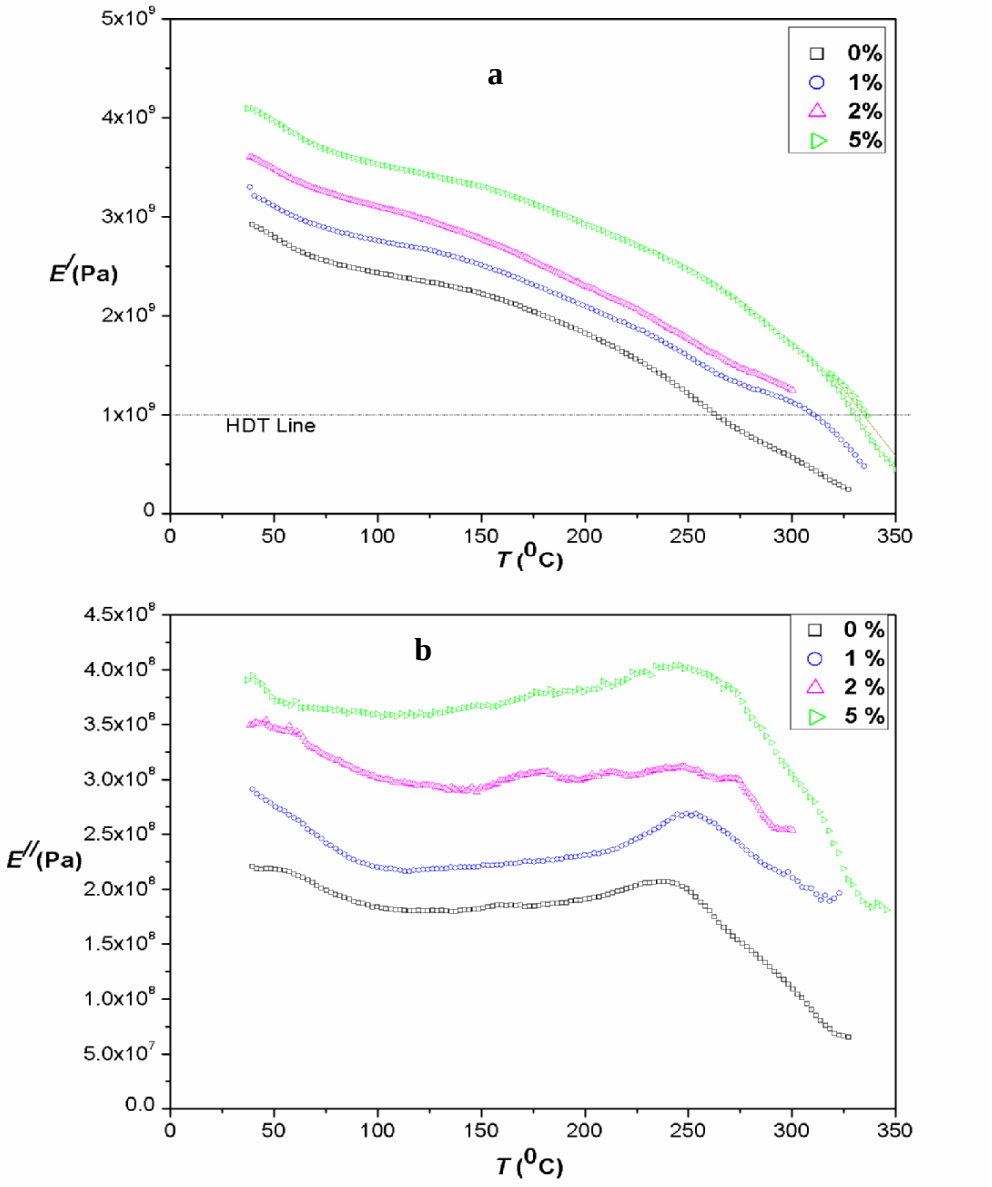

Figure 5.5 Dynamic moduli of nanocomposites with different clay contents (wt%) measured at 1 Hz. (a) Storage modulus ($E^{/}$) (b) Loss modulus ($E^{//}$).

5.5 Mechanical modeling of nanocomposites

The increase in the modulus of polymers by the addition of nanoparticles is a principal advantage of this kind of hybrid materials. So far many mechanical models have been proposed to explain the mechanical properties of polymer nanocomposites [17]. Among these models, the Halpin-Tsai model is widely used to predict the modulus of nanocomposites as a function of filler content from the moduli of the pure matrix and filler material and the aspect ratio of the filler [26]. According to the Halpin-Tsai model, in combination with the analytical continuation theorem [27], the complex modulus $E_c = E_c' + iE_c''$ of the nanocomposite can be predicted from the complex moduli $E_m = E_m' + iE_m''$ and $E_f = E_f' + iE_f''$ of the matrix and of the filler respectively as:

$$E_c = E_m \left[\frac{E_f(1+\varsigma\phi) + E_m(\varsigma - \varsigma\phi)}{E_f(1-\phi) + E_m(\varsigma + \phi)} \right] \qquad (5.1)$$

ς is the shape factor of the filler. For a given aspect ratio *w/t* (*w* width, *t* thickness) of the platelets, ς is equal to $2/3*(w/t)$ for the tensile moduli in the radial direction of the platelets. For the transverse moduli (platelets not aligned in the direction of loading) ς is taken equal to 2 [19]. The storage modulus of the filler is taken as 178 GPa, as reported in literature for MMT type clay platelets[13]. The loss modulus of the filler is assumed to be zero as it is supposed to be purely elastic. For the mechanical moduli of the pure matrix we use our own experimental results (see Fig. 5). ϕ is the volume fraction of the filler in the nanocomposite. In order to convert the weight percentages into volume fractions, the densities of the matrix and clay are taken as 1.3 and 1.98 g/cm^3 respectively. The weight percentage is converted into the volume fraction using [28]:

$$\phi = \frac{w_f / \rho_f}{w_f / \rho_f + (1 - w_f) / \rho_m} \qquad (5.2)$$

where ρ_f is the density of the clay particle and ρ_m is the density of the matrix and w_f is the weight fraction of particles.

Using the above-mentioned known values for the moduli of the pure matrix and the pure filler in the Halpin-Tsai expression (equation 1), the aspect ratio of the filler is determined so that the best fitting of the calculated modulus with the experimental storage modulus at low temperature is obtained. In this way apparent values of the aspect ratio are

obtained, which may be larger or smaller than that of the individual clay platelets because of incomplete exfoliation, aggregation etc. The values are collected in Table 5.1.

The Halpin-Tsai predictions of the storage modulus as a function of temperature for different concentrations of clay particles, along with the experimental data are shown in Fig. 5.6. The experimental data for the storage modulus (E') are fitted well by the Halpin-Tsai model, especially at low temperatures. The calculated moduli deviate from the experimental data at high temperatures above 200 °C. This deviation becomes more significant upon increase of the concentration of clay particles. The deviation of the calculated modulus at elevated temperature may be due to platelet-platelet interactions, which is not considered by the Halpin-Tsai model. [27] At high temperature, when the matrix is soft, rubber like, the particle network has a relatively large contribution to the modulus. Conversely, when the matrix is in the glassy state the contribution from the particle network is relatively unimportant [18].

Table 5.1 Aspect ratio of clay particles calculated by using Halpin-Tsai model

Clay concentration (wt %)	Aspect ratio(w/t)
0.5	93
1	45
2	42
5	23

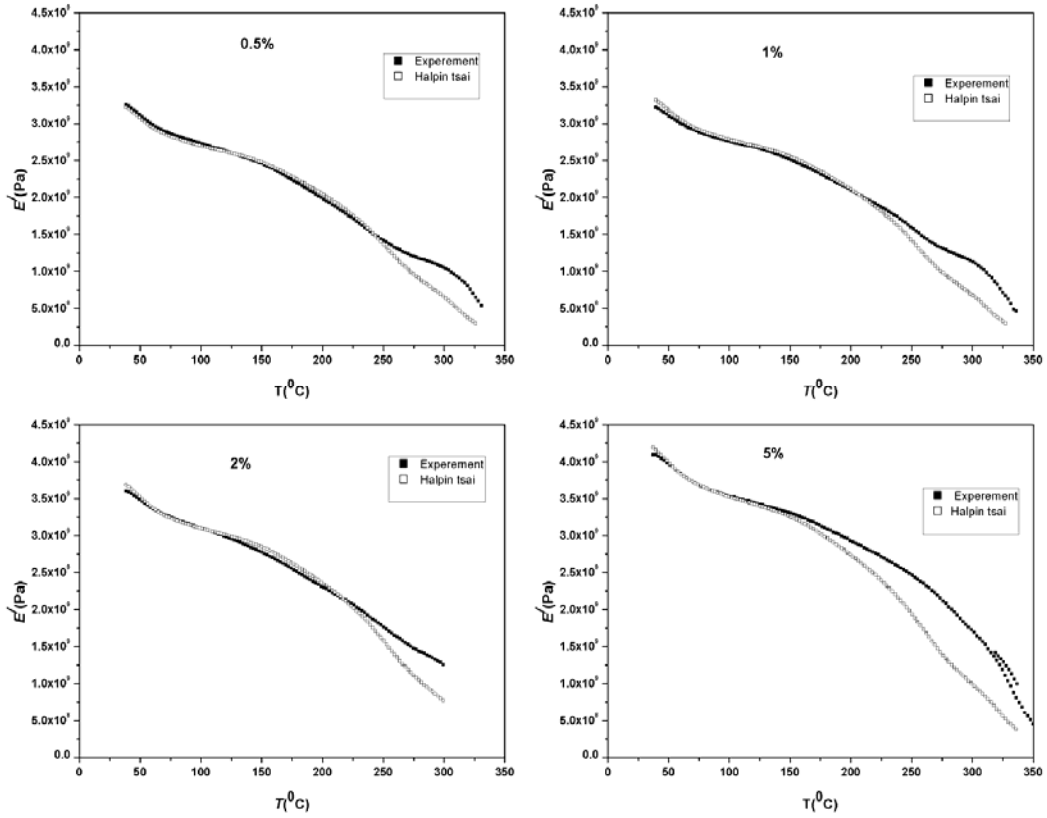

Figure 5.6 Comparison storage modulus ($E^{/}$) determined by Halpin-Tsai model and experimental results with different clay concentrations

The values for the apparent aspect ratios obtained from the fit to the Halpin-Tsai equation are plotted against the concentration of the clay particles in Fig. 5.7. It is clear from Table 5.1 and Fig. 5.7 that these aspect ratios decrease with increase of the concentration of clay particles. When we assume that the decrease of the apparent aspect ratio with increasing clay concentration is due to a decreasing degree of exfoliation, we can estimate for each clay concentration a mean number of platelets in a stack. This mean number of platelets in a stack is calculated by assuming that the width of a stack is the same as that of an individual platelet. By taking the aspect ratio of clay particles at 200 for MMT type platelets (200 nm width, 1 nm thickness)[29, 30], the numbers of platelets per stack corresponding to the aspect ratios from Halpin-Tsai fitting (see Table 1) are calculated. It turns out that for the lowest clay concentration of 0.5%, the stack size is almost 2 platelets per stack. The value rises to roughly 10 platelets per stack for 5% clay. Although a systematic increase in modulus is observed for the range of investigated clay concentrations, it would be even higher if the exfoliation would be better. The stiffness of the nanocomposites is primarily affected by the effective aspect

ratio of the particles. For low concentrations of particles, the effective aspect ratio is high and the relative contribution to the stiffness is large. On the other hand with increasing particle concentration the effective aspect ratio drops and the reinforcing efficiency is decreased. If the aspect ratio drops too much with increase in filler amount then further addition of the filler will not improve the stiffness. The Halpin-Tsai model can explain the modulus of the nanocomposite without considering confinement effects of filler upon the matrix. It means the reinforcing mechanism in nanocomposites is similar to the traditional composites. The aspect ratios determined here are effective values, which may be influenced by effects of distribution, polydisparsity and shape variations of the platelets.

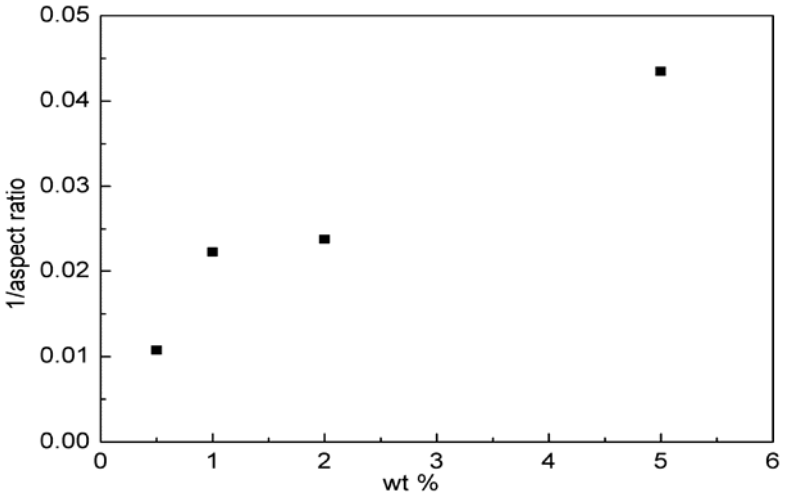

Figure 5.7 Relation between apparent aspect ratio and clay concentration

5.6 Conclusion

The thermoset resin investigated in this study exhibits excellent thermo-mechanical properties, which render it a potential candidate to be used for high-temperature-resistant composites. The incorporation of the clay particles improves the thermo-mechanical properties. The elastic modulus and heat deflection temperature improve with increasing concentration of clay particles. The preparation method discussed in this paper leads to relatively low levels of exfoliation. Shrinkage in one direction upon the evaporation process leads to alignment of platelets, which may also be beneficial for the mechanical properties. The stiffness of the nanocomposites has been modeled by the Halpin-Tsai model. This model reproduces the experimental data reasonably well. From the model analysis it also turns out that the degree of exfoliation decreases upon increasing concentration of clay particles. The agreement of the model prediction with the data supports the idea that the reinforcing

mechanism of the nano-clay composite is similar to micro-composites and not influenced by confinement effects of filler on polymer.

5.7 References

[1] Pavlidou S, Papaspyrides CD. A review on polymer layered silicate nanocomposites. Prog Poly Sci. 2008;33(12):1119-1198.

[2] Ray SS, Okamoto M. Polymer/layered silicate nanocomposites: A review from preparation to processing. Prog Poly Sci. 2003;28 (11):1539–1641.

[3] K.Hbaieb, Q.X.Wang, Y.H.J.Chia, B.Cotterell. Modeling stiffness of polymer clay nanocomposites. Polymer. 2007;48(3):901-909.

[4] Termonia Y. Structure-property relationships in nanocomposites. Polymer. 2007;48(23):6948-6954.

[5] Bitinis N, Hernandez M, Verdejo R, Kenny JM, Lopez-Manchado MA. Recent advances in clay/polymer nanocomposites. Advanced Materials. 2011;23(44):5229-5236.

[6] Xuhai Xiong, Ping Chen, Qi Yu, Nengbo Zhu, BaichenWang, Zhang J, et al. Synthesis and properties of chain-extended bismaleimide resins containing phthalide cardo structure. Polymer International. 2010;59(12):1665-1672.

[7] Haoyu Tang, Naiheng Song, Zihong Gao, Xiaofang Chen, Fan X, Xiang Q, et al. Synthesis and properties of 1,3,4-oxadiazole-containing high-performance bismaleimide resins. Polymer. 2007;48(1):129-138.

[8] Tang H, Li W, Fan X, Chen X, Shen Z, Zhou Q. Synthesis, preparation and properties of novel high-performance allyl-maleimide resins. Polymer. 2009;50(6):1414-1422.

[9] Gu AJ, Liang GZ, Lan LW. A high-performance bismaleimide resin with good processing characteristics. J App Poly Sci. 1996;62(5):799-803.

[10] Cristea M, Gaina C, Ionita DG, Gaina V. Dynamic mechanical analysis on modified bismaleimide resins. J Ther Anal Calo. 2008;93(1):69-76.

[11] Ursache O, Gaina C, Gaina V, Musteata VE. High performance bismaleimide resins modified by novel allyl compounds based on polytriazoles. J Poly Res. 2012;19(10):9968-9968.

[12] Faraz MI, Bhowmik S, De Ruijter C, Laoutid F, Benedictus R, Dubois P, et al. Thermal, Morphological, and Mechanical Characterization of Novel Carbon Nanofiber-Filled Bismaleimide Composites. J App Poly Sci. 2010;117(4):2159-2167.

[13] Fornes TD, Paul DR. Modeling properties of nylon 6/clay nanocomposites using composite theories. Polymer. 2003;44(17):4993-5013.

[14] Ji XL, Jing JK, Jiang W, Jiang BZ. Tensile modulus of polymer nanocomposites. Poly Eng Sci. 2002;42(5):983-993.

[15] Weon JI, Sue HJ. Effects of clay orientation and aspect ratio on mechanical behavior of nylon-6 nanocomposite. Polymer. 2005;46(17):6325-6334.

[16] Anoukou K, Zairi F, Nait-Abdelaziz M, Zaoui A, Messager T, Gloaguen JM. On the overall elastic moduli of polymer-clay nanocomposite materials using a self-consistent approach. Part I: Theory. Comp Sci Tech. 2011;71(2):197-205.

[17] Wang G-T, Liu H-Y, Yu Z-Z, Mai Y-W. Evaluation of Methods for Stiffness Predictions of Polymer/Clay Nanocomposites. Journal of Reinforced Plastics and Composites. 2009;28(13):1625-1649.

[18] Picken SJ, Korobko AV, Mendes E, Norder B, Makarova VV, Vasilyev GB, et al. Mechanical and thermal properties of polymer micro- and nanocomposites. Journal of Polymer Engineering. 2011;31(2-3):269-273.

[19] Es Mv. Polymer-clay nanocomposites : The importance of particle dimensions PhD Thesis. Delft University of Technology, 2001.

[20] Grigoriadi K, A. Giannakas, A. Ladavos, Barkoula N-M. Thermomechanical behavior of polymer/layered silicate clay nanocomposites based on unmodified low density polyethylene. Poly Eng Sci. 2013;53(2):301-308.

[21] Kinloch AJ, A.C.Taylor. The mechanical properties and fracture behavior of epoxy-inorganic micro-and nano-composites. J Mat Sci. 2006;41(11):3271-3297.

[22] E.Unsal, J.Drum, O.Yucel, Nugay II, Yalcin B. Real time measurement system for tracking birefringence,weight,thickness,and surface temperature during drying of solution cast coatings and films. Review of Scientific Instruments. 2012;83(025114):1-10.

[23] J.S.Machell, J.Greener, Contestable BA. Optical properties of solvent cast polymer films. Macromo. 1990;23(1):186-194.

[24] A.M.Nasr. Characterization of polymer films for optical applications. Poly Tes. 2002;21(3):303-306.

[25] Vegt AKvd, L.E.Govaert. Polymeren: Van Keten tot Kunststof: DUP Blue Print, Delft; 2003.

[26] Halpin J, Kardos J. The Halpin-Tsai equations : A review. Poly Eng Sci. 1976;16(5):344-352.

[27] Ozdilek C, Norder B, J.Picken S. A study of the thermomechanical behavior of Boehmite-polyamide-6 nanocomposites. Thermoch Act. 2008;472(1-2):31-37.
[28] Zare-Shahabadi A, Shokuhfar A, Ebrahimi-Nejad S, Arjmand M, Termeh M. Modeling the stiffness of polymer/layered silicate nanocomposites: More accurate predictions with consideration of exfoliation ratio as a function of filler content. Poly Tes. 2011;30(4):408-414.
[29] W.Beall G, E.Powell C. Fundamentals of Polymer-clay nanocomposites. Cambridge: Cambridge University Press; 2011.
[30] Tjong SC. Structural and mechanical properties of polymer nanocomposites. Materials Science & Engineering R-Reports. 2006;53(3-4):73-197.

Appendix

Halpin-Tsai model

Halpin-Tsai model is widely used to predict the stiffness of the composites with various geometries of the filler. The composite modulus predicted by Halpin-Tsai equation is given by:

$$\frac{E_c}{E_m} = \frac{1+\varsigma\eta\phi}{1-\eta\phi} \quad \text{in which} \quad \eta = \frac{(E_f / E_m)-1}{(E_f / E_m)+\varsigma} \qquad (1)$$

where E_c and E_m represent Young's modulus of the composite and matrix, respectively, E_f represents the Young's modulus of filler, ζ is a shape factor depending on geometry and loading direction and ϕ is the filler volume fraction.

The shape factors for the moduli of the composites determined by comparing the model with finite element modeling calculations are given by:

(a) For platelets (width *w* and thickness *t)*

$\zeta = \frac{2}{3}\left[\frac{w}{t}\right]$ in the radial direction of platelets, E_{11} or E_{22}

$\zeta = 2$ perpendicular to the platelets, E_{33}

(b) The shape factors for fibers (length *l*, diameter *d*) are

$\zeta = 2$ perpendicular to the fiber direction

$\zeta = 2\left[\frac{l}{d}\right]$ in the fiber direction,

Rewriting the equation 1 the physical nature of Halpin-Tsai model becomes clearer:

$$E_c = E_m\left[\frac{E_f(1+\zeta\phi)+E_m(\zeta-\zeta\phi)}{E_f(1-\phi)+E_m(\zeta+\phi)}\right] \qquad (2)$$

When $\zeta \to 0$, the Halpin-Tsai equation reduces to series model (lower bound):

$$\frac{1}{E_c} = \frac{\phi}{E_f} + \frac{1-\phi}{E_m} \qquad (3)$$

For $\zeta \to \infty$, the Halpin-Tsai model reduces to parallel model given as (upper bound):

$$E_c = E_f \phi + E_m (1-\phi) \qquad (4)$$

The series model underestimates the nanocomposite modulus. On the other hand the parallel model overestimates the nanocomposite modulus. Halpin-Tsai model works between these two extreme limits.

For randomly oriented particles in the matrix, 3D finite element modeling predicts that the composite modulus can be obtained by averaging over the particle orientation[19]:

$$E_c = \beta_{\|} E_{c\|} + \beta_{\perp} E_{c\perp} \qquad (5)$$

where $\beta_{\|} + \beta_{\perp} = 1$, $E_{c\|}$ and $E_{c\perp}$ are parallel and transverse moduli with respect to the particle alignment calculated using Halpin –Tsai model with $\varsigma = \frac{2}{3}\frac{w}{t}$ for $E_{c\|}$ and $\varsigma = 2$ for $E_{c\perp}$ the platelet particles. The values of $\beta_{\|}$ and $\beta_{\perp}$ are 0.49 and 0.51 respectively for platelet.

Chapter 6

Creep and Recovery Behavior of Bismaleimide/Clay Nanocomposites: Characterization and Modeling

Abstract

In this paper we report creep and recovery behavior of nanocomposites based on a high-temperature-resistant thermosetting matrix. Nanocomposites with up to 2 wt% of organically modified clay were prepared with a high-temperature-resistant Bismaleimide resin. The creep and recovery behavior was investigated under various stress levels and at various temperatures. The addition of clay improves the creep resistance of the matrix. Creep behavior was modeled by a modified form of Burgers' model by introducing a stretched exponential function. This 'stretched Burgers' model satisfactorily describes the creep behavior of the matrix and nanocomposites. A critical analysis of the creep behavior was done, to explain the mechanisms involved in creep. The role of filler on the system dynamics has been also discussed and an interesting finding discovered from the stretched Burgers' model results. The model results suggest that the dynamics of the filled system is independent of the filler, which is scientifically quite interesting in the field of nanocomposites. The multiple cycle creep and recovery behavior of the matrix was also investigated and the Boltzmann superposition principle applied to describe the multistep loading creep response.

6.1 Introduction

Polymers are viscoelastic materials having time dependent mechanical properties. When a constant load is applied the deformation increases with time which is known as creep. Polymeric materials are subjected to different stresses for a period of time during their usage. They are commonly placed under a constant load for a longer duration or stresses are applied repeatedly in a working environment. Therefore, the mechanical response, notably the instantaneous and time dependent deformation, is crucial for applications requiring dimensional stability. Creep is a serious concern for polymers, impairing their service

durability and safety and it constitutes a limitation to their applications in aviation and automotive industries [1]. Thermoset polymers possess excellent dimensional stability because of their cross-linked network structure. Their creep resistance is much better than that of thermoplastics. It is quite hard to deform this kind of polymeric materials, having structure entrapped by entanglements and covalent bonds [2]. Thermosets are widely used as matrix for composites for various applications including aviation, automobile, sports and buildings [3].

The use of nano-sized fillers to modify the polymer properties has received considerable attention. The stiffness, strength, and toughness are improved by the nanoscale inclusions. Promising effects of nanoparticles on creep resistance has also been reported in several studies [4-7]. However, loose agglomerates of particles and poor filler-matrix interactions still impede exploiting their full potential [8]. The literature is overwhelmed by the creep studies of thermoplastic nanocomposites but reports concerning thermosets are very limited and contradictory [9, 10]. Zhang et al. [9] studied the creep response of carbon nanotubes (CNT) epoxy composites. The creep strain of epoxy reduced significantly with CNT at lower weight fraction (up to 0.1- 0.25wt %) and lower stress levels. With increase in CNT to 1 wt% further improvement of the creep resistance was badly affected by poor dispersion. Moreover, the CNT showed poor adhesion with the matrix at higher stress levels. Tehrani et al. [10] reported that the addition of 3wt% multiwall carbon nanotubes (MWCNT) in epoxy reduced the creep, however, the effect is more pronounced under the conditions of elevated temperature and high nano-identation creep load. The effect of graphene on creep behavior of epoxy was investigated in [11]. At low stress level and ambient temperature no difference was observed between the creep response of filled and unfilled epoxy. The graphene platelet-filled epoxy creeps significantly less at elevated temperature and higher levels of stress with optimum filler amount of 0.1wt%. The functionalized surface of graphene has better interactions with epoxy, which lead to increase in creep resistance. Starkova et al. [12] showed that MWCNTs did not influence the creep characteristics of the epoxy matrix, and other mechanical properties also remained unaffected. In another study of epoxy clay nanocomposites by nano-indentation test, 4wt% was found to be the optimal clay concentration to minimize creep strain [13].

The viscoelastic properties of nanocomposites have been modeled using both constitutive models and simulations. Plaseied and Fatemi [14] used the Findley model for predicting the long term creep compliance of 0.5wt% carbon nanofiber filled vinyl ester nanocomposites. Yang et al. [15] explained the creep behavior of polyamide clay nanocomposites by applying the Burgers' model and Findley law. Jia et al. [7] employed the

Burgers' model to illustrate the creep mechanism involved in polypropylene/MWCNT composites. A few examples can be found, in which the creep behavior of thermoset polymers and thermoset nanocomposites have been modeled by a modified form of Burgers' model [16-19]. An important assumption made in these studies is the consideration of characteristic time as a distribution function.

Reviewing the literature it turns out that creep behavior of thermoset nanocomposites is not well understood yet. There is still a lack of systematic experimental studies on the creep and creep-recovery performance of thermoset matrix based nanocomposites. Moreover the creep behavior of high-temperature resistant thermoset nanocomposites is rarely reported. However, the aerospace industry is very keen to use high-temperature resistant thermoset matrix composites. In this regard composites of Bismaleimide are getting attention due to their excellent thermal properties and low cost to performance ratio. Their processability is as easy as that of epoxy resins but performance is much better. The manufacturing defects are also minimum compared to high-temperature-resistant thermoset polyimides [20, 21]. To the best of our knowledge, no studies on the creep behavior of Bismaleimide nanocomposites have been reported yet. This motivated us to study the impact of nano-filler on the creep behavior of a recently developed high temperature-resistant Bismaleimide resin, claimed to be a potential candidate for high performance composites. Their use in structures under the conditions of elevated temperature demands high mechanical stability. It is important to know how the creep response of this resin is affected by the incorporation of nanofiller.

This study aims at investigating the creep and creep recovery of high- temperature-resistant Bismaleimide/clay nanocomposites under various loads and temperatures and to find an appropriate model for the description of creep.

6.2 Experimental

6.2.1 Materials

The resin used was a pre-polymer of Bismaleimide with trade name of "Homide 250" supplied by Hos-technik, Austria, in the form of a yellow powder. Organically modified clay, Cloisite 30B, was obtained from Southern Clay Products, USA. It is Montmorillonite (MMT) modified with bis-(2-hydroxyethyl) methyl tallow alkyl ammonium cations. The solvent *N*-Methyl-2-pyrrolidone (NMP) was obtained from Sigma Aldrich.

6.2.2 Nanocomposite preparation

A pre-polymer resin solution of 30wt% concentration in NMP solvent was prepared by magnetic stirring. An ultrasonication probe Sonotrode UIS-250LS by Hielscher Ultrasonics, GmbH was used to disperse the clay in NMP in a plastic vial of 25ml. The instrument was operated at 50% amplitude and 50% cycle time for 2 hrs to prepare a master batch dispersion with 5wt% clay. After that the master batch was diluted to 2.5wt% and ultrasonicated for 1 hr. Then both the diluted clay dispersion and resin solutions were mixed in appropriate proportions to prepare a resin clay mixture with various concentrations of clay particles. The resin clay solution mixture was magnetically stirred for 8 hr. After that, the mixture was poured in a glass dish. The dish was placed in a vacuum oven at 80 °C for 3 hr to evaporate the solvent and remove any entrapped air. In the mean time, the mixture was stirred intermittently with a spatula to avoid skin formation and agglomeration. The solvent was evaporated and the mixture dried to an extent that it could be easily poured into a mold. We used silicone-rubber molds with slots of dimensions length 25 mm, width 3 mm, and a depth 1 mm. After filing the mold, the samples were cured for 1 hr at each of the following temperatures: 80 °C, 120 °C, 140 °C, 160 °C, 180 °C and 200 °C .
The samples were removed from the molds after curing, and post cured at 220 °C for 4 hr. The samples were finished by removing the overflowed material and burrs using sand paper.

6.2.3 Creep and creep-recovery measurements

Creep and creep-recovery behavior was studied by a three point bending mode flexural tests using a Perkin Elmer DMA 7-e. The sample dimensions were 10 x 3 x 0.6mm. In order to ensure working within linear viscoelastic regime, different stress levels 10-50 MPa at an increment of 10 MPa at 23 °C were applied for plain matrix samples and the resulting strain as a function of time was monitored. The time allowed for both creep and recovery was 30 min at each stage. The recovery was done under almost zero force (20mN). Creep and recovery tests were conducted for organoclay reinforced samples with 1 and 2 wt% at stress levels of 20, 30 and 40 MPa at 23 °C . These tests were also conducted at different temperatures 23 °C, 50 °C, and 100 ^{0}C at a fixed stress of 40 MPa for all materials. Before each measurement a time of 2 min for was allowed to reach thermal equilibrium. Multiple

cycle creep and recovery experiments were also conducted for the pure matrix at 40 MPa at 23 °C by repeating the creep and recovery cycle 5 times for 30 min at each stage.

6.3 Modelling of creep

Modeling of the creep response allows a better understanding of the underlying deformation mechanisms and provides a design tool for long-term load bearing applications. The Burgers' model and Findley law are among the widely used viscoelastic models to describe the creep behavior of polymers. The Burgers model is more appropriate from the physical point of view. It is a combination of Maxwell and Kelvin-Voigt models in series as shown in Fig.6.1 [15].

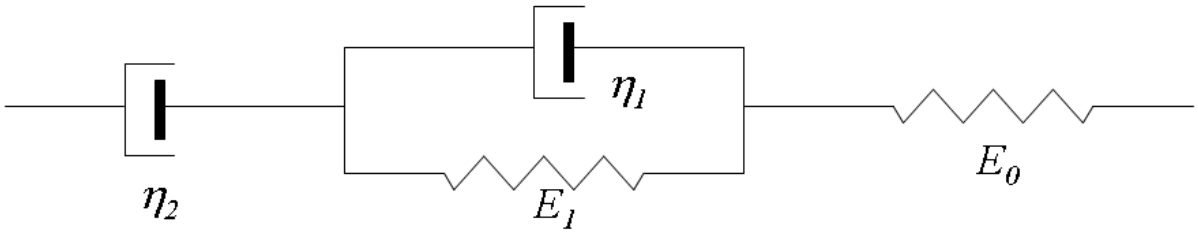

Figure 6.1 Schematic representation of the Burgers' model

Based on the constitutive relations of the elements, the creep behaviour can be represented by the Burgers' model as [15]:

$$\varepsilon(t) = \frac{\sigma}{E_0} + \frac{\sigma}{E_1}\left(1 - \exp\left(\frac{-t}{\tau}\right)\right) + \frac{\sigma}{\eta_2}t \quad \text{in which} \quad \tau = \frac{\eta_1}{E_1} \qquad (6.1)$$

Here t denotes the time after loading and $\varepsilon(t)$ the strain at t, while E_0 and η_2 are the elastic modulus and viscosity of the Maxwell spring and dashpot respectively, E_1 and η_1 the elastic modulus and viscosity of the Kelvin-Voigt spring and dashpot respectively, τ the retardation time and σ the applied stress.

A single retardation time usually is not sufficient to describe the relaxation process in real polymers as there usually is a distribution of retardation times [22, 23]. Secondly for network polymers we assume that there will be no viscous flow, and the recovery should be

complete [18]. Thus the Maxwell viscous element η_2 can be omitted. By incorporating these assumptions into equation 6.1 the modified model we name here as the "stretched Burgers' model" is given by:

$$\varepsilon(t) = \frac{\sigma}{E_0} + \frac{\sigma}{E_1}\left(1 - \exp\left(-\left(\frac{t}{\tau}\right)^n\right)\right) \text{..... (6.2)}$$

where *n* determines the measure of stretching.

The Findley, law is an empirical relation that is often used to describe the long term creep behavior of polymeric materials. It reads [24]

$$\varepsilon(t) = \varepsilon_0 + \varepsilon_1 t^n \text{ ..... (6.3)}$$

where $\varepsilon(t)$ is strain at time *t*, ε_0 the initial instantaneous strain and ε_1 the amplitude of the transient strain and *n* the time exponent, usually assumed to be independent of the stress, its value is generally less than one.

In a number of studies the ability of the Findley law to fit the creep has been found to be quite satisfactory [7, 14, 15, 25]. It has the advantage of being mathematically simple. However, some limitations are associated with this model like the inability to explain the creep mechanism [14].

By comparing the stretched Burgers' equation (6.2) and the Findley equation (6.3) it turns out that in the stretched Burgers' model the strain will always approach a plateau, whereas according to the Findley equation the strain increases without bounds. It can be inferred that for short time scales both models behave similarly. Upon expanding the stretched exponential $\exp\left(-\left(\frac{t}{\tau}\right)^n\right)$ in equation (6.2) for short times ($t < \tau$), and ignoring all but the first terms, equation (6.2) reduces to:

$$\varepsilon(t) = \frac{\sigma}{E_0} + \frac{\sigma}{E_1 \tau^n} t^n \text{ ..... (6.4)}$$

Equating $\frac{\sigma}{E_0}$ to ε_0 and $\frac{\sigma}{E_1 \tau^n}$ to ε_1 equation (6.4) turns into exactly the same form as the Findley power law. Mathematically, the Findley law is the short time expansion of the stretched Burgers' model and for short time scales both models will be equivalent and behave similarly. However, from a physical point of view the stretched Burgers' model is a better option to be used for describing the long term creep behavior of the thermosetting matrices. It is clearly illustrated in Fig. 6.2 that the predicted creep strain curves from both the stretched

Burgers' model and Findley's law coincide for a short time span, while for longer times the Findley law curve deviates from the data considerably. However, the stretched Burgers' model complies with the data for the whole experimental time scale.

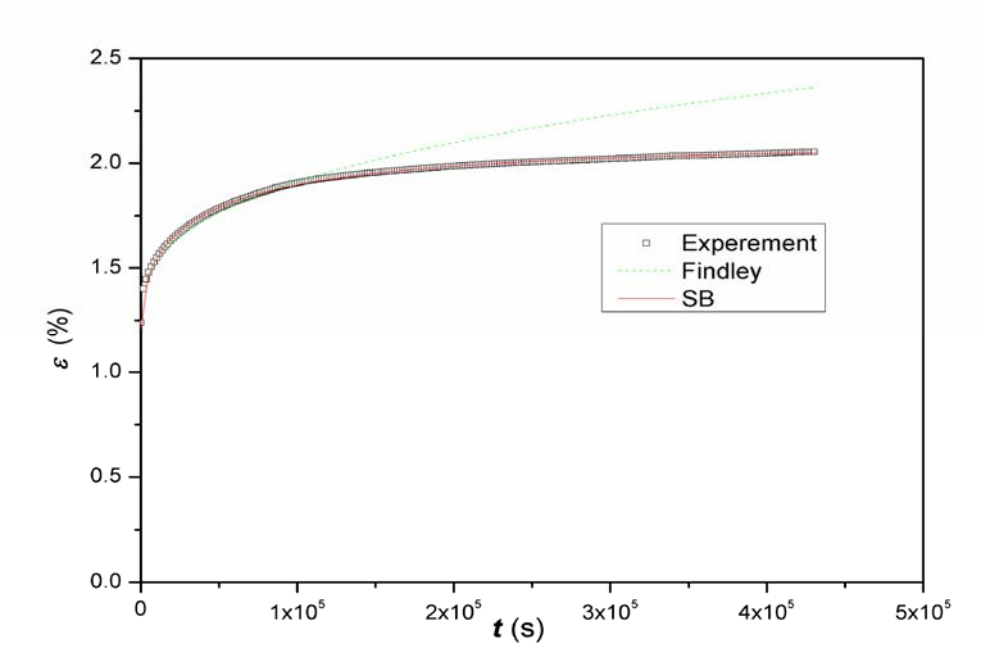

Figure 6.2 Creep of the pure matrix material measured at 40 MPa at 23 °C, together with fitted curves of the stretched Burgers' model (SB) and Findley's law. The Findley curve was forced to coincide with the Burgers curve at short times, as is required from equation. 6.3 and 6.4.

6.4 Results and discussion

6.4.1 Creep and recovery behavior of matrix

In order to have a broader over view of the viscoelastic characteristics of the matrix the samples were loaded for 30 min applying different stress levels and then unloaded for 30 min. The resulting creep and recovery behavior is shown in Fig. 6.3. Figure 6.4 shows the creep compliance ($J = \varepsilon/\sigma$), measured for different stress levels as a function of time. We can see clearly from this figure that the creep compliance curves for all the loading levels roughly fall on the same line. The strain is proportional to the stress, hence the applied loading is within the linear regime.

All the loading curves in Fig. 6.3 have same general features. Deformation increases by raising the stress levels and also gradually increases with time. This time dependence is a characteristic feature of viscoelastic materials [1]. From Fig. 6.3 distinct deformation stages of creep can be identified. There is a relatively large instantaneous increase of the strain, corresponding to the elastic element E_0 in Fig. 6.1, followed by delayed strain or primary creep stage which increases with time at a decreasing creep rate. Finally the material enters into steady creep state or secondary creep. Upon the removal of load some of the strain is recovered immediately which was also instantaneous during the loading and after that the strain decays over time which is the viscoelastic recovery. Most of the strain is recovered during the unloading with minor residual strain left in all the cases which is more visible for higher stress levels. For a perfect viscoelastic solid the material should recover 100% with zero permanent strain [1]. It seems from the recovery curves that the material would reach zero residual stain asymptotically after longer recovery times as the curves are continuously decaying. Secondly it is a thermoset system which is chemically crosslinked and we donot expect viscous flow as the stress levels are within linear viscoelastic limits. So it will recover completely given enough time [2].

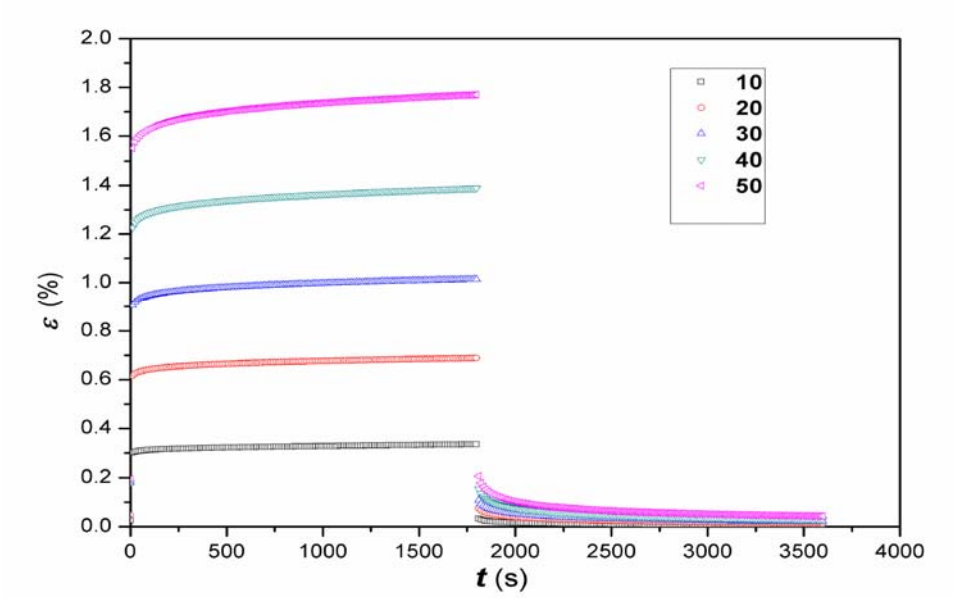

Figure 6.3 Creep and recovery response of the matrix under various stress levels (MPa) at 23 °C

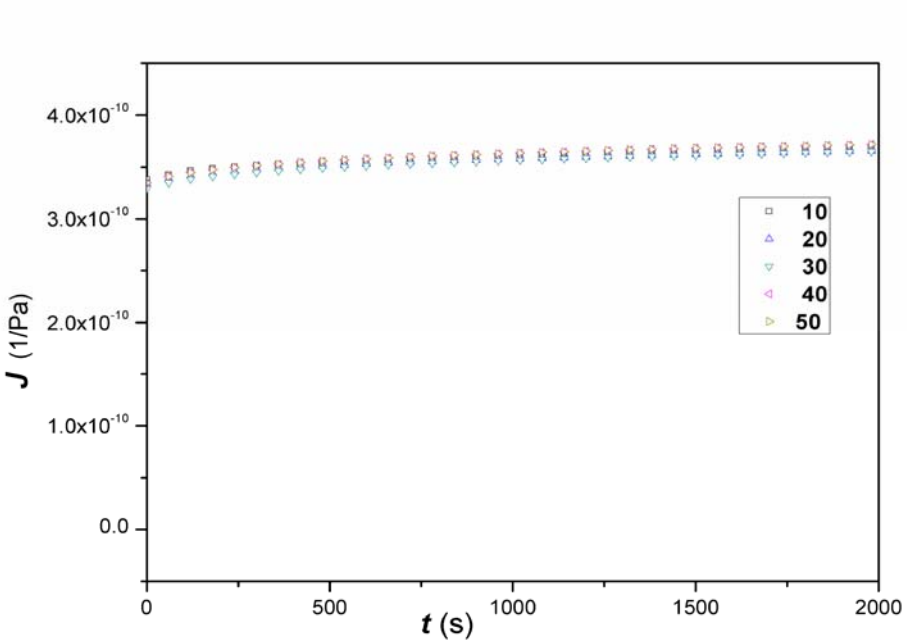

Figure 6.4 Compliance of the matrix as a function of time at different stress levels (MPa) at 23 °C

6.4.2 Effect of temperature on creep behavior

The role of temperature in creep is very critical. The creep rate and the magnitude of deformation usually increase with increasing temperature [15, 25]. Bismaleimides are selected for high-temperature applications, because of their favorable resistance to high temperatures. Their mechanical stability at elevated temperature is crucial. Therefore, we investigated creep and recovery behavior at different temperatures. The matrix was subjected to loading and unloading for 30 min at each stage at different temperatures at a stress level of 40 MPa. The creep and recovery response at different temperatures for the pure matrix material is shown in Fig. 6.5. The increase in deformation for 50 °C, 100 °C and 150 °C is 34%, 60% and 80% respectively compared to that at 23 °C. The initial elastic deformation increases significantly with increase in temperature, which implies that matrix has softened and the stiffness of the matrix is reduced at high temperature. A similar trend was observed in another study, in which the modulus dropped by 85% upon an increase in temperature from 30 °C to 150 °C [16]. The slope of the curves increases with increasing temperature, which means that the rate of viscoelastic deformation is accelerated. The deformation of polymeric materials is facilitated at high temperature and changing the molecular conformation becomes easier. This contributes to an enhanced rate of viscoelastic deformation. It is also observed from Fig. 6.5

that higher the temperature, the sooner the deformation reaches its plateau value. The deformation mechanisms contributing to the creep strain may include stretching of the networks and local segmental motions of the main chain and side chains which are highly sensitive to temperature in the glassy state [2]. The residual strain after removing the load increases with temperature as well, as shown in the recovery part of the Fig. 6.5. The unrecovered strain at 150 °C is 80% higher than that at 23 °C. However, the recovery curves are still decaying and they may reach zero asymptotically.

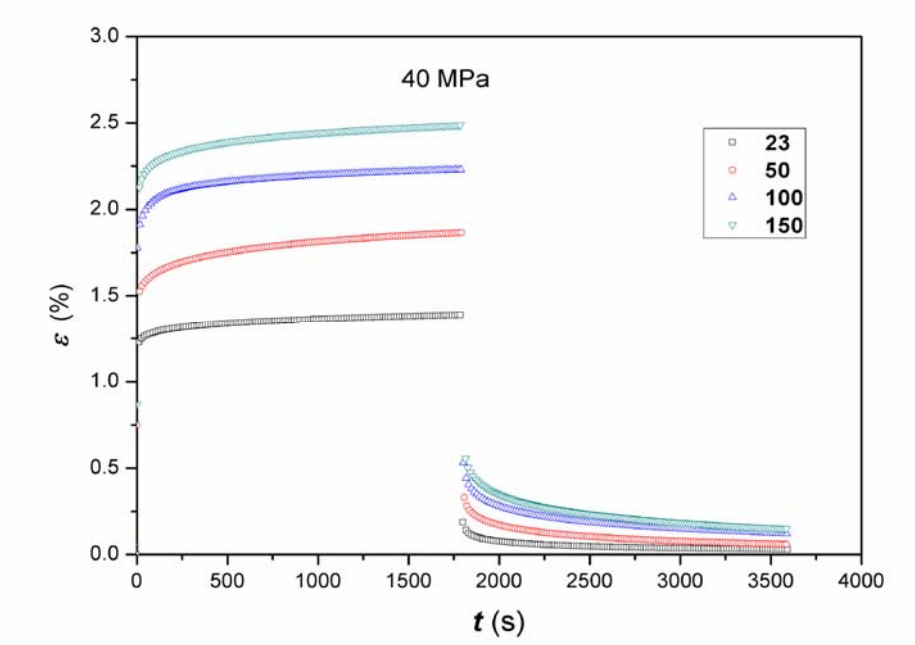

Figure 6.5 Creep and recovery response of matrix under various temperatures at 40MPa

6.5 Creep behavior of nanocomposites

Nanocomposites are claimed to have better creep resistance than unfilled polymeric materials[8]. We have also investigated the creep and recovery behavior of nanocomposites prepared by adding 1 wt% and 2 wt% of organically modified clay particles to the matrix. The creep and recovery behavior under various stress levels at a fixed temperature and under various temperatures at a fixed stress is shown in Fig. 6.6 and 6.7 (**in Appendix**) respectively. With increase in both temperature and stress, the creep strain increases for all materials. For all conditions, the creep strain of nanocomposites is lower than that of the pure matrix. This improvement in creep resistance is due to reduction in both elastic and viscoelastic components of the total creep strain. The improvement in creep resistance is more pronounced

at elevated temperature. For example creep strain at 100 °C under 40 MPa is reduced by 21% and 32% for 1 wt% and 2 wt% clay composites respectively compared to the unfilled matrix. Whereas at 23 °C under 40 MPa the creep strain reduced by 16% for 2 wt% and 5% for 1 wt% clay composite. With increase in temperature, the mobility of polymer chains increases and deformation becomes easier. The clay platelets can act as blocking sites and reduce the chain mobility consequently improving the creep stability [15, 26]. The particles can influence several aspects of molecular motion like stretching of chain segments and friction between molecular chains which in turn decreases the creep strain. The recovery part for nanocomposites also shows some residual strain after unloading which increases with loading levels and temperature as shown in Fig. 6.6 and 6.7 respectively. However, the recovery of nanocomposites is higher than that of matrix; the residual strain is reduced by 50% at 100 °C for 2% of clay loading at 40 MPa. The addition of clay particles improves the stiffness of the material as revealed by the decreased initial strain for composites under all conditions.

6.6 Modeling creep behavior of nanocomposites

Modeling of creep behavior may yield a better understanding of the creep mechanisms, and may allow predictions to be made of the creep behaviour. The prediction of creep is much desired from the perspective of designing structural components. We have applied the stretched Burgers' model (SB) given in equation 6.2 to simulate the experimental data of nanocomposites. To fit the data with the SB model we have assumed that the parameters τ and n will be *independent* of filler concentration. The experimental results for the pure matrix and composites were fitted simultaneously, assuming the same values of τ and n for all materials, and allowing E_0 and E_1 to vary. These fits are shown in Fig. 6.8.

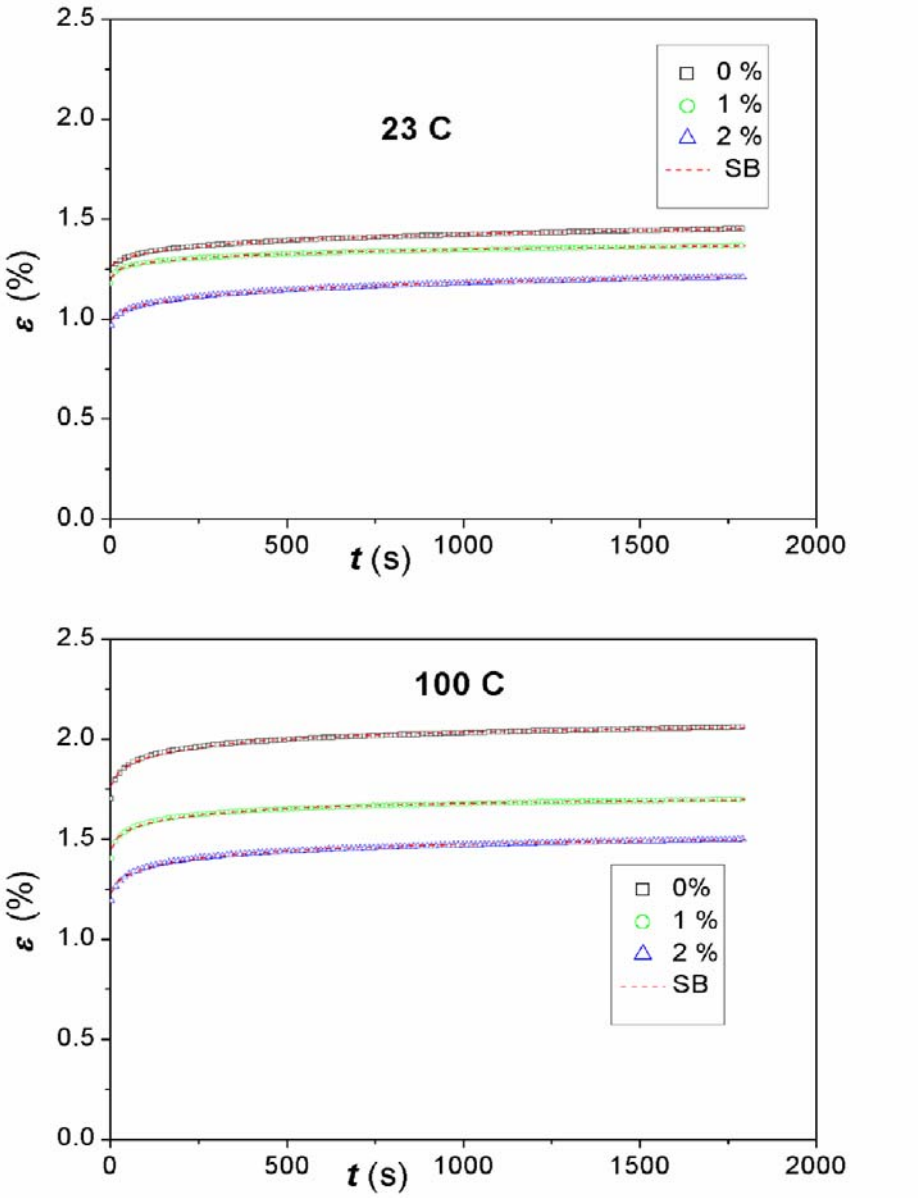

Figure 6.8 Fitted curves of the creep behavior of the nanocomposites by the stretched Burgers' model (SB) at 40 MPa at various temperatures and clay concentrations.

There is very good agreement between the fits and the experimental data. The model parameters of Bismaleimide matrix and its nanocomposites are summarized in Table 6.1. The instantaneous Maxwell spring modulus, E_0, determines the instantaneous strain, which can also be recovered instantaneously upon removal of the stress. The instantaneous modulus E_0 is improved by the addition of clay particles and becomes higher than that of the pure matrix under all conditions.

The increase of E_0 follows a nearly linear increase with the concentration of clay particles at 100 °C. However, at 23 °C the relation between the concentration of clay particles and E_0 is not well-defined as only for the higher concentration of 2 wt% E_0 increases by 30%,

while for 1 wt% the improvement is marginal. These results indicate that the exfoliation of the clay particles for this system is tricky and that it is difficult to obtain reproducible intercalation/exfoliation levels. The relaxation modulus, $E_{1,}$ which represents the stiffness of the material for a short term does not seem to correlate at all with the concentration of clay particles. The modulus, $E_{1,}$ of the pure matrix is extremely large. This can be associated with the dense network structure of the matrix.

The fact that the model fits are quite good confirms the assumption that τ *does not depend on the concentration of clay particles*. Thus the dynamics of the composite is mainly governed by the dynamics of the matrix. This assumption is interesting in itself and this aspect has never been highlighted in creep studies of nanocomposites. This result is very helpful for developing further understanding of the mechanics of the nanocomposites. So it warrants serious research efforts including experimental, theoretical and numerical studies to be conducted for further investigations and establishing the role of the filler on the mobility of polymer chains (composite dynamics). Many research efforts are underway to understand the correlation between the dynamics and mechanical properties of the nanocomposites.

The invariance of τ with filler concentration is also supported by the Halpin-Tsai micromechanical model. According to the Halpin-Tsai model the composite modulus (E_c) is a function of the matrix and filler moduli, filler volume fraction (ϕ) and the shape factor (ς). Following the analytical continuation theorem the complex modulus (E_c^*) can also be calculated from the same Halpin-Tsai expression. The complex modulus has real and imaginary parts. The real part is the storage modulus (E_c') and the magnitude of the imaginary part is the loss modulus (E_c''). According to the Halpin-Tsai model the moduli E_c' and E_c'' both increase by the addition of filler. In most nanocomposite systems the filler modulus is much larger than that of the matrix ($E_f \gg E_m$). Under such conditions for high aspect ratio particles the Halpin-Tsai equation reduces to [27]:

$$E_c^* = E_m^*(1+(1+\varsigma)\phi) \quad \text{..... (6.5)}$$

From this relation (equation 6.5) it is clear that both E_c' and E_c'' increase by a same constant factor for a given volume fraction of filler. Thus the ratio of moduli for filled and unfilled samples remains constant. Moreover, the increase in moduli by a constant factor is also frequency independent. So the relaxation time distribution will be independent of filler concentration. This also implies that in the time domain (creep) the retardation time distribution will be independent of filler concentration. Hence the assumption made in

stretched Burgers' model that τ and n can be chosen to be independent of filler concentration is in line with the Halpin-Tsai theory.

All the parameters determined from the fits of creep strain curves sharply decreased when the temperature is increased from 23 to 100 °C as can be seen in Table 6.1. The elastic stiffness E_0 is reduced by 27 and 17 % for matrix and 2 wt% clay composite respectively by increasing the temperature from 23 to 100 °C. The τ is reduced by 89% with an increase in temperature from 23 to 100 °C. A significant reduction in E_0 indicates that the matrix is softened with the increasing temperature. The reduction in τ at high temperature can be attributed to the accelerated deformation of the polymer. At high temperature the mobility of polymer increases and therefore the deformation is accelerated leading to reduction of the characteristic time scale [9].

The stretched exponent, n, values are also quite low (average 0.35) this implies a wide distribution of τ because n=1 represents for a single relaxation time and n=0 an infinitely wide spectrum of characteristic times [23]. Multiple mechanisms at a molecular scale may lead to a broad distribution of characteristic time scales. However, the specific mechanism taking place at the atomistic scale is not well understood at present. Moreover, the value of n is roughly invariant with the temperature variation as can be seen in Table 1. This means the broadness of the distribution time scales is not changed by temperature variation.

Table 6.1 Stretched Burgers' Model parameters at 40MPa determined by fitting of the model to the experimental data

T **^{0}C**	**Filler content wt%**	***E_0*** **GPa**	***E_1*** **GPa**	***τ*** **s**	***n***
23	0	3.3	10.5	1880	0.33
	1	3.4	14.5	1880	0.33
	2	4.3	9.2	1880	0.33
100	0	2.4	9.39	192	0.36
	1	2.9	11.7	192	0.36
	2	3.5	10.2	192	0.36

In summary, the creep compliance as a function of time is remarkably well described by the stretched Burgers' model. The determined moduli results (E_0 and E_1) are weird due to the difficulty in obtaining the reproducible exfoliated/ intercalated levels for the present system. However, from a physics point of view and the quality of fits is good enough to propose that the stretched Burgers' model very suitable for modeling the thermoset matrices and their nanocomposites.

6.7 Multiple cycle creep and recovery behavior

The materials subjected to cyclic loading can fail at much lower levels of stress than those in static cases. Moreover, the process of physical aging may also happen in viscoelastic materials when subjected to loads for longer times at a certain temperature. Both the cyclic loading and physical aging may change the mechanical properties of the material. We investigated the creep and recovery behavior of the matrix by applying a multistep loading and unloading programme. The multi-cycle creep and recovery behavior of the matrix at a stress level of 40 MPa at 23 °C is shown in Fig. 6.9. The curves in the creep parts have similar shapes for all the five loading cycles. The creep strain increases with the number of creep cycles. From the unloading curves it also appears that the ir-recoverable strain increases with the number of cycles. It may be a consequence of the fact that creep strain has not relaxed completely within the given unloading time. So the residual strain which was not relaxed in previous cycle is still relevant in the next creep and recovery cycle [28]. The Boltzmann superposition principle can effectively describe the creep response of a linear viscoelastic material subjected to multistep loading programme. According to the Boltzmann principle, the creep in a specimen is a function of entire loading history and each loading step makes an independent and additive contribution to the total deformation. The generalized mathematical form of Boltzmann principle is given by:

$$\varepsilon(t) = \int_{-\infty}^{t} j(t-\tau_n)d\sigma(\tau_n) \quad \text{..... (6.6)}$$

where $j(t-\tau_n)$ is the creep compliance function, and τ_n is the time when a load $d\sigma$ is applied.

We used the Boltzmann superposition principle and applied the stretched Burgers' model (SB) to describe the multistep loading creep compliance of the material. There is a reasonable agreement between the creep response predicted by SB using the Boltzmann superposition principle and the experimental data as shown in Fig. 6.9. The fact that fits are so

good for the same parameters of SB model at each loading and unloading step confirms that the material is linear viscoelastic under the applied conditions. There is no contribution of plastic deformation to the creep strain of the material. The increase in irrecoverable strain with increasing the multistep loadings is just a consequence of the loading history of the material.

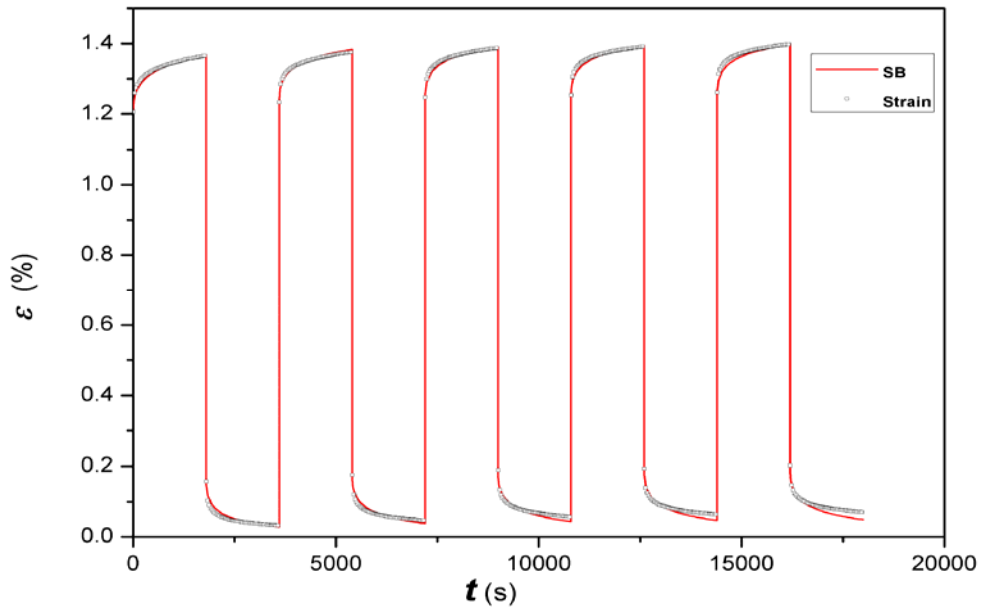

Figure 6.9 Fitted curves of multiloading creep strain of an unfilled sample with the stretched Burgers' model (SB) using Boltzmann superposition (at 23 °C and 40 MPa)

6.8 Conclusion

The investigated thermoset matrix shows good creep stability. Creep strain shows large sensitivity to the temperature and stress levels. The incorporation of clay particles up to 2 wt% further improved the creep stability of the matrix. The creep behavior of the matrix and the nanocomposites has been successfully described by the stretched Burgers' model. The model analysis indicates that the dynamics of the system is mainly controlled by the matrix and is independent of the filler amount. This is an interesting finding from the creep results and has not been reported yet. We believe this is helpful for developing a better understanding of thermoset nanocomposites mechanics. The creep response of the matrix for multistep loading is satisfactorily described by the Boltzmann superposition principle.

6.9 References

[1] Y.M.Haddad. Viscoelasticity of engineering materials. London: Chapman&Hall; 1995.

[2] Stepto RFT. Polymer networks : Principles of their formation structure and properties. London: Blackie Academic&Professional; 1998.

[3] Nair CPR, Mathew D, Ninan KN. Cyanate ester resins, recent developments. In: Abe A, Albertsson AC, Cantow HJ, Dusek K, Edwards S, Hocker H, et al., editors. New Polymerization Techniques and Synthetic Methodologies, vol. 1552001. p. 1-99.

[4] Yang JL, Zhang Z, Schlarb AK, Friedrich K. On the characterization of tensile creep resistance of polyamide 66 nanocomposites. Part I. Experimental results and general discussions. Polymer. 2006;47(8):2791-2801.

[5] Seltzer R, Mai Y-W, Frontini PM. Creep behaviour of injection moulded polyamide 6/organoclay nanocomposites by nanoindentation and cantilever-bending. Composites Part B-Engineering. 2012;43(1):83-89.

[6] Luduena L, Vazquez A, Alvarez V. Viscoelastic behavior of polycaprolactone/clay nanocomposites. J Comp Mat. 2012;46(6):677-689.

[7] Jia Y, Peng K, Gong X-l, Zhang Z. Creep and recovery of polypropylene/carbon nanotube composites. International Journal of Plasticity. 2011;27(8):1239-1251.

[8] Zhou TH, Ruan WH, Yang JL, Rong MZ, Zhang MQ, Zhang Z. A novel route for improving creep resistance of polymers using nanoparticles. Comp Sci Tech. 2007;67(11-12):2297-2302.

[9] Zhang W, Joshi A, Wang Z, Kane RS, Koratkar N. Creep mitigation in composites using carbon nanotube additives. Nanotechnology. 2007;18(18).

[10] Tehrani M, Safdari M, Al-Haik MS. Nanocharacterization of creep behavior of multiwall carbon nanotubes/epoxy nanocomposite. International Journal of Plasticity. 2011;27(6):887-901.

[11] Zandiatashbar A, Picu CR, Koratkar N. Control of epoxy creep using Graphene. Small. 2012;8(11):1676-1682.

[12] Starkova O, Buschhorn ST, Mannov E, Schulte K, Aniskevich A. Creep and recovery of epoxy/MWCNT nanocomposites. Composites Part a-Applied Science and Manufacturing. 2012;43(8):1212-1218.

[13] Lam CK, Lau KT, Zhou LM. Nano-mechanical creep properties of nanoclay/epoxy composite by nanoindentation. Key Engineering Materials. 2007;334-335:669-672.

[14] Plaseied A, Fatemi A. Tensile creep and deformation modeling of Vinyl Ester polymer and Its nanocomposite. Journal of Reinforced Plastics and Composites. 2009;28(14):1775-1788.

[15] Yang J-L, Zhang Z, Schlarb AK, Friedrich K. On the characterization of tensile creep resistance of polyamide 66 nanocomposites. Part II: Modeling and prediction of long-term performance. Polymer. 2006;47(19):6745-6758.

[16] Li F, Larock RC, Otaigbe JU. Fish oil thermosetting polymers: creep and recovery behavior. Polymer. 2000;41(13):4849-4862.

[17] Marais C, Villoutreix G. Analysis and modeling of the creep behavior of the thermostable PMR-15 polyimide. J App Poly Sci. 1998;69(10):1983-1991.

[18] Mosiewicki MA, Marcovich NE, Aranguren MI. Creep behavior of wood flour composites made from Linseed oil-based Polyester thermosets. J App Poly Sci. 2011;121(5):2626-2633.

[19] Sheng X, Akinc M, Kessler MR. Creep behavior of bisphenol E cyanate ester/alumina nanocomposites. Materials Science and Engineering a-Structural Materials Properties Microstructure and Processing. 2010;527(21-22):5892-5899.

[20] Cristea M, Gaina C, Ionita DG, Gaina V. Dynamic mechanical analysis on modified bismaleimide resins. J Ther Anal Calo. 2008;93(1):69-76.

[21] Aijuan Gu, Liang G, Liang D, Ni M. Bismaleimide/carbon nanotube hybrids for potential aerospace application: I. Static and dynamic mechanical properties. Poly Adv Tech. 2007; 18(10): 835–840.

[22] Shaito A, Fairbrother D, Sterling J, D'Souza NA. Ethylene maleated amorphous propylene compatibilized polyethylene nanocomposites: Stress and temperature effects on nonlinear creep. Poly Eng Sci. 2010;50(8):1633-1645.

[23] Dean GD, Broughton W. A model for non-linear creep in polypropylene. Poly Tes. 2007;26(8):1068-1081.

[24] Findley W, Lai J, Onaran K. Creep and relaxation of nonlinear viscoelastic materials: with an introduction to linear viscoelasticity. New York: Dover Publications,Inc; 1989.

[25] Banik K, Karger-Kocsis J, Abraham T. Flexural creep of all-polypropylene composites: Model analysis. Poly Eng Sci. 2008;48(5):941-948.

[26] Dorigato A, Pegoretti A. Tensile creep behaviour of polymethylpentene-silica nanocomposites. Polymer International. 2010;59(6):719-724.

[27] Picken SJ, Korobko AV, Mendes E, Norder B, Makarova VV, Vasilyev GB, et al. Mechanical and thermal properties of polymer micro- and nanocomposites. Journal of Polymer Engineering. 2011;31(2-3):269-273.
[28] Adalja SB, Otaigbe JU. Creep and recovery behavior of novel organic-inorganic polymer hybrids. Polymer Composites. 2002;23(2):171-181.

Appendix

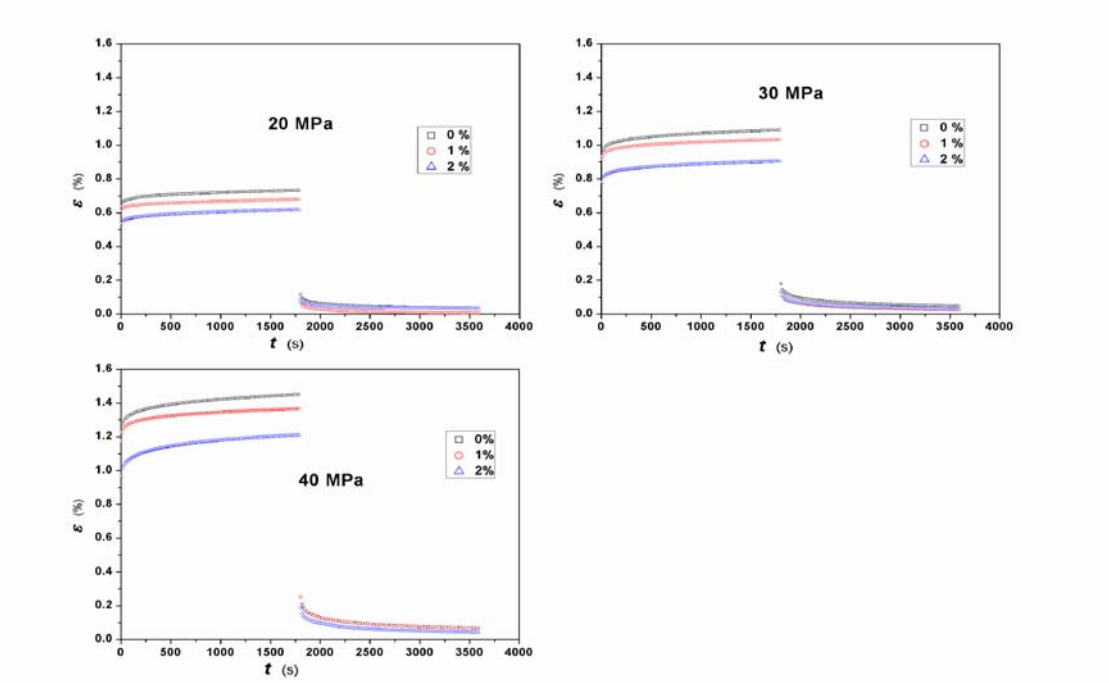

Figure 6.6 Creep and recovery behavior of nanocomposites under various stresses at 23 °C.

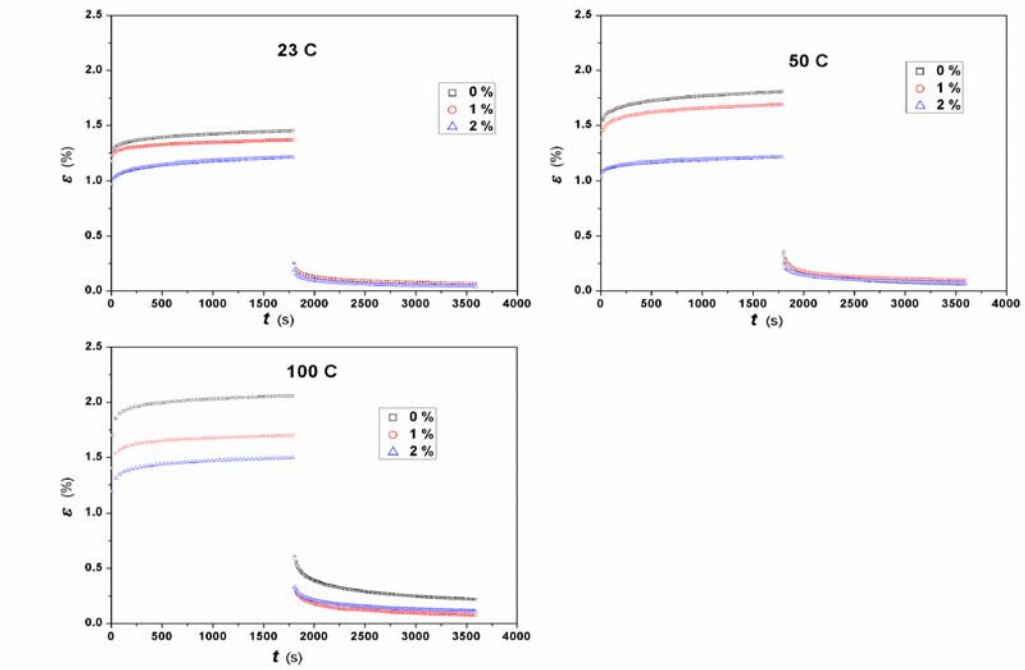

Figure 6.7 Creep and recovery behavior of nanocomposites at different temperatures at 40 MPa.

Chapter 7

Conclusions and recommendations

7.1 Conclusions

The toughest challenge was to work out a strategy for the synthesis of well dispersed and exfoliated nanocomposites and obtain good samples for thermo-mechanical characterization. The resin system used was a one component pre-polymer differing from the conventionally used two monomer components thermoset systems. There was no low viscosity monomer available to disperse the particles and melt blending was not suitable due to the narrow processing window of the matrix. So only solution casting was left as an option for us. This method also introduces the problem on how to get rid of the high amount of solvent having a boiling point above the curing temperature of the resin. Thus indeed the fabrication remained challenging for us. However, the results obtained from the thermo-mechanical characterization indicate that Bismaleimide thermoset nanocomposite resins have the potential to contribute to the development of advanced composites in view of their excellent thermo-mechanical properties. We have observed a HDT of about 260 °C and a T_g about 240 °C for a Bismaleimide resin in this study, which is exceptionally high and surpasses the properties of (normal and advanced) engineering polymers. The cost of the Bismaleimide resin material is also low compared to the competitive high-temperature resistant polymers.

The study of rheology of organoclay dispersions provided a quick insight into the structure and development of clay dispersions and the level of intercalation and exfoliation. The rheological study of organoclay dispersions exhibited some interesting features. The dispersions have the tendency to evolve over time showing distinct stages of evolution. The dispersions exhibited a predominantly elastic behavior. A critical threshold concentration of clay particles is needed to form elastic dispersions. The viscoelastic characteristics of the elastic dispersions resemble that of a critical gel. The critical threshold concentration seems to coincide with the particle overlap concentration. The critical gel-like behavior of the dispersions remained unaffected over time despite the formation of new bonds between the particles contrary to the standard concept of a critical gel in polymeric systems. The formation of a fractal-like structure of the particles we believe is responsible for preserving the critical-gel- like behavior throughout the time window. Time has such a large influence on the

viscoelastic behavior that even the viscous dispersions with clay concentration below the critical threshold showed critical-gel-like behavior after a long time. It is intriguing to identify which mechanism is controlling this viscoelastic behavior. Either it is mainly diffusion controlled process in which the platelets and clusters take time to join together to form a percolated network or the degree of exfoliation increases with time and a larger number of platelets becomes available making new connections and further developing the percolated network. It is also possible that both processes are competing with each other and depending upon the particle concentration one process dominates over the other.

The use of nanoclay has enhanced the thermo-mechanical properties of the matrix. An anisotropic structure is formed because of the shrinkage of the material during curing and the evaporation process of the solvent. The degree of exfoliation is fairly good but gets worse with increase in concentration of particles. The Halpin-Tsai model reproduces the data of experimental moduli reasonably well. The aspect ratio of the clay platelets has been calculated from the room temperature moduli values by using the Halpin-Tsai model. The apparent aspect ratio decreases with increase in concentration of particles. This means the degree of exfoliation is reduced with increase in concentration of clay particles. The Halpin-Tsai model does not take the particle network into account. We believe interfacial interactions and the associated particle network formation may explain the observed discrepancy between the model predictions and experimental data at high temperatures i.e. when the matrix becomes soft and the particle contribution is considerable.

The creep resistance of Bismaleimide themosets is extremely high because of the densely crosslinked network structure. The matrix recovers completely upon removal of the load. The creep resistance of Bismaleimide nanocomposites is further improved by the incorporation of nanoclay. The widely used linear viscoleastic models such as the Burgers' model and the Findley power law model have their limitations when used for network polymers. The Findley power law is unable to explain the creep mechanism. Also, the Findley power law has no strain bound which is not meaningful for thermosets from a physical point of view. Thermosets, in principle should have a time limited strain without viscous creep flow. Furthermore the assumption of a single relaxation time in the Burgers' model is also not appropriate for real systems. In real polymer systems the relaxation time is distributed over rather wide time scales. The modified form of the Burgers' model in which the Maxwell viscous element is omitted the retarded creep compliance is considered as a stretched exponential function reproduces the creep strain over time for the matrix and the nanocomposites remarkably well. In our fitting procedure of the data with the stretched

Burgers' model we adopted a different approach than others. We imposed additional constraints on fitting by setting the boundary conditions that the retardation time (τ) and stretching exponent (n) should be invariant of the filler concentration. This means that we assume that dynamics of the nanocomposites is wholly controlled by the matrix dynamics and thus must be independent of the filler concentration. That this approach works is an important and interesting finding that is also be supported by the dynamic Halpin-Tsai micro-mechanical model. This result implies that research questions on the role of filler on the matrix dynamics have to be critically evaluated. The ability to model the mechanical properties is also helpful for optimizing and predicting the thermo-mechanical properties of nanocomposites in general.

7.2 Recommendations

We would like to propose some future work to address the some remaining research questions that appeared during the course of this study.

- Time dependent evolution of the organoclay dispersions is an interesting phenomenon. Systematic experimental studies are needed in order to develop the understanding of the mechanism involved in evolution of dispersions. Rheology coupled with optical analysis and scattering techniques might provide better insight into the on going evolution process.
- The solvent NMP is emerging as a preferred candidate to obtain good dispersions of organoclay particles. It is worth investigating its physio-chemical properties in detail to explain what underlies this success. This understanding will be helpful for further fine tuning of the chemistry of the particles and matrix materials to obtain even better dispersed nanocomposites.
- The Bismaleimide resin chemistry is not very well defined which hampers understanding of the interfacial interactions and interface properties. It would be worth properly understanding the resin chemistry. It will help to better understand the process-structure-property relations and allow designing of combinations of materials meeting the desired characteristics.
- For thermosets the properties are mainly determined by the network and it is crucial to know the curing kinetics so as to know how the network is affected in the presence of nanoparticles. However, due to the presence of solvent in this study the normal calorimetric techniques used for curing kinetics characterization are not suitable. This

warrants developing other strategies that could be used reliably to determine the curing kinetics of solvent based systems.

- Halpin-Tsai model does not take into account particle network effects or indeed a possibly inhomogeneous composite structure. Theoretical models need to be developed that can accurately determine the mechanical properties based on the structure of nanocomposites including interfacial effects.
- In order to verify the stretched Burgers' model and the boundary conditions proposed in this study additional systematic studies should be done on various thermoset nanocomposite systems In the present study it is tricky to obtain a reproducible level of intercalation and exfoliation. A large set of data with a reasonably reproducible level of intercalation/exfoliation is needed to validate the model further and establish the additional boundary conditions we imposed on the fitting (same τ and n for matrix and nanocomposites).
- The high-temperature resistant Bismaleimide nanocomposite matrix is worth investigating for the fabrication of three phase fiber reinforced nanocomposites, an emerging concept. Because mainly fiber reinforced composites are used in practice a well dispersed nanofilled matrix might further enhance the mechanical properties, toughness and erosion resistance of the composite, in addition to potential weight savings. It is useful to know how feasible it is to be used with standard composite manufacturing processes and what the effect of using a nanocomposite matrix is on the properties of fiber reinforced composites.

Summary

In this thesis we report the synthesis, characterization and thermo-mechanical properties of a high-temperature resistant themoset nanocomposite system based on an aero-space-grade Bismaleimide resin. Various processing techniques with various fillers are used. The emphasis is on establishing the relationship between the structure and mechanical properties of nanocomposite systems. We characterized the nanocomposite systems experimentally using rheology, X-ray diffraction, Thermo-mechanical and microscopic techniques. The mechanical properties e.g. viscoelastic properties are interpreted in terms of the microstructure and explained by using micromechanical and viscoelastic models.

In order to get insight into the structure of clay particles in the form of suspension we studied the rheology of organoclay dispersions before curing. We investigated the development of organoclay dispersions over time with the help of rheometry by applying small amplitude oscillatory deformation. Dispersions evolve over time with distinct stages into a percolating network. In most of the cases with various clay concentrations the behavior of dispersions was elastic solids-like. There is a critical threshold concentration of clay particles at which the dispersions initially behave as elastic solids and below which they form viscous fluids. This critical threshold seems to coincide with overlap concentration of the bodies of revolution of the particles, which is at a low clay concentration (of the order of 0.5% w/w). This overlapping of the bodies of revolution of particles may also limit the degree of exfoliation. Complete exfoliation is hardly ever achieved, as usually the concentration of particles used is much larger than the critical threshold concentration. Moreover, surprisingly, the frequency dependency of the mechanical moduli of the dispersions resemble that of a critical gel (a system just at the cross over between a visco-elastic solid and a visco-elastic fluid), normally reported for cross-linking polymers. This aspect has not been highlighted yet for clay dispersions. Interestingly the critical gel-like behavior of the dispersions persisted throughout the evolution over time.

Thermo-mechanical properties of nanocomposite systems prepared with both carbon nanofiber and organoclay were investigated. The matrix itself and the nanocomposite system show excellent thermal properties and reasonable mechanical properties, better than the normal engineering polymers. The use of carbon nanofiber did not produce significant improvement in mechanical properties due to the poor adhesion of the fiber with the matrix. However, the use of organo clays shows systematic increase in mechanical properties and

heat deflection temperature with the concentration of clay particles. The evaporation of solvent during curing leads to alignment of clay particles, which may also be beneficial for the properties of the nanocomposite. The stiffness of the nanocomposite was modeled by the Halpin-Tsai model. The model reproduces the data reasonably well. XRD results and the apparent aspect ratio obtained by Halpin-Tsai fitting indicate that the nanocomposite system is not completely exfoliated, and that the degree of exfoliation decreases with increasing particle concentration.

We also investigated creep behavior of the nanocomposite system. The matrix shows very good creep stability and the use of nanofiller further enhances it. Application of the Findley power law and the Burgers model, which are widely used to describe the creep behavior of polymers, is critically evaluated. Their limitations to describe the creep behavior of thermoset matrices are discussed. We used a modified form of Burgers' model which we named the 'stretched Burgers model' (SB) to describe the creep behavior of thermoset matrix and the nanocomposite. The stretched Burgers model reproduces the time-dependent creep compliance remarkably well. We made assumptions in fitting the data that retardation time scale distribution should be independent of filler concentration. The very good fitting of data supports the assumption. This means that the dynamics of the nanocomposite system is mainly governed by the dynamics of the matrix. This is an interesting assumption in our study and never highlighted in creep studies of nanocomposites. We believe that this finding is helpful for developing a better understanding of the mechanics of nanocomposites and of the role of filler on the dynamics of the matrix, which is greatly debated. The stretched Burgers model appears to be very suitable for describing the creep behavior of thermoset systems both from a physical point of view and concerning the quality of the fits.

Samenvatting

In dit proefschrift rapporteren we de synthese, de karakterisering en de thermo-mechanische eigenschappen van een hoge-temperatuurbestendige, thermoharder nanocomposietsysteem op basis van een luchtvaartkwaliteit bismaleimidehars. Verscheidene verwerkingstechnieken met verschillende vulmiddelen zijn toegepast. De nadruk ligt op het vastleggen van het verband tussen de structuur en mechanische eigenschappen van nanocomposiet systemen. We hebben de nanocomposiet systemen experimenteel gekarakteriseerd met reologie, röntgendiffractie (XRD), en microscopische technieken. De mechanische (o.a. visco-elastische) eigenschappen zijn geïnterpreteerd in termen van de mikro-structuur, en zijn verklaard met micromechanische en visco-elastische modellen.

Om inzicht te krijgen in de structuur van kleideeltjes in suspensievorm hebben we de reologie van organoklei-klei dispersies bestudeerd. We hebben de ontwikkeling in de tijd van organokleidispersies onderzocht met behulp van reometrie, door oscillerende deformatie met kleine amplitudes toe te passen. Dispersies evolueren mettertijd met duidelijke stadia van tot een percolerend netwerk. In de meeste gevallen met verschillende kleiconcentraties gedroegen de dispersies zich als een elastische vaste stof. Er is een kritieke drempelconcentratie van de kleideeltjes boven welke de dispersies zich als elastische stoffen gedragen, en waar beneden ze in eerste instantie visceuze vloeistoffen vormen die zich na enige tijd ontwikkelen tot viscoelastische vaste stoffen. Deze kritieke drempelconcentratie lijkt samen te vallen met een overlapconcentratie van de omwentelingslichamen van de deeltjes Deze drempelconcentratie is ongeveer 0.5 gew%. Dit overlappen van de omwentelingslichamen van de deeltjes kan ook de mate van exfoliëren beperken. Volledige exfoliatie slechts wordt zelden bereikt aangezien de gebruikte deeltjesconcentratie meestal veel groter is dan de kritische drempelconcentratie. Bovendien en verrassend vertoont de frequentieafhankelijkheid van de mechanische moduli van de dispersies gelijkenis met die van een kritische gel (een systeem precies bij de overgang tussen een visco-elastische vaste stof en een visco-elastische vloeistof), die wordt gevonden voor verknopende polymeren. Dit is niet eerder gevonden voor kleidispersies. Interessant is dat het kritische-gelachtige gedrag van de dispersies persistent is tijdens de evolutie met de tijd.

Thermomechanische eigenschappen van nanocomposietsystemen met zowel koolstofnanovezels en organokleideeltjes zijn onderzocht. De matrix zelf en e nanocomposieten hebben uitstekende thermische eigenschappen en redelijke mechanische eigenschappen, beter dan de normale technische polymeren. Het gebruik van koolstofnanovezels geeft geen significante verbetering van mechanische eigenschappen door de slechte adhesie van de vezel met de matrix. Echter, het gebruik van organoklei geeft systematisch een verhoging in mechanische eigenschappen en warmtedeflectietemperatuur met toenemende kleideeltjesconcentratie. Het verdampen van oplosmiddel tijdens het uitharden leidt tot uitlijnen van kleideeltjes, wat ook voordelig kan zijn voor de eigenschappen van het nanocomposiet. De stijfheid van het nanocomposiet is gemodelleerd met het Halpin-Tsai model. Het model reproduceert de data redelijk. XRD resultaten en de schijnbare aspectverhouding, verkregen uit de Halpin-Tsai fit, geven aan dat het nanocomposietsysteem niet volledig geëxfolieerd is, en dat de mate van exfoliatie afneemt met toenemende deeltjesconcentratie.

We hebben ook het kruipgedrag van de nanocomposieten onderzocht. De matrix vertoont zeer goede kruipstabiliteit en het gebruik van nanovulmiddel versterkt dit verder. De Findley machtsfunctie en het model van Burgers, die algemeen gebruikt worden om kruipgedrag in polymeren te beschrijven, zijn kritisch geëvalueerd. Hun beperkingen om het kruipgedrag van thermosettende matrices te beschrijven wordt bediscussieerd. We introduceerden een gemodificeerde vorm van het model van Burgers dat we het “streched Burgers” (SB) model noemen om het kruipgedrag van de thermohardende matrix en het nanocomposieten te beschrijven. Het SB-model reproduceert de tijdafhankelijke kruip opmerkelijk goed. We hebben enkele interessante aannames gebruikt om de data te fitten die nog niet in de literatuur zijn toegelicht. We gebruiken een aanvullende randvoorwaarde bij het fitten van het model, door aan te nemen dat de retardatietijdsverdeling niet afhankelijk is van de vulmiddelconcentratie. Dit betekent dat de dynamica van het nanocomposietsysteem voornamelijk bepaald wordt door de dynamica van de matrix. Dit is een interessante aanname in die niet eerder is is geintroduceerd in studies over kruip van nanocomposieten. Deze aanname werkt zeer goed. We geloven dat deze vinding helpt bij het ontwikkelen van een beter begrip van de mechanica van nanocomposieten en de rol van vulmiddel op de dynamica van de matrix. Het SB-model lijkt zeer geschikt voor het beschrijven van het kruipgedrag van thermohardende systemen, zowel vanuit een fysisch oogpunt en wat betreft de kwaliteit van defits.

Acknowledgements

Accomplishing a PhD degree is a significant point in ones life, thanks to Almighty Allah who blessed me to obtain this level of knowledge and gave me strength and support to carry on this challenging journey. Every achievement or success is not always an individual effort but it has contribution from many others directly or indirectly. This is the time now to extend my gratitude to those persons and institutions which were part of me during this research period and played vital role in various forms to achieve this milestone.

First of all I am grateful to Higher Education Commission of Pakistan for providing financial support by awarding scholarship to carry out PhD in The Netherlands. I would never have been dream to go abroad and study in such an advanced country without their financial support. Moreover, I really acknowledge their fare and transparent selection process which provides the opportunity to meritorious students. I must also take this opportunity to thank Nuffic, the Dutch higher education body which coordinated HEC scholar's placement in universities and facilitate the timely distribution of scholarship and other administrative issues. I am really thankful to Ms. Loes Minkman our correspondent in Nuffic who was very kind, helpful and responsive to the issues faced during this study period.

The person whom I am really indebted for achieving this PhD milestone is my supervisor, Prof. dr. Stephen J. Picken. He always encouraged me during the tough times of research and came up with brilliant ideas to carry on my research in a concluding way. It was he who never lost confidence on me although I lost at many times. I found him great mentor, scientist, visionary and super intelligent with full of smart ideas. He was always very kind and open to discuss ideas and clear my concepts and understandings of the subject. He really helped me to apply the analytical models for data fittings. He spent a fair amount of time to read my thesis and correct the writings to conclude my thesis in time despite having much busy schedule. But how can I forget to acknowledge my co-supervisor Dr.Ir.N.A.M. Klaas Besseling, indeed not. His contribution to this thesis is also beyond my expressions. He proposed many scientific interesting aspects to probe during my research to make it more genuine and academically accepted. I am really impressed by his extraordinary scientific nature of thinking and critical analysis. I am honest to say that he inculcated in me the scientific way of doing the things and how to analyze them critically. I am really thankful to him and feel sorry for him as he has to do a lot of work on my manuscript writings, due to my

non native English speaking background and inexperience in scientific writing. He really taught me like a toddler. I appreciate his patience for working with me and honing my writing skills. I am grateful to him for being so kind to me that whenever I knocked his door for discussion or queries he spared his time without pre-planned appointments which is not common in Dutch culture. I would like to work with my supervisors life long if given the opportunity and wish them happiness and success in their scientific endeavours in future.

I must also pay thanks to Alexander Korobko (Sasha), post doc at the section of Nano Structured Materials (NSM) for being so kind and helpful for me during my PhD. I must say his role was a kind of co-supervisor in my research. He came up with many brilliant ideas during the research and helped me a lot in applying the quantitative techniques and taught me how to work with the model fittings and calculation procedures. He was also very kind for helping me thesis editing and formatting the graphical work for manuscripts.

I am thankful to the NSM secretaries Karin and Wil for their kind, hospitable and cooperative behavior during the time which I spent in this section. They always welcomed me with smiling face and helped for all the administrative issues proactively. I always bothered them for translating the official letters written in dutch but never find a sign of tease on their faces. So I will remember their kind attitude in times to come.

The role of technicians in experimental research is very vital due to their profound experience in dealing with the machines, obtaining the accurate data and handling the samples smartly. I am grateful to Ben Norder who trained me to work with the thermal analysis machines (DSC, DMA, TGA) used to characterize the samples and working of the Rheometer which I used extensively as well. I am thankful to Marcel Bus supervisor of the chemistry lab where I performed all my experimental work. He taught me how to work with the chemicals safely and do the experiments in a safer and cleaner way. He was very friendly in working. I am also thankful to Pieter Droppert for his technical help.

Staying abroad for a long time and doing the research makes one very tired and bored and missing own society and culture. Thus for achieving this PhD milestone a friendly and cooperative social network is necessary. I also got a chance to meet many people from Pakistan and other nationalities in Delft who provided me friendly company and co-operated at many occasions. First of all I extend my gratitude to my office colleague Xiayon Yang, the best Chinese guy I ever met. Sharing the same office we spent plenty of time on discussing different issues including science, culture and personal affairs. I really developed a reasonable knowledge about the Chinese culture, society, politics and tourism through frequent long discussions with him and become fond of China to go there and experience the life. Besides

that his personal behavior was really very friendly and cooperative, the reason why I always called him “my friend” whenever I need to speak to him. I wish him my heartiest wishes for the completion of his thesis. I would really miss him on my defence day as he will be departed to China by that time, but let see if he invites me in future to visit China to compensate it. I also thank my other section colleagues Zhen Liu, Haining, Piotr Glazer, Saida El Asjadi for giving me a friendly environment and helping me in various ways. I thank to all members of NSM section (which is no more existing now) for giving me the opportunity to do my research in that group with encouraging support on all levels.

I also take this opportunity to acknowledge some of my other international friends whom I met in Deflt. Luis Arteaga (from Bolivia) stayed with me as my room mate is a great person by character and knows how to live with differences. I developed many positive things from him specially how to live with different cultures and backgrounds in harmony. I am thankful to Denis Takeo Goto (from Brazil) and Yoshihiro Mizutani (from Japan). I really had a wonderful time with them in Aerospace faculty during my research when they came in Delft as a guest researcher. I am proud to have a friend like Dipanjay Dewanji (from India) who always provided me the social support with his sincere and professional guidance at many times. I must acknowledge that I would never have explored so many European places if I had not met him. Thanks Dipanjay for giving me such a wonderful company and making my stay in Europe to be memorable. Your friendship always means to me above the frontier barricades. I wish you and your wife Sanchita a happy and prosperous life.

One can not deny the fact that in abroad it is really very comfortable to have some fellows of your native country. I was lucky enough to have so many Pakistani friends in Delft which makes me to feel like in Pakistan. We celebrated many parties together off and on and at special occasions which makes life a bit easier. I take this opportunity to thank all those Pakistani fellows in Delft for supporting me during this research and giving their friendly company. I would like to mention few persons who were really close to me and I had a wonderful time in their friendship. The first pakhtoon friend I made in my life is Hamayun Khan (GM), I am proud of your friendship, very sincere, intelligent, kind, hospitable, and helpful. I will remember the happy time we walked and cycled in the sunny days to explore the nature and lush green fields around Delft. Your hospitality to bring the parathas in faculty and have a lunch together and company for a cup of tea, all were amazing. How one can miss, “Shah-e-Delft” among Pakistani students, the person well known to every one, Shah Muhammad from Talagang. I had very friendly time with him and also have the honour to stayed with him as my room mate. He was altogether a sincere person with full of knowledge

about domestic and international affairs. I am thankful to him for supporting me and giving his honest suggestions during the tough times of research. I must acknowledge Syed Iftikhar Kazmi, darling of all, a very honest, kind, sympathetic, generous and a man of values. I am proud of your friendship. I wish you a very success in your PhD soon. I am also thankful to find a very nice friend Hanan Sheikh during my final stage of PhD. I am really grateful for his hospitality for offering delicious Pakistani foods frequently to me, which is priceless thing to find abroad. I also enjoyed his funny jokes with harsh critical thinking as well. I am also thankful to my other friends Faisal Kareem, Cheema, Zahid Shabir, Awais, Aleem, Shahzad Gishkori, Akram , Ibrahim, Faheem Raees for their friendly and supporting company.

Now the time to acknowledge the persons most important and dear to me, my parents. From my existence in the world to raise me to the level to become an effective society member all is due to their prayers, efforts, support, and unconditional love to me. They did not get any education but understand the value of education and wanted their son to get the highest standard education. They provided me all the means I needed by sacrificing their comforts and most important giving up their right to serve them in their old age when it was time from my side to pay back. They allowed me to go abroad for PhD and continued their prayers for my success during the days and nights. I must say that I am nothing to achieve these mile stones in my life it is the power of their sincere prayers that today I am at this stage. But I am thankful to Allah that their prayers and efforts became true and fruitful. Mom and Dad I hope now you take this PhD token from my side as your pride. But I need you at all stages of my life, God bless you with long and healthful life. I must acknowledge my elder brother Shafiq for taking care of the family and social affairs in my absence and supporting the family through thick and thin and preserving its fabric structure. He suffered himself and his family life but never bothered me so I can focus on my studies. I must thankful to him for giving me his love as elder brother and treating like his kid. My younger brother Faisal also deserves to be appreciated and acknowledged through his support by handling the administrative issues during my scholarship application as I was not free to go to the offices and solve the bureaucratic issues. He also fulfilled duties owed to me in my absence by taking care of my parents and their medication He kept me in touch with family by calling me when I missed them and supported me in tough times. I am thankful to my brother’s wife Salma for her kind, loving and serving attitude to all our family members. In this selfish and individualism age she still managed to lead a joint family life. I wish her kids also get high quality education and be obedient to her. I am also thankful to all my sisters for their sincere prayers for my success and their so kind and loving attitude towards me. I wish all of them for

a prosperous and healthy life. I must acknowledge the innocent and pure love of my nephews and nieces to me which makes my life colourful. I wish very success to my nieces Sidra, Iqra, Sana, Nabeela, Aniqa and my nephews Adnan, Shafqat, Ammar, Umar , Abubakar , Ali, all are very dear to me. In my family how can I forget my cousin Naveed, the man who motivated me to come abroad and pursue my PhD. His constant inspiration to me right from Pakistan to date is invaluable source for me to accomplish this task. He supported me all the times and was right on the spot when I needed. I was lucky to have his company in Netherlands, which relieved me from home sickness.

Last but not least I must acknowledge the Dutch society for their openness, kindness, helping attitude, honesty, straight forwardness, and acceptance for the internationals. I never felt any problem in communication and any kind of prejudice during this long and prime time of life which I stayed over here. I always find people respecting others and talking with a smiling and friendly tune. I just annoyed with the Dutch weather else the best place in the world to live in. I learned many positive things during my stay over here and I wish to translate them in my personal behavior and transfer to my society as well. At the end thanks to TU Delft for accepting me to do my research in the world top technical university and providing me all the quality resources I needed generously. Giving me so independence to channel my research and asking me to come up with ideas to explore the world of science is just sheer character of TU Delft. I would try my best to contribute to my society and world through the knowledge and skills which TU Delft imparted to me. I wish to come again and again in this paradise of science and technology to refresh me and fill with the knowledge.

Curriculum Vitae

Muhammad Iftikhar Faraz was born on 10th April, 1980 in Satiana Banglow, district Faisalabad, Pakistan. He got his primary education in the government school of his native town. He studied at University of Engineering and Technology Taxila from 2000-2004 and received his BSc in Mechanical Engineering. He did his master in Manufacturing Engineering from University of Engineering and Technology Lahore from 2004-2006. He also served as a lecturer in National Textile University Faisalabad from 2004-2005. After his master he joined National Engineering and Scientific Commission Islamabad and involved in research and development activities in the field of manufacturing from 2006-2007.

He moved to The Netherlands in December 2007 and joined the Faculty of Aerospace Engineering in the department of Aerospace Materials and construction at TU Delft. He worked there till June 2010. Later on he moved to the department of Chemical Engineering at TU Delft in June 2010 and started his PhD with Prof. dr. Stephen.J.Picken. He has published his research work in several international conferences and journals well known in the field of Polymers and Composites. One of the articles has already published and three are under the review process. His major interests are in the field of Materials Engineering with special focus on Polymer nanocomposites and fiber reinforced composites. Mr. Faraz in his future plans intends to join a university back in Pakistan and do the teaching and research job. He also wants to do the social work and contribute his best to promote the education and uplifting the life standards of people in rural areas. Traveling and tourism is his main hobby.